Investigation of Load-Slip Behavior and Fatigue Life of Headed Shear Stud Connector

Md Manik Mia

A Thesis in
The Department of
Building, Civil and Environmental Engineering

Presented in Partial Fulfillment of the Requirements
for the Degree of Master of Applied Science (Civil Engineering) at
Concordia University, Montreal, Quebec, Canada

July 2017

© Md Manik Mia, 2017

CONCORDIA UNIVERSITY
School of Graduate Studies

This is to certify that the thesis prepared

By: Md Manik Mia

Entitled: Investigation of Load-Slip Behavior and Fatigue Life of Headed Shear Stud Connector

and submitted in partial fulfillment of the requirements for the degree of

Master of Applied Science (Civil Engineering)

complies with the regulations of the University and meets the accepted standards with respect to originality and quality.

Signed by the final examining committee:

Dr. Ashutosh Bagchi	*Chair*
Dr. Lucia Tirca	*Examiner*
Dr. M. Zahangir Kabir	*Examiner*
Dr. Anjan Bhowmick	*Supervisor*

Approved by _____
Chair of Department or Graduate Program Director

_____
Dean of Faculty

Date: _____

Abstract

Investigation of Load-Slip Behavior and Fatigue Life of Headed Shear Stud Connector

Md Manik Mia

The use of composite structures in highway bridges has become a widespread practice and for developing composite action between steel beam and concrete slab, shear connectors are widely used. These shear connectors transfer the longitudinal shear forces developed at the interface between concrete slab and steel beam. Among different types of shear connectors, headed shear stud is most commonly used in practice. The strength and ductility of these connectors greatly influence the capacity of composite structures. In bridges, these shear studs are subjected to rapidly fluctuating stresses which may result in fatigue failure during the lifetime of the structure. Thus, the fatigue resistance of shear studs in composite beams is significant for the safe of whole structure and needs to be well investigated. The aim of this research work is to investigate the load-slip behavior and fatigue life of headed shear studs and assess the strength and fatigue requirements of current Canadian Standard, CSA S6-14. A three-dimensional finite element (FE) model of push out test is developed using commercial software package ABAQUS for predicting both fatigue life and static strength of headed shear studs. The FE model included both geometric and material nonlinearities. For fatigue life prediction both fatigue crack initiation life and crack propagation life are estimated. Excellent correlation against the test results for both fatigue life and static strength of shear stud is found. After validation, an extensive parametric study has been performed to investigate the effects of different parameters on load-slip behavior and fatigue life of shear stud connectors. Results from the FE analysis were also compared with current code of practices, such as European code (EC4), American code (AASHTO LRFD), Canadian code (CSA

S6-14). The parametric study showed that both AASHTO and CSA S6-14 usually overestimate the static strength of headed shear stud connectors. The design provisions of European code, EC4 is found to give conservative estimation of shear capacity of headed shear stud. For fatigue life of shear stud a significant underestimation was found in case of AASHTO LRFD, while notable amount of overestimation was observed in case of CSA S6-14 demanding more study in this area. Currently, there is no provision available for fatigue life of shear studs when they are subjected to tension. This research project also examines the applicability of the current Canadian fatigue curves for design of shear studs when they are subjected to tension.

ACKNOWLEDGMENTS

At first I would like to express my gratitude to the blessings of Almighty God, the Beneficent and the Merciful for enabling me to complete the study successfully.

I have the pleasure to state that I got an excellent opportunity to complete this thesis under supervision and guidance of Dr. Anjan Bhowmick, Associate Professor, Department of Building, Civil and Environmental Engineering, Concordia University, Montreal, Canada. I am greatly indebted to him for all his guidance, assistance and enthusiastic encouragement throughout the progress of this thesis. Without his help, it would be very difficult for me to complete this thesis.

A special thanks goes out to my colleagues especially Kallol Barua, Md Imran Kabir for their moral support and encouragements. Finally, I would like to thank my parents and my elder brothers and sisters for their continuous support and enthusiasm throughout my life.

CONTENTS

LIST OF FIGURES

LIST OF TABLES

List of Symbols

F_{u}	Minimum tensile strength of the stud steel
$\mathrm{A_{sc}}$	Cross-sectional area of one stud shear connector
$\mathrm{f'_c}$	Concrete compressive strength
F_y	Yield stress
$\emptyset_{sc}$	Resistance factor for shear connectors
q_r	Shear resistance
d	Diameter of shear stud
γ_{v}	Partial safety factor
f_{ck}	Cylindrical compressive strength of concrete
E_{cm}	Elastic modulus of concrete
α	Reduction coefficient
h	Overall height of the stud
N	Total number of cycles
$\Delta\sigma$	Stress range
σ_{max}	Maximum applied stress
σ_{min}	Minimum applied stress
R	Stress ratio
C	Fatigue constant
m	Slope of the design curve
$\Delta\tau_R$	Stress range

N_R	Number of stress range cycles
$\Delta\tau_c$	Reference stress range
N_c	Number of cycles at $\Delta\tau_c$
k	Constant term with the value of $2.08x10^{22}$
γ	Fatigue life constant
F_{srt}	Threshold stress range
$\frac{\Delta\varepsilon}{2}$	Strain amplitude
$\frac{\varepsilon_{el}}{2}$	Elastic strain amplitude
$\frac{\varepsilon_{pl}}{2}$	Plastic strain amplitude
σ'_f	Fatigue strength coefficient
N_{init}	Crack initiation life
ε'_f	Fatigue ductility coefficient
b	Fatigue strength exponent
c	Fatigue ductility exponent
E	Elastic modulus
K'	Cyclic strength coefficient
n'	Cyclic hardening exponent
da/dN	Crack growth rate
ΔK	Stress intensity factor range
K_{max}	Maximum stress intensity factor
K_{min}	Minimum stress intensity factor
N_{prop}	Crack propagation life

a_o	Initial crack size
a_f	Final crack size
ΔK_{th}	Threshold stress intensity factor range
N_{Total}	Total fatigue life
D	Damage paramter
f_{max}	Maximum nominal shear stress
Q_{max}	Maximum cyclic load
Q_{min}	Minimum cyclic load
Q_{ult}	Static strength of headed shear stud
P_{sh}	Static strength of shear stud
a	Crack size

List of Abbreviations

AASHTO	American Association of State Highway and Transportation Officials
ASTM	American Society for Testing and Materials
ASCE	American Society of Civil Engineers
BS	British Standards
CAFL	Constant Amplitude Fatigue Limit
CHBDC	Canadian Highway Bridge Design Code
CSA	Canadian Standards Association
EC	Euro Code
ECCS	European Convention for Constructional Steelwork
FE	Finite Element
FEA	Finite Element Analysis
LEFM	Linear Elastic Fracture Mechanics
LRFD	Load and Resistance Factor Design

Chapter 1 Introduction

1.1 General

Highway bridges are often designed to achieve composite action by connecting concrete slab on top of steel beam allowing them to act as one unit. The use of steel-concrete composite beams in buildings and bridges are widespread practice now. Horizontal shear developed at the interface between steel section and concrete deck slab must be resisted to develop full flexural strength of the composite member. To resist this horizontal shear at the interface, connectors are used and these shear connectors are embedded in the concrete slab as shown in Figure 1.1. By using shear connectors, the load-carrying capacity of a girder could be increased by 50% than non-composite girder (Shariati *et al*. 2012). The strength and ductility of these shear connectors greatly influence the flexural strength of composite beams.

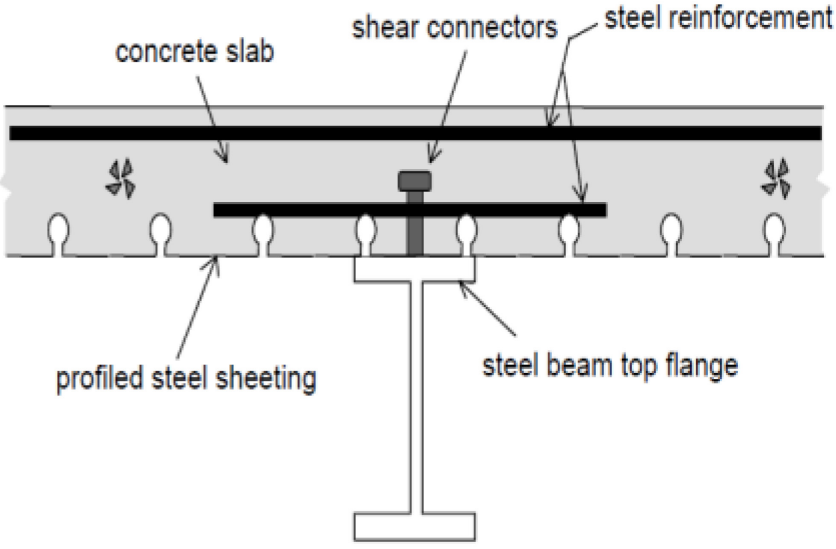

Figure 1.1. Headed shear stud connectors between concrete slab and steel beam (Shariati *et al*. 2012)

A synopsis of the research work involved in this thesis are discussed in this chapter with its significance and contributions. This research investigates the load-slip behavior of headed shear stud, a common shear connector used in steel-concrete composite bridges. Two smaller studs i.e. 19 mm and 22 mm and three larger shear studs i.e. 25 mm, 27 mm and 30 mm have been used. Also, the fatigue life of shear stud using finite element analysis is also investigated. The following Section 1.2 provides the background of the study and the motivation of this research is discussed in Section 1.3. Section 1.4 presents the research objectives and the next Section 1.5 discusses scope and limitations of this study. Finally, an outline of the thesis contents is presented in Section 1.6.

1.2. Background

Although, the American Institute of Steel Construction (AISC), in addition to European and Canadian codes, have provisions for strength and ductility of the composite member, load-slip behavior of headed shear studs has not been studied extensively (Mirza and Uy 2008). The main factors affecting the behavior of shear studs are strength of concrete and connector. Experimental push-out tests have been done to evaluate both shear capacity and load-slip behavior of shear connectors (Nguyen and Kim 2009). In a push-out test, a specimen is loaded till failure and the ultimate load is divided by the number of studs to get shear capacity. Figure 1.2 shows a typical push-out specimen. Shear studs with diameters less than 1" (25 mm) are called standard diameter studs and studs used in composite bridges are either 3/4" (19 mm) or 7/8" (22 mm). The studs greater than 1" (25 mm) in diameter are called large diameter studs. Many shear studs are required in high shear zone to provide full shear connection resulting a long welding time and difficulty to remove a deteriorated slab and a dense distribution of shear studs can cause difficulty for the workers in case of smaller shear studs are used (Lee *et al*. 2005). Thus, use of larger shear studs, such as 25, 27 and 30 mm are now getting attraction from engineers, however, a very few works

have been done on larger shear studs. Badie *et al*. (2002) proposed the application of a new shear stud of 1¼" diameter to reduce the number of required studs in design. Currently, the use of 1¼" diameter or shear stud larger than 1¼" in diameter is not allowed by AASHTO LRFD (2007) due to lack of test and design criteria (Mundie 2011).

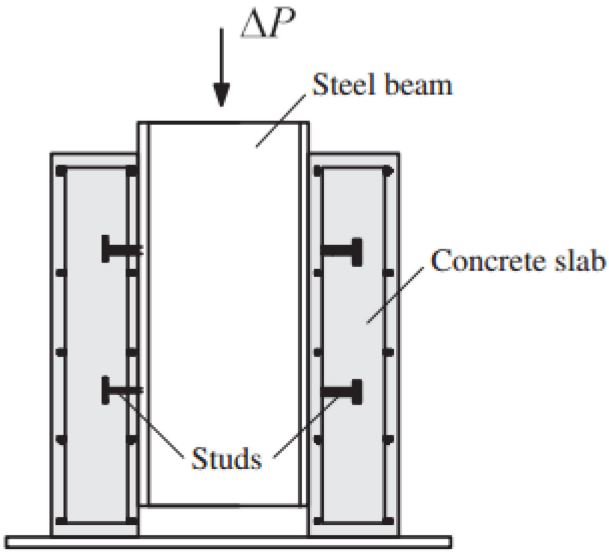

Figure 1.2. A typical push-out specimen

Shear studs are often subjected to repeated loadings and these repeated loads can initiate micro-cracks in stud materials which may propagate with the continued application of cyclic stress. This process is known as fatigue. Fatigue failure can be dangerous since it occurs suddenly without significant prior deformations. Shear stud connectors are very sensitive to fatigue. Behavior of shear studs subjected to fatigue load was the main research objective in earlier studies on the fatigue behavior of steel-concrete composite beams. Push-out specimen shown in Figure 1.2 was used in most of the tests. In current Canadian Highway Bridge Design Code (CHBDC), shear studs must satisfy both strength and fatigue requirements. The shear connection must be capable of developing full plastic capacity of the steel cross-section to satisfy strength requirements. In order

to satisfy fatigue requirements, demands due to the application of load must be lower than the shear stud fatigue capacity determined from an empirical fatigue capacity curve (Ovuoba and Prinz 2016).

1.3. Motivation of this Research

A recent study by Alkhatib (2012) revealed that Canadian Standards Association, CSA-S06 overestimates the shear capacity of 22.2 mm shear stud when compared with test results. This is one of the main motivations of this research work. Badie *et al*. (2002) pointed out that using alternate headed and headless studs has no harmful effect on slippage but it was recommended to investigate the effects of using only headless studs. To investigate this issue, two small shear studs (19 and 22 mm) and one large shear stud (25 mm) are taken and load-slip behavior is investigated.

For many years, the American Association of State Highway and Transportation Officials (AASHTO) Load and Resistance Factor Design (LRFD) Specification and Canadian Highway Bridge Design Code (CHBDC) used the test results of Slutter and Fisher (1966) for fatigue requirements. In 2010, a supplement to the 2006 publication of the CHBDC has made modification to the fatigue requirement of shear stud, based on the work of Zhang (2007), to be consistent with that of other fatigue details (CSA S6-14). In the work of Zhang (2007), a regression analysis was carried out on a large collection of push-out test data carried by previous researchers and log-log relationship is found to approximate closely if fatigue detail category D is considered while AASHTO LRFD still uses log-linear curve for fatigue life prediction. Lee et al. (2005) pointed out a notable amount of underestimation by AASHTO LRFD for large shear studs: 25, 27 and 30 mm. Findings from this research investigation provided another motivation for closer evaluation of the current codes for fatigue and strength requirements of shear studs. The fatigue resistance of headed shear stud is best determined through testing which is very expensive and time-consuming. It is

often impractical, or sometimes impossible, to test full-size structural components. Thus, a numerical method is required to predict fatigue life of headed shear stud well.

1.4. Research Objectives

The research work carried out in this thesis is to investigate the issues pointed out in Section 1.3 to provide further insights and understandings. The main research objectives are outlined as follows:

- To investigate the load-slip behavior of two small headed shear studs used in steel - concrete composite bridges such as 3/4" (19 mm) and 7/8" (22 mm). It is done by developing a three-dimensional finite element (FE) model that is capable of simulating accurate behavior of push-out specimen.
- To investigate the load-slip behavior of three large headed shear studs: 25, 27 and 30 mm and evaluation of current code of practices for strength requirements of shear stud connectors.
- To investigate the load-slip behavior of headless shear stud.
- To propose a finite element based approach using the push-out test specimen for fatigue life estimation of shear studs.
- To evaluate current code of practices, such as Canadian code (CSA S6-14), American code (AASHTO LRFD), European code (EC4), British code (BS 5400) for fatigue life estimation of headed shear studs.
- To investigate the effects of different parameters such as concrete strength, slab thickness, stud spacing on fatigue life of shear stud.
- To investigate the fatigue life of shear studs when they are in tension.

1.5. Scopes and Limitations

There are several factors that affect the shear capacity obtained from finite element (FE) analysis of a push-out specimen. These are boundary conditions, material properties of shear stud, concrete damage modeling, loading conditions. The material nonlinearities are included in the developed FE model and concrete damage plasticity is also defined to investigate the concrete strength effects on both shear capacity and fatigue life of shear studs. In spite of these, there are some limitations of this research. There are some differences in the mechanical behavior of shear studs between full-scale beam tests and push-out tests. The result from push-out test needs to be interpreted for use in composite bridge beams but this relation is not included in this thesis work for simplicity. Push-out tests are standard procedure and are used for investigating load slip behavior for many years (Bro and Westberg 2004). To estimate total fatigue life, crack is not explicitly modeled. Rather, it is assumed that crack will generate at the most stressed area and the critical location is identified by finite element (FE) analysis.

1.6. Outline of the Research

The composition of the thesis is organised into six chapters. Each chapter begins with an introduction giving an overview of that chapter.

Chapter 1 presented a short background of strength and fatigue requirements of headed shear stud and explains the motivation of this thesis work and approaches to be used to accomplish the objectives.

Chapter 2 presents a comprehensive review on the previous works which relates to the interests of this thesis work. In addition to discussing various experimental and analytical works, relevant

design rules are also presented. The literature review is mainly divided into two categories which are static shear capacity and fatigue life of shear studs.

Chapter 3 explains the finite element (FE) model developed to investigate load-slip behavior and fatigue life of shear studs. The finite element method generally consists of three major parts: pre-processing, solution techniques and post-processing. In this chapter, pre-processing and solution will be discussed in details. The pre-processing, in which the author has developed a three-dimensional finite element (FE) model to investigate load-slip behavior of shear studs using push-out specimen. Finite element model must be validated against test results to ensure its accuracy and reliability. At the end of this chapter, validation of FE model is shown against two test results.

Chapter 4 presents the load-slip behavior of headed shear studs. The shear capacity obtained from FE analysis is compared with current code of practices such as CSA S6-14 and EC4.

Chapter 5 discusses the proposed finite element based approach for fatigue life estimation of shear studs using push-out specimen. This chapter also presents and evaluates the fatigue strength requirements of Canadian Standard (CSA S6-14), American code (AASHTO LRFD), European code (EC4) and British code (BS-5400). The effects of several parameters on fatigue life such as stud spacing, slab thickness, concrete strength are also discussed. Finally, some insights on shear stud subjected to tensile loading are discussed.

Chapter 6 provides the summary of the conclusions gathered throughout this study as well as recommendations for future works.

Chapter 2 Literature Review

2.1. Introduction

The literature review consists of four major parts which are discussed in this chapter. In Section 2.2, a general background of different types of shear connectors used in composite structures is presented. In this study, headed shear stud has been selected since this types of shear studs are widely used for steel-concrete composite bridges. In Section 2.3, current static and fatigue design specifications of different codes i.e. CSA S6-14, AASHTO LRFD, EC4 and BS 5400 are reviewed. Following this, the techniques which are used for calculating fatigue life are discussed with their development, applications and limitations. Finally, an extensive study of previous works on shear studs is reviewed in Section 2.5.

2.2. General Background

Composite structures are widely used nowadays because of their lightweight and strength. In composite structures, shear connectors are used to transmit the shear forces developed across steel-concrete interface. These shear connectors are welded on top of steel beam and primary purpose is to prevent horizontal movement and separation between steel beam and concrete slab which allows them to act as one unit. The capacity and ductility of these shear connectors greatly influence the flexural strength of composite beams. Inadequate design results loss of strength of composite beams causing complete failure of the systems. Various types of shear connectors such as headed stud shear connectors, channel connectors, block with hoops connectors, post-installed shear connectors, T connectors, Perfobond rib connectors, T-Perfobond connectors, Crestbond connectors etc. These are illustrated in Figure 2.1. Among different types of shear connectors,

headed shear stud connectors, developed during the 1940's by Melson Stud Welding Company, are most common and widely used in steel-concrete composite bridges. The common advantage of this connector is that welding is very fast and it anchors well in concrete (Xie *et. al*. 2011). One drawback of headed shear stud connector is that it is very sensitive to fatigue and care must be taken if used in fatigue prone sites. Perfobond rib shear connector was developed in late 1980's in Germany to reduce the fatigue problems of shear studs used in bridges. It provides a good resistance in vertical and horizontal directions by forming a dowel action of concrete flow through rib holes and it is a good alternative of headed shear studs. One of the disadvantages of this shear connector lies with the placement of the transverse bottom reinforcement in slab. Although, perfobond rib shear connectors are better than headed shear stud connectors in case of fatigue, these are not yet adopted by industries and experimental investigation is going on. In 2009, Vienna *et al.* proposed a new alternative headed shear stud connector known as T-perfobond stud connector. This connector was developed by adding a flange to the plate and it was found that the resistance of T-perfobond shear connector is higher than perfobond rib shear connector. Another type of shear connector used in steel-concrete composite bridges is T-connector and it is a standard T section welded to the steel plate with two fillet welds. Another most common shear connector is channel shear connector. The capacity of this connector is higher than headed shear stud connectors and thus, it enables a fewer number of channel connector compared to large number of headed shear stud connectors (Maleki *et al*. 2008). The current code of practices for the use of channel shear connectors in North America i.e. CSA S6-14 and AASHTO LRFD are based on the experiments carried out by Slutter and Fisher (1966) at Leigh University.

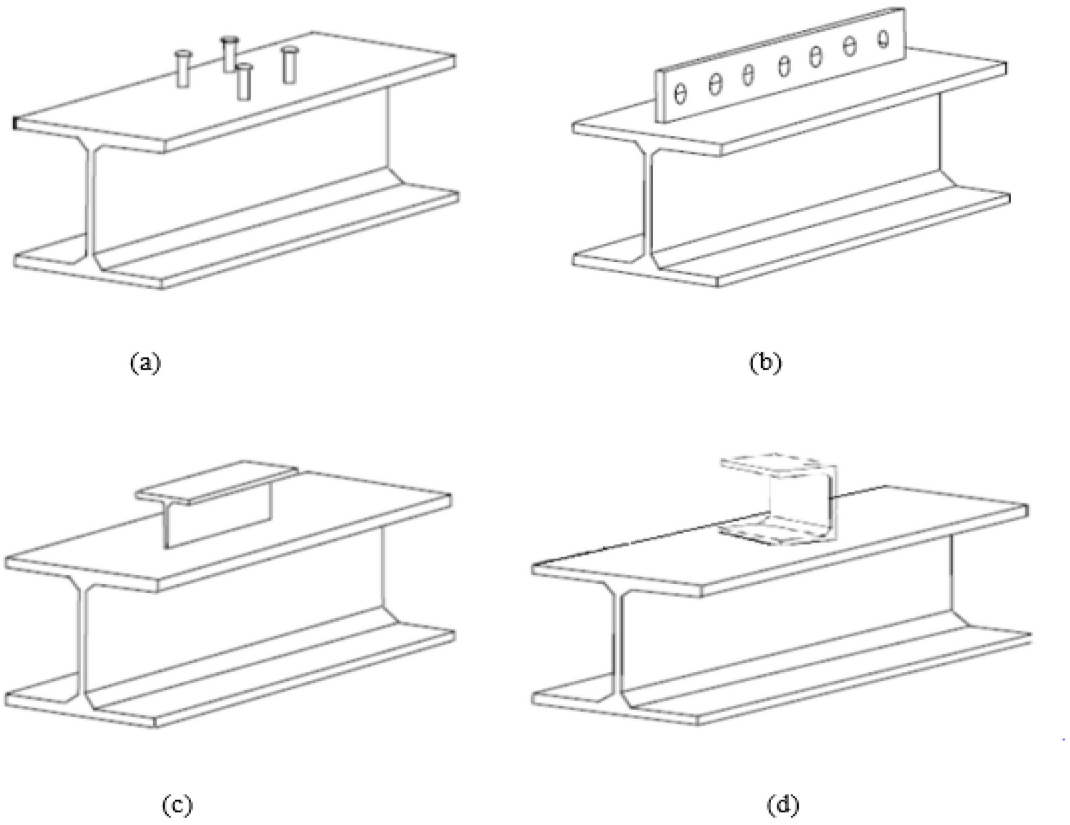

Figure 2.1. (a) Headed stud shear connector, (b) Perfobond rib shear connector, (c) T shear connector, (d) Channel shear connector

2.3. Static and Fatigue Design Specifications for Headed Stud Shear Connector

2.3.1 Static Design Specifications

To find out static strength and load-slip behavior of headed shear stud connectors, push-out tests are mostly used worldwide. A typical push-out specimen consists of a steel beam on which shear connectors are welded on both flanges and embedded in concrete slab. The specimen is loaded until failure and the recorded ultimate load is divided by the number of studs to get static strength of shear stud connectors. It is assumed that the load is transmitted from steel beam to concrete slab uniformly through shear studs for simplicity (Viest 1956). This method was first used in

Switzerland in 1930's for studying shear capacity of spiral shear connectors. The design provisions in AASHTO LRFD and CSA S6-14 are based on the research done by Ollgaard *et al.* (1971) for static strength and Slutter and Fisher (1966) for fatigue life prediction of shear stud.

The Canadian Standards Association CSA S6-14 states that the factored shear resistance, q_r of a headed stud shear connector with h/d ≥ 4 shall be taken as Clause 10.11.8.3.2.,

$$q_r = 0.5\emptyset_{sc}A_{sc}\sqrt{(f'_c E_c)} \leq \emptyset_{sc}F_u A_{sc} \quad (2\text{-}1)$$

where F_u = minimum tensile strength of the stud steel, A_{sc} = cross-sectional area of one stud shear connector, f'_c = concrete compressive strength and $\emptyset_{sc}$ = resistance factor for shear connector.

It has been also suggested that the spacing of shear connectors shall not be less than 4d (d = diameter of shear stud) nor greater than 600 mm. Equation 2-1 is also used by AASHTO LRFD to calculate static strength of headed shear stud. The left-hand side of the inequality of Equation 2-1 represents the shear stud strength and is affected by modulus of elasticity and compressive strength of concrete while the right-hand side represents the tensile strength of the shear stud (Jayas *et al.* 1988). CSA S6-14 specifies some restrictions on the placement of the slab reinforcement and stud spacing which can be seen from Figure 2.2. The minimum cover to the top and bottom reinforcement is 70 mm and 50 mm respectively and the clear distance between the head of the stud to the bottom transverse reinforcement should be at least 25 mm. One interesting thing to mention here is that CSA S16 and AASHTO LRFD both limit minimum spacing of shear stud as 6 stud diameters while CSA S6-14 specifies to 4 stud diameters.

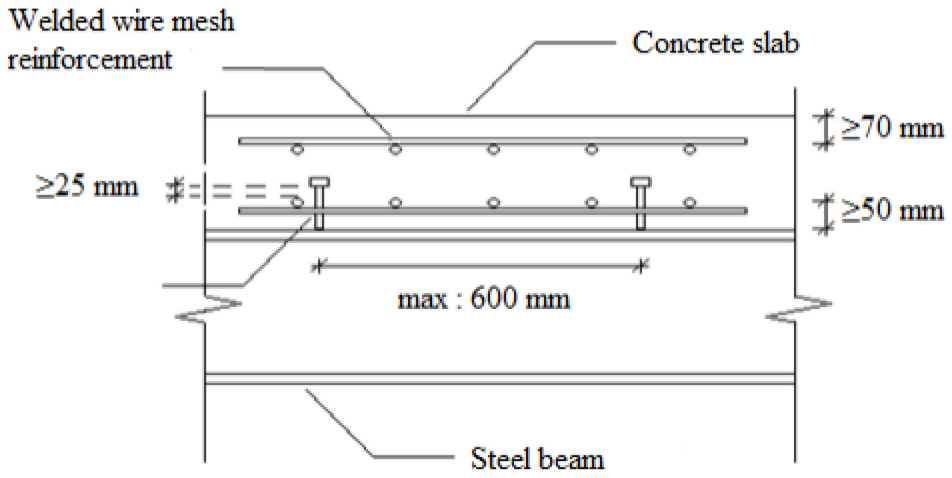

Figure 2.2. Detailing requirement based on CSA S6-14 for composite bridge decks (Alkhatib 2012)

According to Eurocode-4, the static strength of shear stud in composite beam should be taken as the lesser of Equation 2-2 and Equation 2-3.

$$q_r = 0.8 f_u (\pi d^2/4) \,/\gamma_v \tag{2-2}$$

$$q_r = 0.29 \alpha d^2 \sqrt{(f_{ck} E_{cm})}/\gamma_v \tag{2-3}$$

where f_u = ultimate strength of stud steel

f_{ck} = cylindrical compressive strength of concrete

E_{cm}= Elastic modulus of concrete

$\alpha = 0.2(\frac{h}{d} + 1) \leq A_{sc} f_u$; h and d are overall height and diameter of the stud respectively and γ_v is a partial safety factor (= 1.25). Equation 2-2 represents the shear failure of the shear connector, while Equation 2-3 represents the concrete failure around the shear connector.

2.3.2. Fatigue Design Specifications

Repeated or fluctuating stress can initiate micro-cracks in materials which may propagate with the continued application of cyclic stress. This process is known as fatigue and the fatigue problem of shear studs used in steel-concrete composite bridges has been paid a great attention in recent years. AASHTO LRFD and Canadian Highway Bridge Design Code provisions on fatigue of headed shear studs are based on the results of fatigue tests by Slutter and Fisher (1966) at Leigh University of Pennsylvania. In their study, 44 samples were tested (35 samples of 19 mm (3/4-in.) and 9 samples of 22.2 mm shear studs) under constant amplitude stress cycles. They proposed a curve fitting through the test data from loading the test samples in one direction. Slutter and Fisher (1966) found that stress range is the most important parameter affecting fatigue life and they proposed Equation 2-4 to relate stress range and number of cycles a specimen can sustain before failure:

$$log(N) = A - B\,\Delta\sigma \tag{2-4}$$

where N is total number of cycles and $\Delta\sigma$ is the stress range. The stress range is defined as $\Delta\sigma = \sigma_{max} - \sigma_{min}$ where σ_{max} and σ_{min} are the maximum and minimum applied stress respectively. There are another two parameters in fatigue life prediction such as stress ratio, R =$\sigma_{min}/\sigma_{max}$, and mean stress, $\sigma_m = (\sigma_{max} + \sigma_{min})/2$ but it has been found that these two parameters have negligible effect on fatigue life (Fisher et al. 1970). In Equation 2-4, A and B are two parameters found from regression analysis. Slutter and Fisher (1966) determined these two parameters as 8.072 and 0.1753 respectively when $\Delta\sigma$ is expressed in ksi. AASHTO LRFD 2012 specifies these two parameters as 8.061 and 0.1834 respectively. Thus, the fatigue life can be related to stress range by the following Equation 2-5 based on AASHTO LRFD (2012).

$$log(N) = 8.061 - 0.1834\,\Delta\sigma \quad (2\text{-}5)$$

Fatigue requirement of shear studs in CSA S6-14 have been modified in order to be consistent with other fatigue details based on an investigation by Zhang (2007). Zhang (2007) carried out a regression analysis on a series of test results and it was observed that the mean regression line of a log stress range versus log fatigue life plot could be approximated by fatigue category D curve (Commentary of CSA S6-14, Clause 10.17.2.7). is considered. The threshold stress range for fatigue category D is consistent with the previous value used for shear studs as 48 MPa. The current CSA S6-14 code Equation is as follows:

$$log(N) = logC - m\,log\,\Delta\sigma \quad (2\text{-}6)$$

In Equation 2-6, N and $\Delta\sigma$ represent total number of cycles and stress range respectively. C is a constant given in Table 10.4 ($721x10^9$ for category D) and m is the slope of the design curve and is taken as 3.0.

Eurocode-4 specifies the fatigue strength of welded headed shear stud as follows:

$$(\Delta\tau_R)^m N_R = (\Delta\tau_c)^m N_c \quad (2\text{-}7)$$

In Equation 2-7, N_R is the number of stress-range cycles, $\Delta\tau_R$ is the stress range, $\Delta\tau_c$ is the reference value at 2 million cycles with $\Delta\tau_c$ equal to 95 MPa, m is the slope of the design curve equal to 8.0.

According to British Bridge Code, BS 5400, fatigue strength of shear stud can be determined from the following Equation 2-8,

$$(\Delta\tau_R)^m N_R = k \quad (2\text{-}8)$$

In the above Equation, k is constant with a value of $2.08x10^{22}$, m is the slope of the fatigue strength curve normally taken as 8.0, N_R is the predicted number of cycles to failure of stress range $\Delta\tau_R$.

2.4. Fatigue Life Prediction Techniques

At present, there are two basic approaches that are used to calculate total number of cycles a component can sustain before failure:

(a) Use of $\Delta\sigma - \mathrm{N}$ curves based on experimentally determined relationships,

(b) Use of Fracture Mechanics Approach.

2.4.1. $\Delta\sigma - N$ Approach

In this approach, a curve of $\Delta\sigma - N$, where stress range $\Delta\sigma$ is usually the independent variable and N is the dependent variable, is established through testing of different weld details. Based on the severity of the stress raisers, the test results are divided into different fatigue categories which are mostly common in civil engineering structures. There are two different sets of fatigue curves used in the design: $\Delta\sigma - N$ curves for European Convention for Constructional Steelwork (ECCS) and American Association of State Highway and Transportation Officials (AASHTO). Among these two types of design curves, the $\Delta\sigma - N$ curves used in AASHTO is also used in Canadian Highway Bridge Design Code. The fatigue design curves which are used in current Canadian Highway Bridge Design Code CSA S6-14 is illustrated in Figure 2-3. In Figure 2-3, there are seven different design fatigue curves designated as A to E, representing the fatigue strengths from highest to

lowest. All the curves have the same slope of 3 and are uniquely defined by fatigue life constant, γ. It has been experimentally proved that if the applied stress range is less than a certain value, then the fatigue life tends to become infinite. This certain value is known as constant amplitude threshold stress range, F_{srt} which is represented by the horizontal portions of the $\Delta\sigma - N$ curves in the following Figure 2.3. To obtain $\Delta\sigma - N$ curves, the full-scale specimen is subjected to constant amplitude load cycles until failure and to get a design curve, a regression analysis is done on the fatigue test data. The design $\Delta\sigma - N$ curve is taken as the mean minus two standard deviation (Klippstein 1987). But this approach is no longer used in current CSA S6-14 code. Rather, to evaluate the fatigue resistance of shear connectors, the mean fatigue curve is used instead of mean minus two standard deviations. One of the major shortcomings of $\Delta\sigma - N$ approach is that there is no distinction between crack initiation life and crack propagation life and little information about crack initiation and crack propagation characteristics can be deducted.

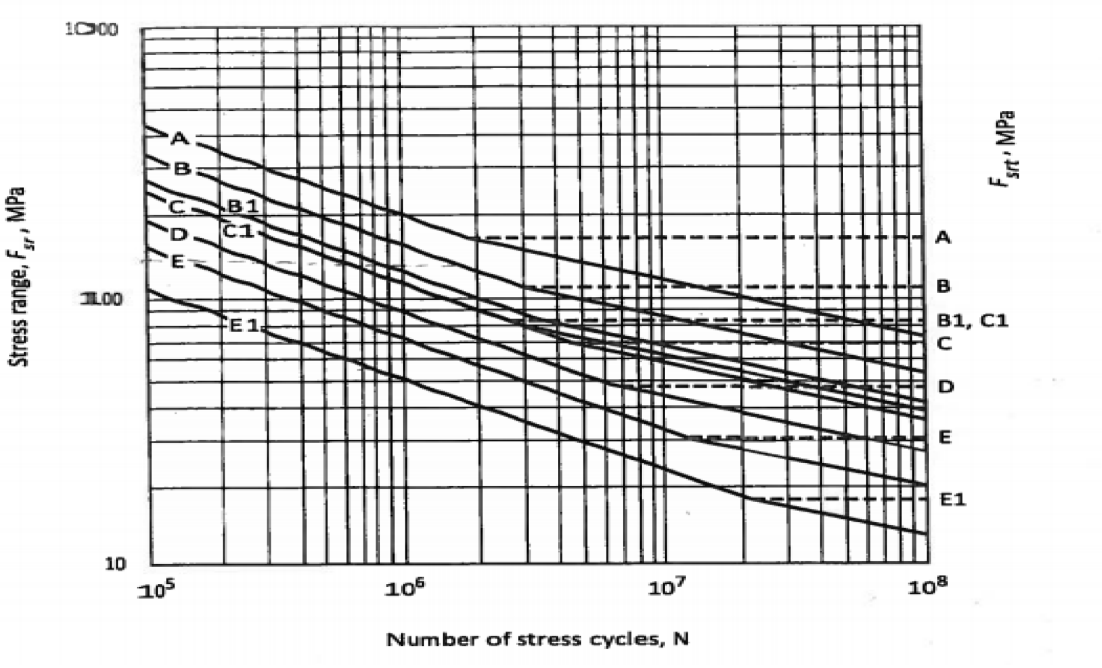

Figure 2.3. Stress range versus number of cycles (CSA S6-14)

2.4.2. Fracture Mechanics Approach

Fracture mechanics is a part of engineering discipline which deals with the crack growth and deals with the stress field around the crack tip. Cracks may initiate at high stress concentrated areas, high residual stress areas or at initial flaws. These cracks can grow within the structure in a stable manner under the application of cyclic loading until it reaches a critical size and becomes unstable and fails. There are three stages of crack growth:

A. Crack initiation stage

B. Stable crack propagation stage

C. Unstable crack propagation stage

In crack initiation stage and stable crack propagation stage, if proper repair is done, the structure can be saved but if it reaches unstable stage, complete failure can occur. The total fatigue life is the sum of crack initiation and crack propagation life. Crack initiation life is calculated using empirical correlation approach and stable crack propagation life is calculated using linear elastic fracture mechanics (LEFM) approach. In the empirical correlation approach, different empirical damage parameters, D, is used to correlate with N, total number of cycles before failure. This empirical correlation approach is divided into three categories: a) Stress-based method, b) Strain-based method, c) Energy-based method.

2.4.2.1 Stress-based Method

The stress-based method emphasizes nominal stresses in the critical cross-section and compares them with traditional $\Delta\sigma - N$ curves. It does not emphasize on local stresses and strains and

normally employs elastic stress concentration factors. In some cases, it has been observed that fatigue life found from stress-based method differs from the test value by more than two orders of magnitude (Everett 1992). This method is more suitable for high-cycle fatigue where the applied stress is within the elastic range.

2.4.2.2 Strain-based Method

The strain-based method is widely used for calculating fatigue crack initiation life and it will be used in this study. For this reason, it is described extensively in this section with its background. It was developed in early 1960's for low cycle fatigue of ductile materials but this method can also be used for high cycle fatigue where small plastic strains exist (Stephens et al. 2001). Although most engineering structures are designed in a way so that the nominal load remains elastic, practically it is never achieved and stress concentration occurs, which leads to crack formation. In contrast to stress-based method, strain based method deals with the plastic deformations which occur in localized regions. The basic assumption of this method is that it assumes a material in a highly strained area behaves similarly as a smooth specimen under cyclic strain controlled loading. After knowing the localized strains, the crack initiation life can be calculated using un-notched strain life properties of the material.

a) Crack Initiation Life:

According to strain-based method, crack initiation life can be estimated from the following Equation 2-9.

$$\frac{\Delta\varepsilon}{2} = \frac{\varepsilon_{el}}{2} + \frac{\varepsilon_{pl}}{2} = \frac{\sigma'_f}{E}(N_{init})^b + \varepsilon'_f (N_{init})^c \quad (2\text{-}9)$$

where $\frac{\Delta\varepsilon}{2}$ = strain amplitude i.e. half of the total strain range

$\frac{\varepsilon_{el}}{2}$ = elastic strain amplitude

$\frac{\varepsilon_{pl}}{2}$ = plastic strain amplitude

σ'_f = fatigue strength coefficient

N_{init} = crack initiation life

ε'_f = fatigue ductility coefficient

b = fatigue strength exponent

c = fatigue ductility exponent

The elastic part of the above Equation 2-9 is known as Basquin's equation (Basquin 1910) and the plastic part is known as Coffin-Manson relationship (Tavernelli and Coffin 1962). The fatigue material properties σ'_f, ε'_f, b and c are found from regression analysis of $\frac{\Delta\varepsilon}{2}$ – N test results. The elastic and plastic strain components are recorded from cyclic stress-strain hysteresis loops and the test is performed by subjecting the specimen under strain controlled cyclic loading. The cyclic stress-strain curve is described by Ramberg-Osgood Equation,

$$\varepsilon = \frac{\sigma}{E} + \left(\frac{\sigma}{K'}\right)^{1/n'} \tag{2-10}$$

where K' and n' are cyclic strength coefficient and cyclic hardening exponent respectively. It is necessary to use the Equation 2-10 in case of cyclic loading in finite element analysis instead of monotonic stress-strain relationship (Josi et al. 2010). Equation 2-9 is valid only for completely reversed cycle scenario i.e. R = -1. But practically, in most of the cases R is greater than -1. Smith

et al. (1970) proposed the following Equation 2-11 which is known as Smith-Watson-Topper model, to account this issue,

$$\frac{\Delta\varepsilon}{2} = \frac{(\sigma'_f)^2}{\sigma_{max}E}\,(N_{init})^{2b} + \frac{\sigma'_f\,\varepsilon'_f}{\sigma_{max}}\,(N_{init})^{b+c} \qquad (2\text{-}11)$$

where σ_{max} is the maximum local stress accounting for plasticity and σ'_f, ε'_f, b and c are the same parameters as mentioned earlier in Equation 2-9.

b) Crack Propagation Life:

Once the crack is initiated, it starts to propagate with the subsequent load cycles. In this stage, crack front grows more and more until failure occurs. Generally, at crack front, high concentration of stresses leading to plastic deformation occur (Fisher et al. 1997). According to Paris (1963), the logarithm of crack growth rate, da/dN is proportional to logarithm of stress intensity factor range, ΔK. This relationship can be expressed as:

$$\frac{da}{dN} = C\,(\Delta K)^m \qquad (2\text{-}12)$$

where $\Delta K = K_{max} - K_{min}$ and C and m are material constants. As per guidelines of ASTM standard E647 (ASTM 2000), ΔK can be taken as $\Delta K = K_{max}$ if stress ratio, R, is less than 0 indicating that only tension portion has been considered. If Equation 2-12 is integrated from an initial crack size, a_o to a final crack size, a_f, then crack propagation life, N_{prop} can be determined using the following Equation,

$$N_{prop} = \int_{a_o}^{a_f} \frac{da}{C\,(\Delta K)^m} \qquad (2\text{-}13)$$

It has been observed that crack does not propagate if the stress intensity factor is less than a certain value known as threshold stress intensity factor range, ΔK_{th} (Dowling 1999). Thus, Equation 2-13 can be modified as follows:

$$N_{prop} = \int_{a_o}^{a_f} \frac{da}{C\,(\Delta K^{\,m} - \Delta K_{th}{}^{m})} \tag{2-14}$$

If we add crack initiation life and crack propagation life found from Equation 2-11 and Equation 2-14 respectively, total fatigue life or endurance can be obtained. Thus,

$$N_{Total} = N_{init} + N_{prop} \tag{2-15}$$

One important thing can me mentioned here that C, m and ΔK_{th} used in Equation 2-14 can be found from laboratory tests. For this study, C, m and ΔK_{th} has been taken from the tests of Josi and Grondin performed in I.F. Morrison Laboratory of the University of Alberta and Syncrude Research Laboratory (Josi et al. 2010).

2.4.2.3 Energy-based method

In this method, energy is used as the damage parameter, D to correlate with the fatigue life and total absorbed energy at fatigue failure is assumed to depend on the sustained total number of cycles. Different types of energy have been proposed as a damage parameter per cycle such as total strain energy density, plastic strain energy density, and plastic and tensile elastic strain energy density. If mean stress is needed to predict in case of deformation controlled situations, plastic and tensile elastic strain energy density per cycle is more suitable. Plastic strain energy density per cycle is more appropriate if there is large plastic strain. Although this method is a promising method, it is not used widely and research is going on in this method (Chen et al. 2005).

2.5. Research on Headed Stud Shear Connector

The test performed by Slutter and Fisher in 1966 at Leigh University is considered one of the major sources for fatigue research. They tested 44 push-out specimens to determine the fatigue life. Fatigue life found from their test was very low in comparison to beam test of King *et al.* (1965). They attributed this lower resistance to little interaction in push-out test between stud and concrete slab whereas beam tests allow full interaction. But it was confirmed that push-out results agreed well with full scale beam tests later in research works of Mainstone and Menzies (1976). In this section, both the push-out and full scale beam tests carried out by previous researchers will be extensively reviewed.

2.5.1. Tests by Slutter and Fisher (1966)

AASHTO LRFD and Canadian Highway Bridge Design Code are based on the research work of Slutter and Fisher (1966) who tested 35 push-out specimens having the concrete slab connected with steel beam by 19 mm shear stud, 9 push-out specimens of 22.2 mm shear stud and 12 push-out specimens for channel shear connectors. From these tests, Slutter and Fisher (1966) found that fatigue life is a function of stress range and peak load in fatigue design is insignificant. The effect of minimum stress was found to be significant only in case of stress reversals. Under the same stress ranges, it was observed that fatigue life is less in unidirectional loading than reversal loading. Following Equation 2-16 was proposed based on 44 fatigue test data points for 19 mm and 22.2 mm shear studs.

$$log\,\mathrm{N} = 8.072 - 0.1753\Delta\sigma \qquad (2\text{-}16)$$

where stress range $\Delta\sigma$ is in ksi and N is the total number of cycles. It is important to mention here that one-face push-out test setup was used in their test and load was applied to the centerline of the concrete slab creating an eccentricity. The inherent eccentricity leads to closer stud subjected to tensile stress and further studs to compressive stress. It is due to this additional tensile stress, Slutter and Fisher (1966) got underestimated value when compared with composite beam tests. Eurocode 4 recommends to use standard two face push-out test specimen to prevent inherent eccentricity (Lee et al. 2010). They also tested channel shear connectors which is out of the interest of this study, so it is not described here.

2.5.2. Tests by Mainstone and Menzies (1967)

Both static and fatigue tests on push-out specimens were performed on stud shear connectors, channel and bar connectors. In case of stud shear connectors, 11 static and 23 fatigue tests were performed using 19 mm dia and 100 mm height of shear studs and both unidirectional and reversal loading conditions were considered. Some variations in strength can be expected if concrete strength varies and this variation was found to be more in case of stud shear connectors compared to bar and channel shear connectors from their research works. The following fatigue strength Equation 2-17 was proposed:

$$f_{max} = k_o N^{-\alpha} \quad (2\text{-}17)$$

where f_{max} is the maximum nominal shear stress and k_o and α are constants, N is the total number of cycles.

2.5.3. Tests by Hallam (1976)

The author investigated the behavior of headed stud shear connectors under repeated loading using 17 push-out specimens of 19 mm diameter and 76 mm height of shear studs. Thirteen fatigue tests with constant amplitude but varying stress range, one static test and four fatigue tests using programmed spectrum of amplitudes were performed. There were two studs on each side of push-out specimen. When one stud failed, the corresponding slab was removed and pre-cast concrete slab was bolted and the test was continued until the second stud was also failed. Different parameters that affect fatigue life, especially concrete strength, were studied and the effect of concrete strength was found as an important factor for fatigue life, which is a contradiction to the findings of Slutter and Fisher (1966). This thesis investigates the effects of concrete strength on fatigue life. The following Equation 2-18 was proposed by Hallam (1976):

$$log\,\mathrm{N} = 7.303 - 5.993\,\mathrm{q} \tag{2-18}$$

where $\mathrm{q} = \frac{\mathrm{Q_{max}} - \mathrm{Q_{min}}}{\mathrm{Q_{ult}} - \mathrm{Q_{min}}}$; $\mathrm{Q_{max}}$, $\mathrm{Q_{min}}$ and $\mathrm{Q_{ult}}$ are maximum cyclic load, minimum cyclic load and static strength of headed shear stud respectively. The adequacy of Miner's linear cumulative damage rule for fatigue life under variable amplitude repeated loading was also examined and it was found that Miner's rule can be safely used for predicting fatigue life in case of variable amplitude repeated loading.

2.5.4. Tests by Oehlers and Foley (1985)

To investigate fatigue strength of stud shear connections, 129 push-out tests were performed and it was observed that static strength of stud shear connectors reduces as soon as cyclic loads are applied. The diameter of stud was 12.7 mm and height was 75 mm. Both the load ranges and peak

load was varied to understand the reduction of static strength of stud connections. The load range was varied from 0.10 P_{sh} to 0.47 P_{sh} while the peak load was varied from 0.18 P_{sh} to 0.75 P_{sh} where P_{sh} is the static strength of shear stud. It was noticed that about 50% static strength reduced in two fatigue tests and 73% reduced in another test which is similar to the findings of Mainstone and Menzies (1967). Several important conclusions were made: (1) the peak load does not affect the crack propagation rate but does affect endurance or fatigue life, (2) the remaining strength of shear stud can be assumed directly proportional to the uncracked area, (3) the load range is found to be most important factor on endurance causing tension in one side of a stud, (4) the crack growth rate can be assumed to be constant at a given stress range.

2.5.5. Tests by Naithani et al. (1988)

An attempt was made to investigate the performance of a new type of standard push out specimen using 18 mm diameter of shear stud under dynamic loads and using the test results, the following Equation 2-19 was proposed:

$$log\,\mathrm{N} = 7.595 - 0.02827\,\mathrm{S} \tag{2-19}$$

where S is the stress range. In their tests, stress range was varied to investigate the effects on it keeping the concrete strength constant. It was found that Equation 2-16 proposed by Slutter and Fisher (1966) gave higher stress range for a connector than Equation 2-19. For 2 million cycles, Equation 2-16 gave stress range 58.7 MPa while using their new standard push-out set up, they got 48.2 MPa. Finally, the author concluded that Equation 2-19 would result lower value than the equation 2-16 resulting safe and more accurate design.

2.5.6. Tests by Oehlers (1990)

An experimental investigation of 14 push-out specimens was performed by the author to investigate the deterioration of static strength under fatigue loads. Three tests among fourteen were to determine static strength of headed shear studs. The diameter and height of the studs were 12.7 mm and 74.9 mm respectively. The failure mode of shear stud under displacement control procedure was that stud had sheared off in a plane parallel to the flange surface which is also seen in this thesis work. In case of fatigue endurance tests, there were three zones at which fatigue cracking and then fracture occurred and one failure zone was at weld collar/shank interface which is also assumed in this thesis work. Another important conclusion was that monotonic strength was found to decrease linearly under fatigue loads. Current code of practices assume that static strength remains intact until the fatigue life is reached but based on the test results, the author showed a linear decrease of remaining strength. The following Equation 2-20 was proposed by the authors,

$$N_e = N_f\left(1 - \frac{P_m}{P_s}\right) \tag{2-20}$$

where Ne is the number of cycles to cause static strength to reduce from P_s to P_m and N_f is the theoretical fatigue life found from fatigue endurance test.

2.5.7. Tests by Gattesco and Giuriani (1997)

The fatigue resistance of headed stud shear connectors for different slip amplitudes and for a given slip history was investigated by eight tests. Instead of using push-out test, direct shear test proposed by the authors was used and one single stud connector was taken to remove the difficulties in

results interpretation. The concrete strength was constant 39 MPa and diameter and height of headed shear studs were 19 mm and 125 mm respectively. It was concluded that if the connection slip reaches more than 1 mm which can occur in long-span beams, the fatigue life can be as low as 10^4 cycles and the stud fracture found to propagate from the front or back of the stud shank.

2.5.8. Tests by Shim et al. (2001)

To design shear connectors in steel-concrete composite bridges with precast decks, experimental tests using push-out tests and bridge model tests were performed. The behavior of the shear connection in precast deck was discussed in addition to ultimate strength and fatigue endurance. The diameter and height of the studs were 19 mm and 150 mm respectively. Based on the test results, the following Equation 2-21 was proposed:

$$log\,\mathrm{N} = 7.8869 - 0.021\,\Delta\sigma \tag{2-21}$$

When the above equation is compared with the equation used in AASHTO LRFD, it was found that Equation 2-21 gives higher resistance.

2.5.9. Tests by Badie et al. (2002)

The most common types of shear studs used in steel-concrete composite bridges are 19 and 22 mm. The authors reported the development and application of 31.8 mm diameter shear stud. Since the static strength of 31.8 mm shear stud is almost double than 22 mm shear stud and fatigue strength is also higher, fewer studs would be required in design. The full-scale beam tests revealed that full composite action could be achieved and the slippage or deflection of the beam found was

less. It was noted that using alternate headed and headless studs has no harmful effect on slippage but it was recommended to investigate the effects of using only headless studs. Fatigue testing showed that the α values in AASHTO LRFD equation can be used for 31.8 mm shear stud but the proposed Equation 2-22 (31.8 mm) and Equation 2-23 (22 mm) by the authors were recommended:

$$\alpha(\text{MPa}) = 278.8 - 31.4\, log\, \text{N} \tag{2-22}$$

$$\alpha(\text{MPa}) = 277 - 32.1\, log\, \text{N} \tag{2-23}$$

2.5.10. Tests by Lee et al. (2005)

The authors performed push-out tests using 25 mm, 27 mm and 30 mm shear studs to investigate ultimate and fatigue strength and compared with EC4 and AASHTO LRFD. The fatigue life found from the tests were slightly lower than EC4. Partial composite beams with about 38% degree of shear connection were performed to compare static strength with the value obtained from push-out tests. It was concluded that the ultimate strength of shear stud from partial composite beam tests are 1.59 times larger than that from push-out tests. This finding is contradiction to research works of Mainstone and Menzies (1976) who indicated that push-out test results are close to composite beam tests. One of the reasons may be due to degree of shear connections assumed in Lee et al. (2005) tests. One of the major conclusions pointed out was that the design strength equation of EC4 can be safely used for shear studs up to 30 mm shear studs but in case of AASHTO LRFD equation, the safety factor should be increased. This finding is investigated in this thesis. Two other conclusions from their tests were that fatigue strength equation of EC4 and AASHTO LRFD for larger shear studs need to be improved conservatively and fatigue strength of larger shear studs are slightly lower than that of normal studs.

2.5.11. Tests by Hanswille et al. (2007)

71 push-out tests were performed using 22 mm diameter and 125 mm height of shear studs to determine the reduced static strength after high-cycle preloading. The further aspect was to examine damage accumulation on the fatigue life. It was concluded that the linear damage accumulation hypothesis of Miner (1945), which is used in current codes is not accurate and unsafe. From their tests, it was observed that crack initiated at stud root at 10%-15% of the fatigue life and non-linear decrease of residual strength was observed contradicting the findings of Oehlers (1990), who observed linear decrease of residual strength. Another important observation was that peak load, P_{max}, of the cyclic loading has a significant effect on the crack formation, which was found to occur at stud root.

2.5.12. Tests by Mundie (2011)

Twelve push-out tests using 1-1/4" and the other twelve using 7/8" diameter shear studs were performed to ensure the applicability of AASHTO LRFD fatigue strength equation. Three stress ranges 18, 22 and 26 ksi were used. It was concluded that semi-log fatigue design equations of AASHTO LRFD significantly underestimates the fatigue life of shear studs, especially at low stress ranges. It was recommended to investigate whether there are any variations found from push-out test results by performing full scale composite beam tests. Finally, it was pointed out by the authors to investigate whether the concrete strength has any effect on fatigue life of shear stud, which is another research motivation of this thesis work. As mentioned earlier in Section 2.5.3, there are some dissimilarities among the previous research works especially between Slutter and

Fisher (1966) and Hallam (1976) about the effect of concrete strength, which has been investigated in this thesis work.

2.5.13. Tests by Alkhatib (2012)

To investigate the effects of some parameters such as reinforcement mesh position, shear stud height, presence of stud head, shear stud spacing, steel flange surface treatment, thirty-three push-out tests were performed by Alkhatib (2012). Also, the performance of a new type of shear stud i.e. adjustable stud was also checked experimentally. It was found that flange treatment has some effect on ultimate capacity of shear studs and the coating on flanges results a decrease in ultimate capacity. It was noticed that ultimate capacity of headless shear studs was higher than headed studs by 15.6% for 200 mm long shear studs and it was concluded that the abnormality of the tests and for 150 mm long studs, ultimate capacity was found to be similar. As pointed out in Section 2.5.9. Badie et al. (2002) concluded that the alternate headed and headless studs have no harmful effect on slippage. However, it was recommended to investigate the effects of using only headless studs. Thus, another motivation of this thesis work is to investigate the ultimate strength of headless studs than that of headed studs.

2.5.14. Tests by Ovuoba and Prinz (2016)

Six composite push-out specimens using 19 mm diameter shear stud were tested under repeated cyclic loads at stress ranges varying between 4.4 ksi and 8.7 ksi to address the lack of existing experimental data near the assumed constant amplitude fatigue limit (CAFL). Based on the test results the authors suggest a fatigue limit of 6.5 ksi which is near the existing limit of 7 ksi in current AASHTO LRFD. All specimens were tested by subjecting to unidirectional loading and

crack was seen to initiate at stud weld base and propagated into the beam flange resulting little damage to the surrounding concrete as was observed in other research works (Slutter and Fisher (1966); Hallam (1976)) and this type of failure mode is seen in case of high-cycle loading where applied stress ranges are low. The fatigue lives obtained from the tests were combined with fatigue data sets available in literature and analyzed with a probabilistic method called MLE. It was concluded that current AASHTO S-N curve underestimates fatigue capacity for fatigue life of shear stud.

2.6. Summary of Chapter

This chapter has presented the literature review which is relevant to this study. Although many experimental works were done on headed shear stud connectors, there is no analytical study available for fatigue life prediction. Few analytical studies on the development of nonlinear finite element model to study the load-slip behavior are found but they are limited to smaller shear studs. This thesis describes a nonlinear finite element model developed using ABAQUS to study the load-slip behavior of both standard (19 and 22 mm) and larger shear studs (25, 27 and 30 mm).

There is no study available when shear studs are in tension. Shear studs are subjected to tension in finger plate expansion joint and no guidelines are in Canadian Standards Association, S6-14 about shear studs when they are in tension. This thesis presents a finite element (FE) based approach for fatigue life estimation of headed shear stud connectors for both shear and tensile loading conditions.

Chapter 3 Development of Finite Element Model for Static and Fatigue Strength of Shear Stud

3.1. Introduction

The focus of this chapter is to discuss the development of finite element (FE) model which has been used for both static and fatigue life investigation. In section 3.2, a basic description of different important features including FEA software used in the development of the modeling are presented. Following section 3.3 will discuss push-out model with geometry, boundary conditions, material properties, FE mesh, contact interactions, analysis methods used to investigate static strength and load-slip characteristics of headed stud shear connectors. Finally, validation of the developed FE model for static strength investigation has been shown in Section 3.4.

3.2. Description of FEA Software

In this thesis work, commercial software package ABAQUS is used to investigate the load-slip characteristics and fatigue life of headed shear stud connectors. ABAQUS is a general purpose advanced nonlinear finite element analysis (FEA) software which can be used for different analysis purposes such as heat transfer, stress and other engineering complex applications. ABAQUS/Standard, ABAQUS/Explicit and ABAQUS/CAE are three core products of ABAQUS suite. ABAQUS/Standard is an implicit analysis method where equilibrium is obtained through an iterative process. In this method, the stiffness matrix is updated at the end of every iteration. In many FE problems, ABAQUS/Standard face difficulty converging because of contact or material complexities. When convergence cannot be obtained easily the increment size is decreased and that results in a large number of iterations. In those situations, analysis using ABAQUS/Standard is very expensive since each iteration requires a large set of linear equations to be solved. In

addition, when three dimensional models have large number of contact points, which is the case in this research, implicit procedure must iterate to satisfy all the contact conditions. This may result in extremely small time increments and possible divergence. On the other hand, in ABAQUS/Explicit method no iteration is involved. ABAQUS/Explicit provides the solution of analysis by explicitly advancing the kinematic state from the previous increment. ABAQUS/Explicit uses the central difference method, which is one of the most commonly used time integration procedures. It has been observed that ABAQUS/Explicit can effectively handle severely nonlinear behavior such as rolling of hot metal, slow crushing of energy devices, column buckling, high speed loading etc. Also, it is more attractive for quasi-static simulations of contact problems and has been found more reliable for fracture mechanics problems. ABAQUS/CAE provides a complete modeling and visualization environment where one can easily create, edit, monitor, diagnose a problem. The job management and ease of result visualization, easy-to-use environment makes it more attractive to the new users.

3.3. Push-out Model

3.3.1. Geometry of push-out model

The push-out specimen as shown in Figure 3.1 used in the test of Lee *et al*. (2005) has been taken in this study. The push-out specimen consists of concrete slab, steel beam, rebar and headed shear studs. The thickness of steel beam and concrete slab are 14 mm and 200 mm respectively.

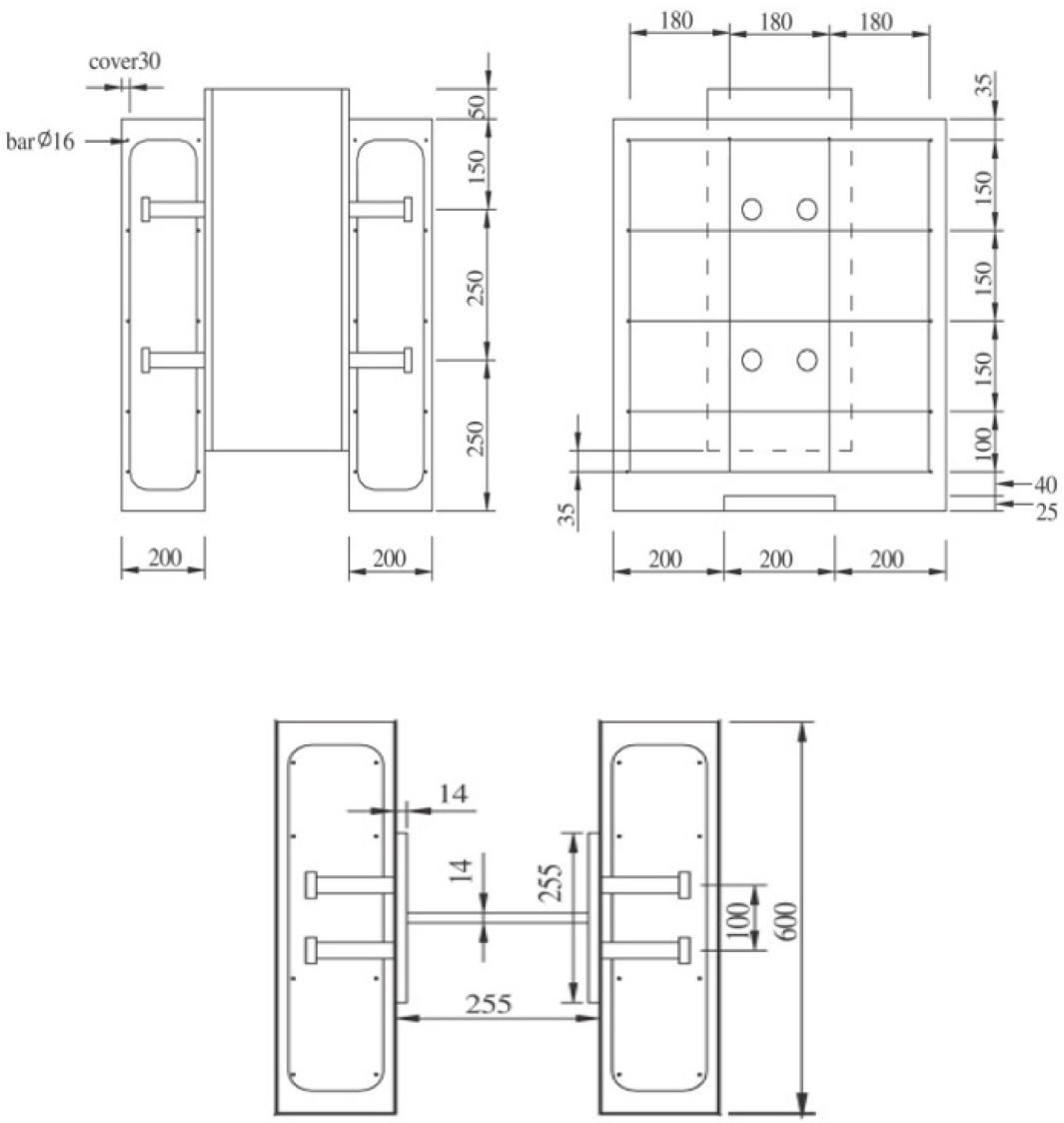

Figure 3.1. Geometry of push-out specimen (Lee *et. al*. 2005)

Two smaller studs i.e. 19 mm and 22 mm and three larger headed shear studs i.e. 25 mm, 27 mm and 30 mm have been used. The dimensions of the studs are shown in Table 3.1. It may be noted here that headed shear studs are modeled using the exact geometry as shown in Figure 3.2 to consider the complicated contact interactions and fracture mechanisms. Reinforcement bars are

modeled as solid parts and embedded in concrete slab; all the nodes are tied to concrete slab allowing no slip between them.

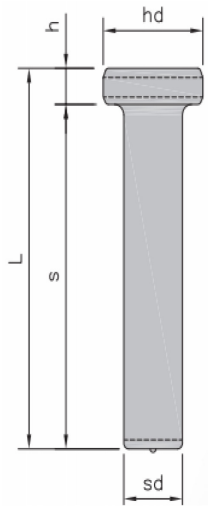

Figure 3.2. A typical headed shear stud

Diameter of studs (s_d) (mm)	Stud head height (h) (mm)	Overall stud height (L) (mm)	Stud head diameter (h_d) (mm)
19	9	125	31
22	11	155	35
25	11	155	38
27	12	155	41
30	12	155	44

Table 3.1. Dimensions of headed shear studs used in FE analysis

Due to the symmetry of push-out specimen, a quarter of the whole model has been used and appropriate boundary conditions are applied to replicate the whole model.

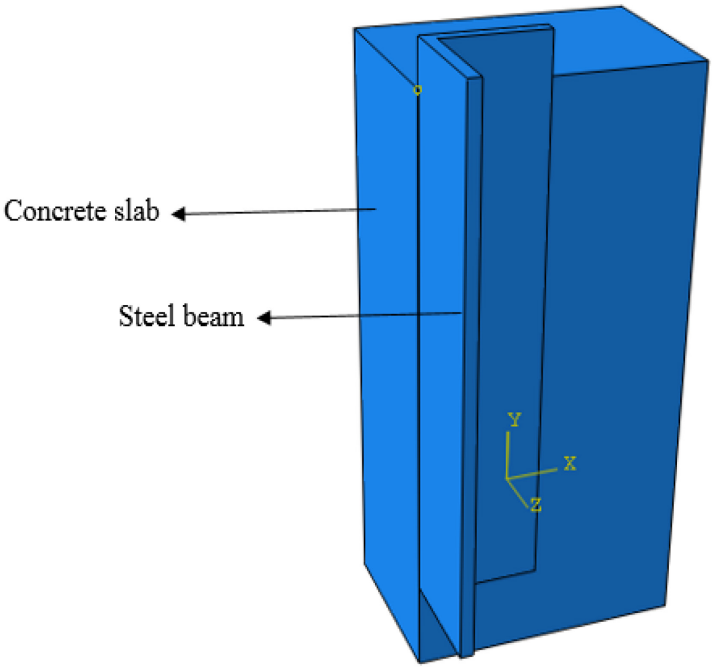

Figure 3.3. A quarter of push-out specimen

3.3.2. Boundary Conditions

Boundary conditions are very important for the simulation of experimental program and any inappropriate boundary conditions may cause completely different and wrong results. In this thesis, selecting proper boundary condition becomes very important to simulate the exact test with which the FE analysis results are compared. Nodes on the top face of the steel section were constrained to a reference point and displacement loading was applied at that reference point. Different loading rate was checked to get accurate results and 0.01 mm/sec downward is found to be the most appropriate loading rate. The X-axis symmetric boundary condition (BC) is applied to surface 1 and all the nodes lying in surface-1 are restricted from moving in X-direction and rotation about Y and Z axis are restrained as shown in Figure 3.4. The Z-axis symmetric BC is applied to surface 2, the middle of the steel beam web so that all the nodes of steel beam web are restrained

in Z-direction and rotation about X and Y axis are also restrained. All translational and rotational movements are restrained at the bottom surface of concrete slab denoted by surface 3.

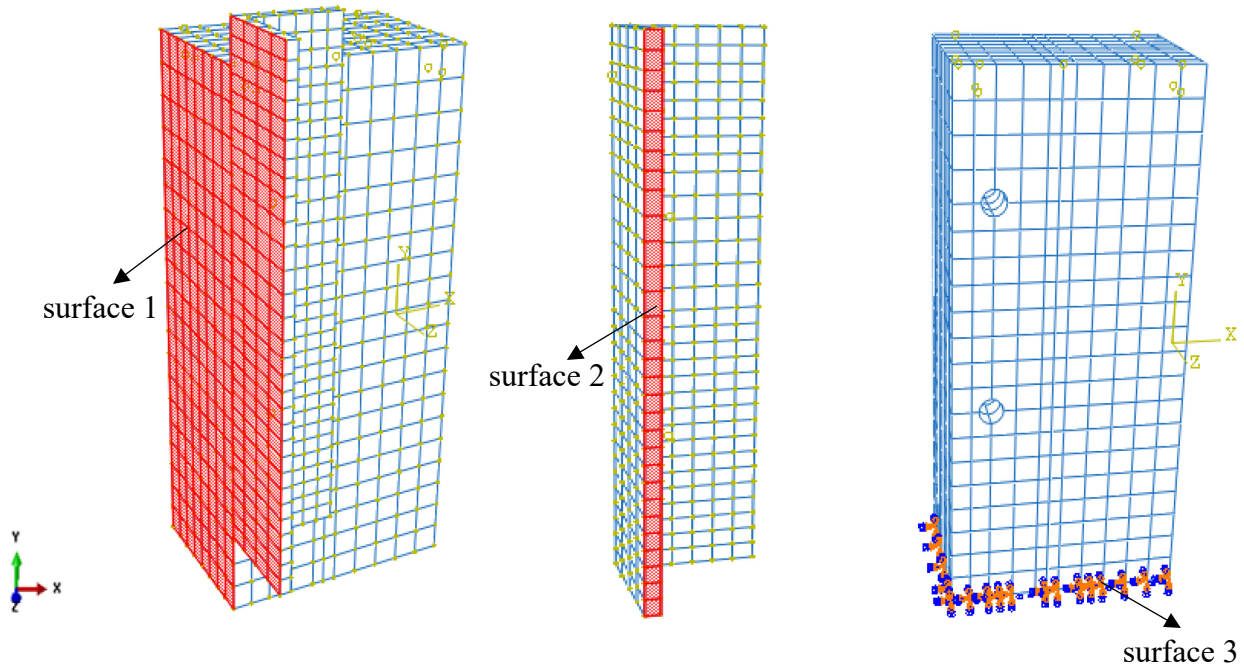

Figure 3.4. Boundary conditions for FE model

These boundary conditions have been selected on the basis of accurate load-slip behavior prediction of headed shear stud and an excellent correlation is found with test results.

3.3.3. Contact and Intearction

Surface-to-surface contact procedure was used in ABAQUS/Explicit with normal behavior ("Hard" conatct) and tangential behavior ("frictionless" formulation). A frictionless interaction has been used between steel beam and concrete slab as shown in Figure 3.5. The reason for using frictionless interaction is to ensure the proper test condition beacause in tests of Lee *et al*. (2005), the bonding at the interface between the flanges of the steel beam and the concrete slab was prevented by greasing the flange. The mechanism assumed in this interaction is that the load will be transferred from steel beam to the headed shear studs and, eventually to the concrete slab.

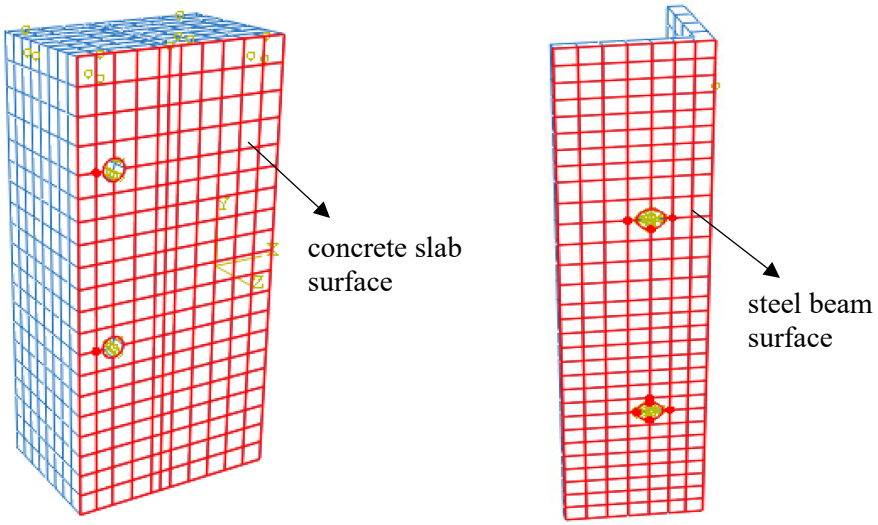

Figure 3.5. Surfaces used for interaction between concrete slab and steel beam

In order to simulate proper test condition, it is very important to use proper constraint between different parts of the push-out specimen in FE analysis. The nodes of the concrete slab and steel beam around the studs are constrained to the surfaces of shear studs by using tie constraint. In Abaqus, it is necessary to define master and slave surfaces accurately. In case of concrete slab-shear stud interface, shear studs have been selected as master surface and concrete slab as slave. In case of steel beam-shear stud interface, steel beam has been selected as master surface. In the time of defining tie constraint between pair of surfaces, surface-to-surface discretization method has been used to get more accurate results.

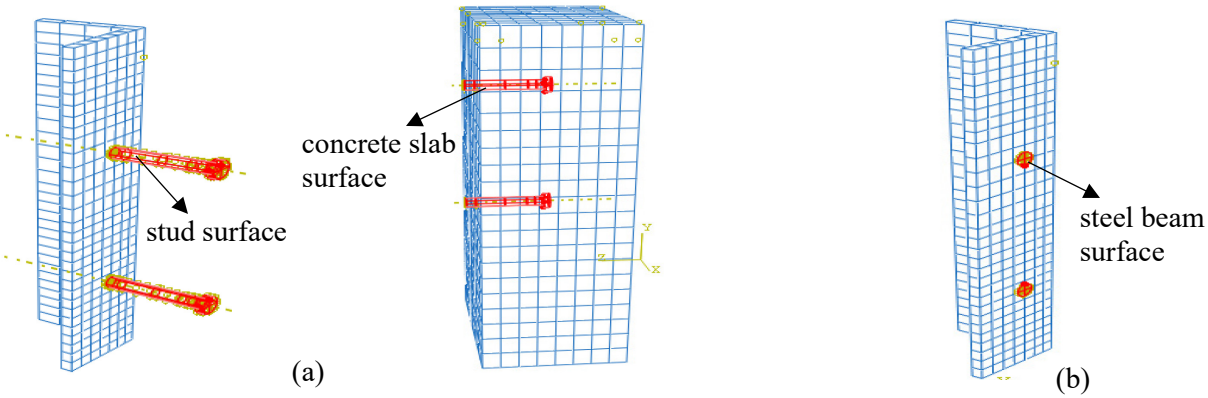

Figure 3.6. Constraints used in FE analysis; (a) surfaces in tie constraint between concrete slab-stud, (b) steel beam surface used in tie constraint with shear stud

To constraint rebar with concrete slab, embedded constraint has been used in which the translational DOF of the nodes on the rebar elements were constrained to the interpolated values of the corresponding DOF of the concrete elements. Absolute tolerance method was used in defining this constraint where a distance has been predefined for constraining the embedded nodes with host elements. For applying load, displacement control procedure has been followed. To do so, MPC constraint has been used between load surfaces (top surface of steel beam) and reference point as shown in Figure 3.7.

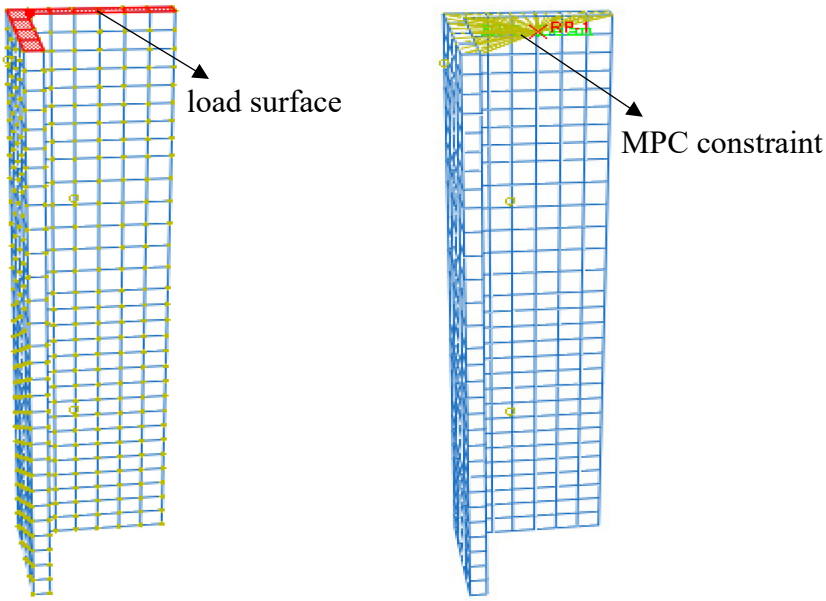

Figure 3.7. MPC constarint between load surface and reference point

3.3.4. Analysis Method

Although, RIKS method was previously used to investigate the behavior of shear connection in push-out test, ABAQUS/Explicit analysis method is used in this study. ABAQUS/Explicit is found more effective than ABAQUS/Standard in many problems such as crack and failure of concrete material. Compared to implicit analysis method, the stiffness matrices need not be inverted, thus, each increment in ABAQUS/Explicit analysis method is relatively inexpensive. The analysis time

of this analysis method can be reduced by using mass scaling or increasing loading rate. Both geometric and material nonlinearities are introduced in the FE analysis.

3.3.5. Load Application

All the nodes lying on the load surface were constrained to reference point 'RP-1' and downward displacement was applied at that reference point till failure. Total step time was fixed based on the ultimate slip criterion i.e. at a slip in which ultimate load is reduced by 10%. As mentioned earlier, downward loading 0.01 mm/sec is found to be the most appropriate loading rate. The loading rate has been decided appropriate on the basis of quasi-static assumption in which the load is applied so slowly that the structure also deforms very slowly as to appear a static condition. It can be noted here that in ABAQUS, an anlaysis can be called quasi-static analysis if the ratio of internal energy (ALLIE) and kinetic energy (ALLKE) is at least 5% or greater which is shown in Figure 3.8.

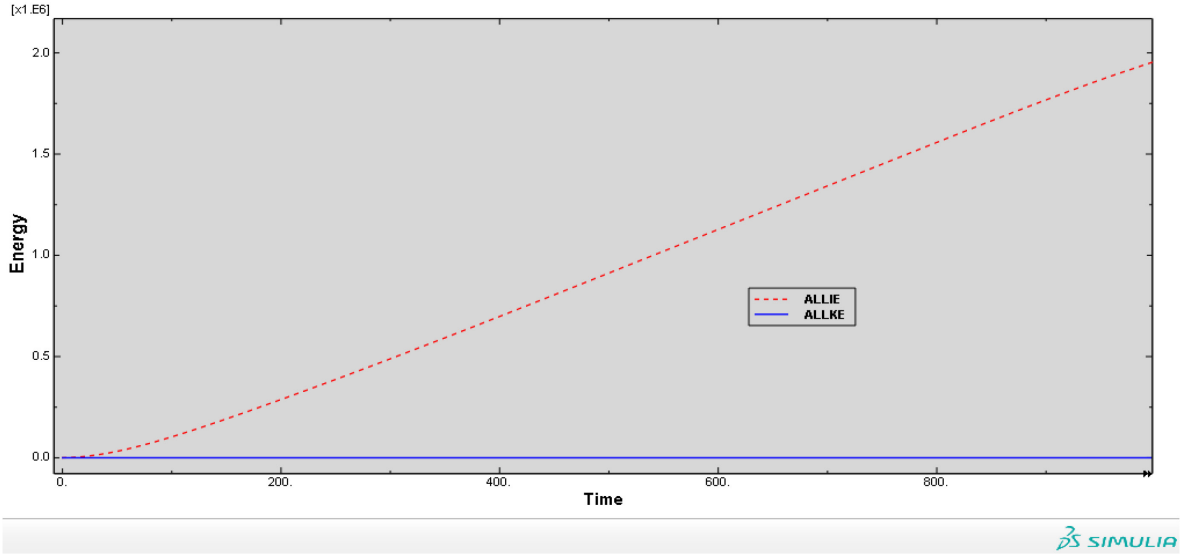

Figure 3.8. Typical Internal and kinetic energy curve for 19 mm shear stud (concrete strength 25 MPa)

3.3.6. FE Mesh

To obtain accurate resuts, a good quality mesh is very important since a coarse mesh reduces the analysis time considerably but the accuracy of results are not acceptable while too fine mesh increases the analysis time. This is why in this thesis work, considerable efforts has been made for proper selection of mesh size.

In order to achieve an accurate results, three dimensional solid elements have been used particularly hexahedrals. Solid elements can be used for linear and nonlinear simulations involving contacts, plasticity successfully. For concrete slab, steel beam and headed shear studs, a three-dimensional eight-node element (C3D8R) was selected to reduce convergance issues. C3D8R is an eight node brick element with reduced integration and each node has three translational degrees of freedom. This element type also prevents mesh locking when material response is incompressible by providing a constant volumetric strain and it is very suitable in case of nonlinearity problems.

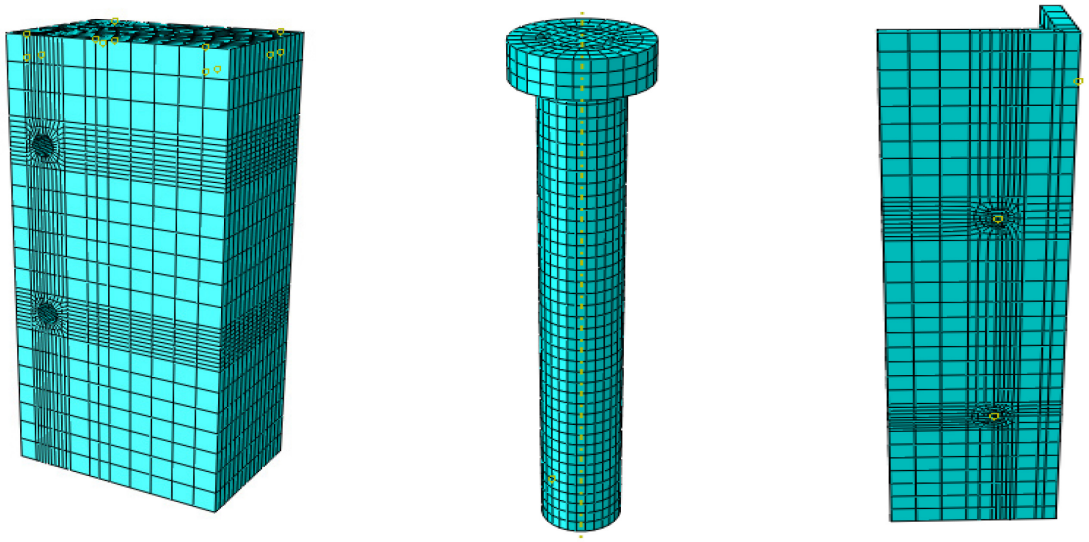

Figure 3.9. FE model mesh used for push-out specimen

T3D2 truss element with linear approximation of displacement was used for rebars and this element has two nodes and three translational degrees of freedom. The mesh size near stud was reduced to get more accurate results since that area is our interst to see the effects of applied displacement. It can be noted here that relative displacement was measured between the nodes on steel beam and concrete slab near the stud. This is another reason to choose finer mesh near the stud.

3.3.7. Material Properties

3.3.7.1. Reinforcement and structural steel meaterial properties

For both structural and reinforcement steel, bi-linear stress-strain relationships have been assumed as shown in Figure 3.10. and in Figure 3.11. which represets a simple elastic-plastic model. Poisson's ratio was taken 0.3 for structural and reinforcement steel material.

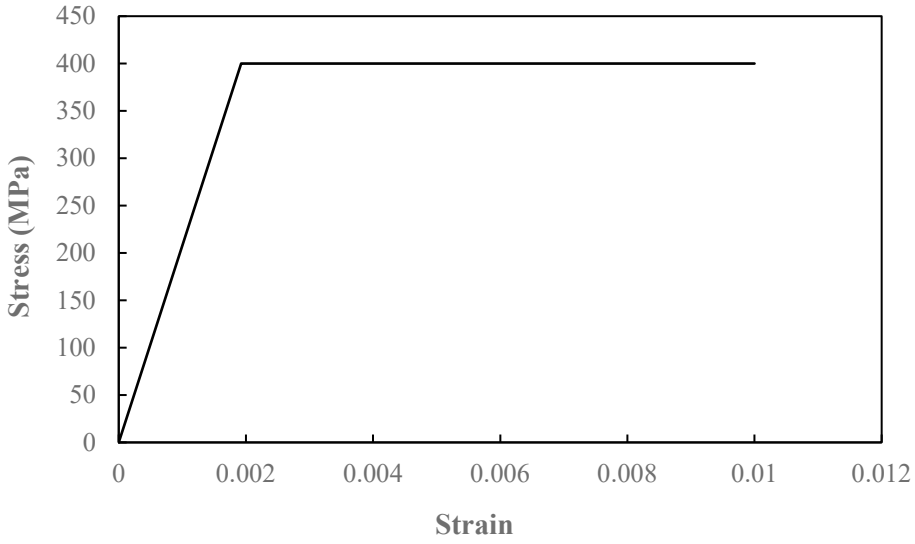

Figure 3.10. Stress-strain relationships for reinforcement steel

The modulus of elasticity and yield strenth used for reinforcement steel are 208000 MPa and 400 MPa while for structural steel are 210000 MPa and 320 MPa respectively.

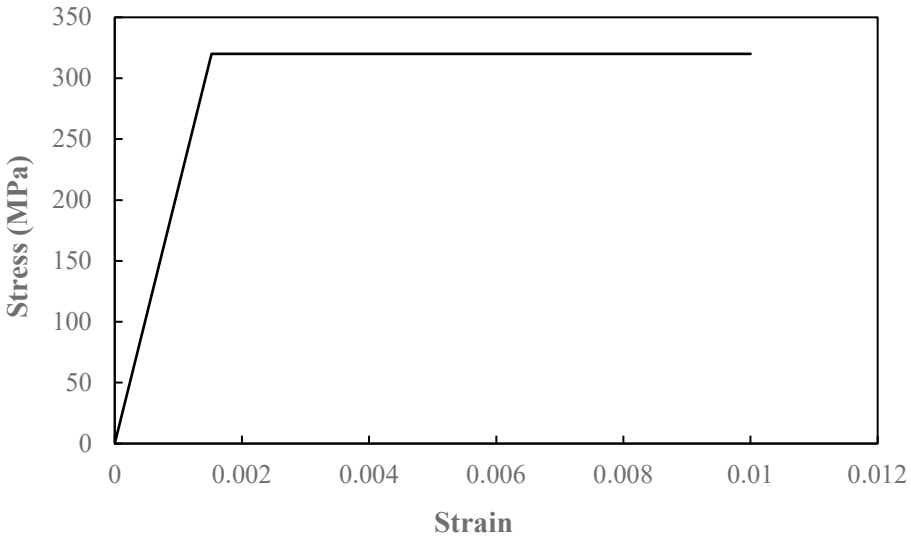

Figure 3.11. Stress-strain relationships for structural steel

3.3.7.2. Headed shear stud material properties

Headed shear stud plays an important role and a key element for push-out FE analysis. As mentioend in Section 3.3.1, two types of headed shear studs are used in order to investigate load-slip characteristics and static strength. Now-a-days 19 mm and 22 mm shear studs are most common in use in steel-concrete composite bridges and any higher diameter of shear studs are called larger studs. In this thesis work, 25 mm, 27 and 30 mm shear studs have been investigated because currently there ae no guidelines in CSA S6-14 for the shear studs greater than 25 mm diameter.

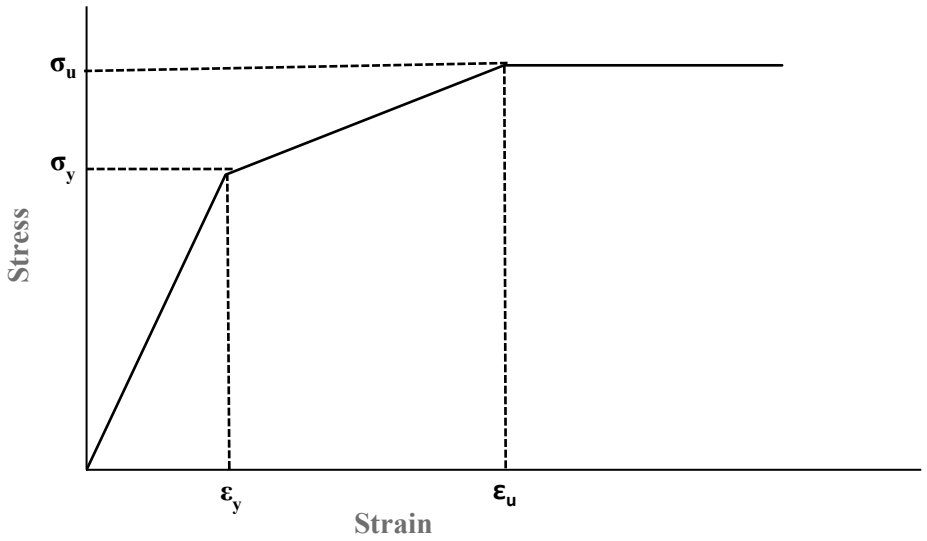

Figure 3.12. Stress-strain relationships for headed shear stud connector

Diameter of stud (mm)	Modulus of elasticity (MPa)	Yield strength σ_y (MPa)	Ultimate strength σ_u (MPa)
19	208000	350	480
22	208000	350	480
25	208000	353	426
27	208000	353	426
30	208000	353	426

Table 3.2. Material properties of headed shear studs used in FE analysis

The material properties for 19 and 22 mm shear studs have been used from tests of Gattesco and Giuriani (1996) and for larger shear studs, the material properties used in the tests of Lee *et al*. (2005) are used in FE analysis as shown in Table 3.2. To achieve exact load-slip relationship, it is very important to use material damage and failure options and in ABAQUS, there are different

types of ductile damage options. In this thesis work, to get appropriate damage and failure options, lot of analyses were performed and use of ductile and shear damage options together give close results to test. Damage initiation criterion and damage evolution responses are defined when specifying ductile damage and shear damage opptions. Damage initiation criterion specifies a fracture strain where the stiffness of the shear stud starts to degrade, and how the shear stud material will degrade, damage evolution describes that. The corresponding fracture strain, stress triaxiality, strain rate, damage evolution were selected based on trial-and-error method to get best aggrement between FE analysis and test results. Poisson's ratio has been taken as 0.3 for shear stud material.

3.3.7.3. Concrete material properties

The nonlinear behavior of the concrete material as shown in Figure 3.13 was used by Nguyen and Kim (2009), which represents uniaxial stress-strain of concrete. In this thesis work, this uniaxial stress-strain curve of concrete has been used with slight modifications. There are three parts in this stress-strain curve. In first part, stress increases linearly up to $0.4 f'_c$. The Young's modulus is calculated based on the following formula as mentioned in CSA A23.3-14 (Clause 8.6.2.3),

$$E_{concrete} = 4500\sqrt{f'_c} \quad (3\text{-}1)$$

where f'_c and $E_{concrete}$ are in MPa. The second part of the curve is an ascending part up to $0.9 f'_c$ where f'_c is the 28-days concrete cylindical compressive strength. The peak stress is used $0.9 f'_c$ as suggested in Clause 10.1.6 of CSA A23.3-14. The strain ε_{c1} related to $0.9 f'_c$ has been taken as 0.0022 and Poisson's ratio has been taken as 0.2 for concrete. The third part of the curve is an descending part up to $r f'_c$, where the value of r is the reduction factor and the value of r has been taken from the study of Ellobody *et al*. (2006) and the ultimate strain ($\alpha\varepsilon_{c1}$) of concrete is used as

0.0035 as suggested by CSA A23.3-14.

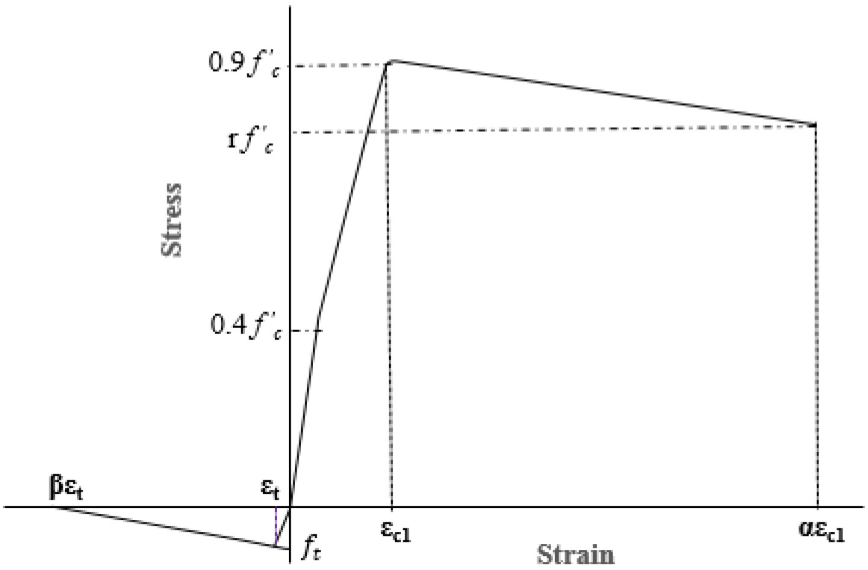

Figure 3.13. Stress-strain relationships for concrete material

For concrete in tension, the tesile stress is assumed to increase linearly till crack and f_t is calculated based on the Clause 8.6.4 of CSA A23.3-14 guldeline which is,

$$f_t = 0.6\sqrt{f'_c} \tag{3-2}$$

where f_t and f'_c are in MPa. After f_t, tensile stress decreases linearly to zero. The strain ($\beta\varepsilon_t$) at zero tensile stress has been taken as 0.005 as used by Nguyen and Kim (2009).

3.4. Preliminary Validation of FE Model

In this section, a preliminary validation of developed FE model with assumed material properties is shown. The results of FE model must be compared with the experiment in order to make it more reliable. Figure 3.14. is the validation of developed FE push-out model for 19 mm shear stud and it has been compared with the test results of Gattesco and Giuriani (1996). In their tests, compressive cube strength of concrete (fcu) was used as 32.5 MPa and thus, compressive cylinder strength of concrete is assumed as 26 MPa (0.8 f_{cu}) in FE analysis.

Stud diameter	19 mm
Overall stud height	125 mm
Stud head diameter	31 mm
Stud head height	9 mm
Yielding tensile stress	350 MPa
Ultimate tensile stress	480 MPa

Table 3.3. Material properties of headed shear stud used in tests of Gattesco and Giuriani (1996)

The ultimate strength from the FE analysis has been found as 108.46 kN, which is very close to test result as can be seen from Figure 3.14. The ultimate slip value was reported 9.70 mm in test of Gattesco and Giuriani (1996) while from FE analysis, it has been found as 9.61 mm. The slip at which the load is reduced by 10% from its peak has been used as ultimate slip as was used in the research work of Lee *et al.* (2005).

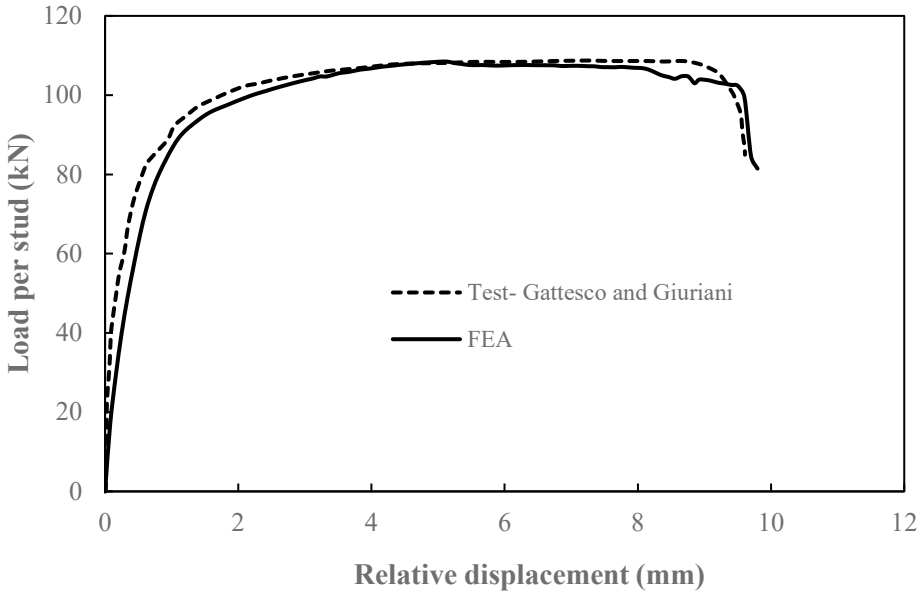

Figure 3.14. Validation of FE push-out model with test results (19 mm shear stud)

Lee *et al*. (2005) performed nine push-out tests on three stud diameters of 25, 27 and 30 mm to investigate experimentally static and fatigue behavior of large shear stud connectors. For each diameter of shear stud, three tests were done. Table 3.4 shows comparison of FE analysis results with the test results. In the tests of Lee *et al*. (2005), the yield and ultimate strength of headed shear stud were 353 MPa and 426 MPa respectively. The yield strength of reinfrocement and structural steel were 400 MPa and 320 MPa respectively. It is important to note here that since three tests were performed for each diameter by them, the average value is used for comparison purpose. From the following Table 3.4 and Figure 3.15, an excellent correlation can be seen between test results and FE analysis for larger shear studs.

Diameter of Stud (mm)	Test Results					FEA Results	
	Specimen	Staic strength (kN)	Average (kN)	Ultimate slip (mm)	Average (mm)	Staic strength (kN)	Ultimate slip (mm)
25	ST25B1	176.4	180.13	6.33	6.79	175.394	8.59
	ST25B2	176.7		6.72			
	ST25B3	187.3		7.31			
27	ST27C1	208.2	211.2	9.19	8.82	208	9.12
	ST27C2	238.5		8.36			
	ST27C3	186.9		8.92			
30	ST30C1	222.8	232.27	9.39	9.36	242.92	10.02
	ST30C2	240.0		9.24			
	ST30C3	234.0		9.46			

Table 3.4. Comparison of FE analysis results with test results of Lee *et al*. (2005)

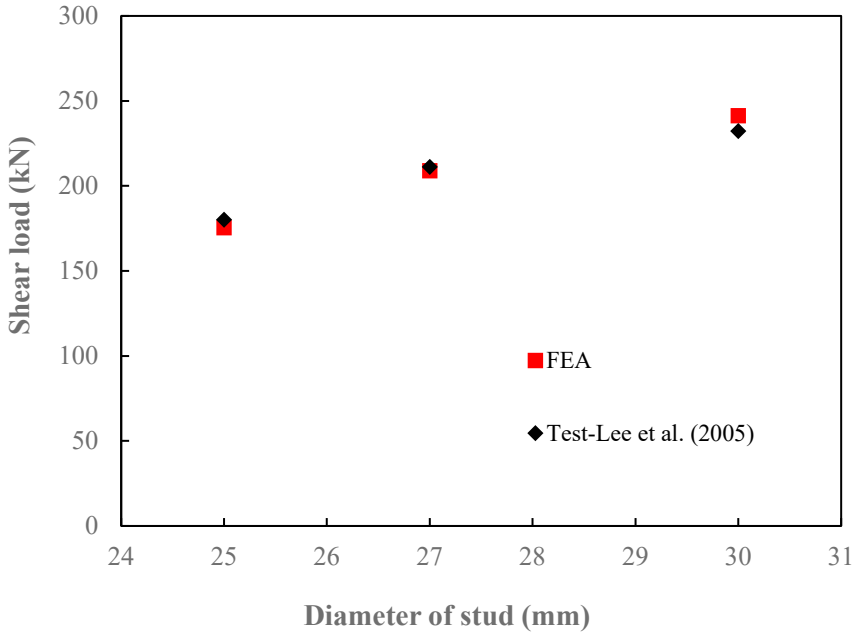

Figure 3.15. Validation of FE push-out model with test results (25,27 and 30 mm shear stud)

3.5. Summary of Chapter

In the finite element analysis of composite push-outt tests, the main component is headed shear stud and ability to model the failure of shear stud would be of primary concern. ABAQUS offers some good choices to model the failure of material. This chapter presents the development of a three-dimensional finite element model using ABAQUS to represent the real push-out test in which both ductile and shear damage of shear stud are used to get accurate load-slip behavior. In the developed finite element (FE) model, both geometric and material nonlinearities were considered and it is validated against test results and an excellent correlation is observed. In addition to failure of shear stud, boundary conditions, mesh, application of loads are also considered to be important factors to obtain good aggrement with test results.

Chapter 4 Load-Slip Characteristics of Headed Shear Stud Connectors

4.1. Introduction

The strength of concrete and diameter of shear stud are the two important factors that influence the load-slip behavior of headed shear studs. The aim of this chapter is to discuss the shear capacity and slip characteristics of both small and larger headed shear studs using the developed FE model. The developed FE model is validated against test results of Gattesco and Giuriani (1996) for smaller shear studs and for larger shear studs, it is validated against test results of Lee *et al.* (2005). The developed FE model is capable of describing slip characteristics and well compared with test results. Section 4.2 presents FE analysis results of shear capacity and ultimate slip variation with concrete strength. An experimental study of Alkhatib (2012) on 22.2 mm headed shear stud reveals an overestimation of shear capacity by CSA S6-14. To investigate this finding further, two smaller shear studs, 19 and 22 mm and three larger shear studs 25, 27 and 30 mm have been analysed and the shear capacities are compared with that predicted by CSA S6-14 and EC 4. This comparison is described in Section 4.3. The failure mode of shear studs found from FE analysis will be presented in Section 4.4. Badie *et al*. (2002) concluded that using alternate headed and headless studs has no harmful effect on slippage but it was recommended to investigate the effects of using only headless studs. To shed more light on this issue, in Section 4.5, headless shear studs of 19, 22 and 25 mm are taken and the shear capacity and slip characteristics are compared with the headed shear studs. Finally, a comparison of previous test results with current code of practices, such as CSA S6-14 and EC4 is shown in Section 4.6.

4.2. Push-out FE Analysis Results

Five different concrete strength 25, 30, 35, 40 and 45 MPa are taken for analysis and the slip at which the load has reduced by 10% from its peak is taken as ultimate slip (Lee *et al*. 2005).

4.2.1. FE analysis results for 19 mm shear stud

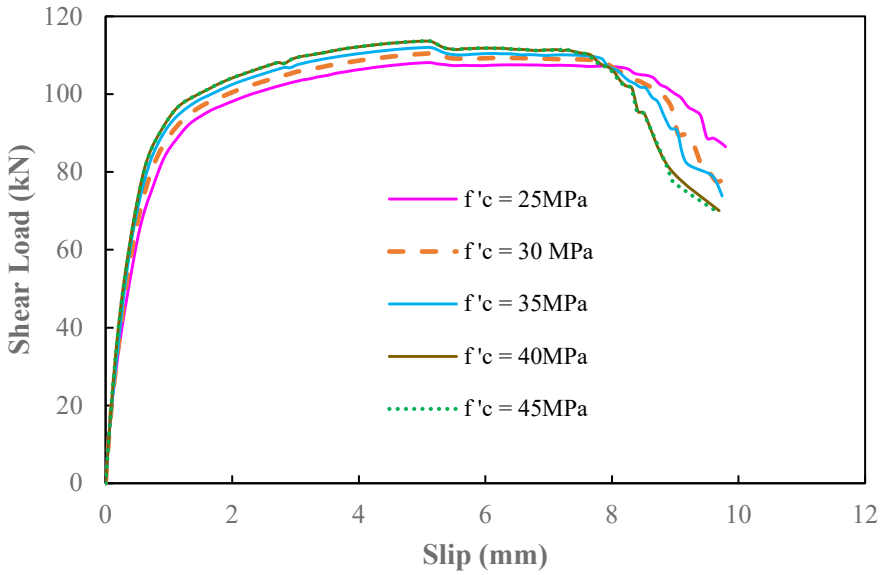

Figure 4.1. Effect of concrete strength on load-slip behavior for 19 mm shear stud

Concrete strength (MPa)	Ultimate slip (mm)	Maximum shear load (kN)	Shear load at ultimate slip (kN)
25	9.18	108.08	97.28
30	8.82	110.44	99.39
35	8.57	111.98	100.78
40	8.21	113.63	102.27
45	8.11	114.84	103.35

Table 4.1. Variation of ultimate slip and load with concrete strength for 19 mm shear stud

4.2.2. FE analysis results for 22 mm shear stud

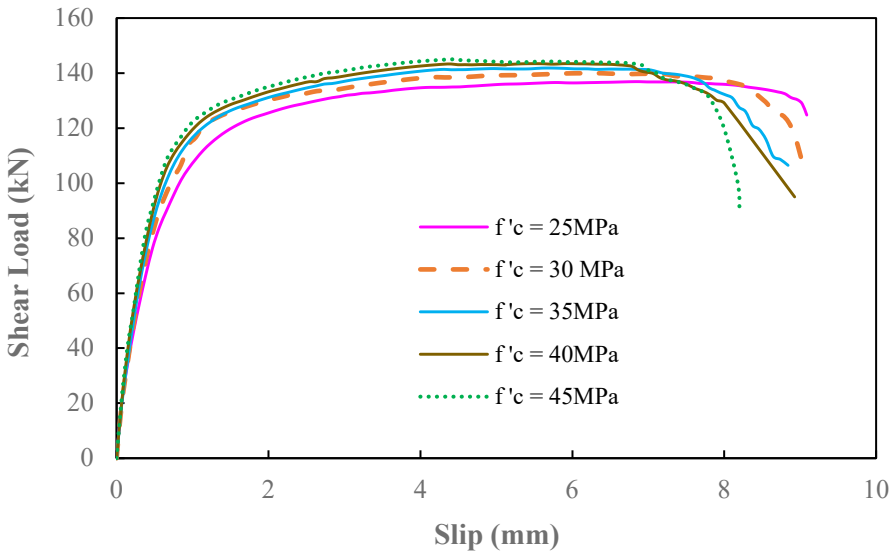

Figure 4.2. Effect of concrete strength on load-slip behavior for 22 mm shear stud

Concrete strength (MPa)	Ultimate slip (mm)	Maximum shear load (kN)	Shear load at ultimate slip (kN)
25	8.81	136.88	123.20
30	8.65	139.94	125.94
35	8.19	141.84	127.65
40	7.99	143.43	129.08
45	7.82	145.00	130.50

Table 4.2. Variation of ultimate slip and load with concrete strength for 22 mm shear stud

4.2.3. FE analysis results for 25 mm shear stud

The ultimate shear load and slip are found higher than 19 and 22 mm which can be seen from Figure 4.3 and Table 4.3.

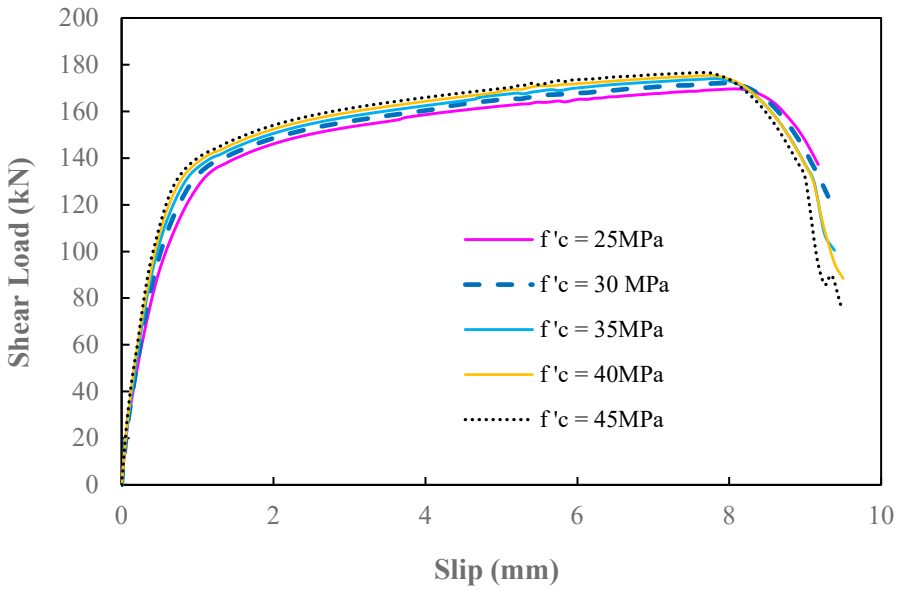

Figure 4.3. Effect of concrete strength on load-slip behavior for 25 mm shear stud

Concrete strength (MPa)	Ultimate slip (mm)	Maximum shear load (kN)	Shear load at ultimate slip (kN)
25	8.89	169.60	152.64
30	8.77	172.09	154.88
35	8.63	173.99	156.59
40	8.59	175.39	157.85
45	8.49	176.63	158.97

Table 4.3. Variation of ultimate slip and load with concrete strength for 25 mm shear stud

4.2.4. FE analysis results for 27 mm shear stud

The following Figure 4.4 shows that the ultimate strength of the connector increases with the increase of concrete strength while the slip decreases. This is because concrete damage plasticity is defined in the developed FE model to account concrete strength effects on static shear strength.

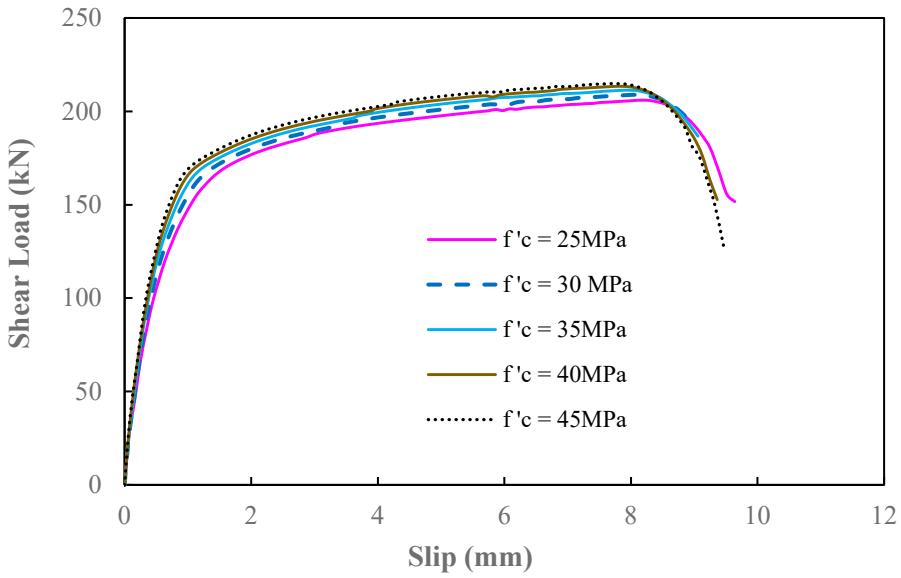

Figure 4.4. Effect of concrete strength on load-slip behavior for 27 mm shear stud

Concrete strength (MPa)	Ultimate slip (mm)	Maximum shear load (kN)	Shear load at ultimate slip (kN)
25	9.16	205.97	185.37
30	9.12	208.88	187.99
35	8.99	211.33	190.20
40	8.87	213.40	192.06
45	8.81	214.88	193.39

Table 4.4. Variation of ultimate slip and load with concrete strength for 27 mm shear stud

4.2.5. FE analysis results for 30 mm shear stud

The ultimate shear load and slip are shown in Figure 4.5 and Table 4.5. It can be noted here that the ultimate strength of 30 mm shear stud for concrete strength 25 MPa is found about 2.21 times

higher than 19 mm headed shear stud. In the research work of Badie *et al*. (2002), the ultimate strength of 31.8 mm was reported almost two times higher than 22.2 mm shear studs for 32 MPa concrete strength demanding less number of studs if larger shear studs are used.

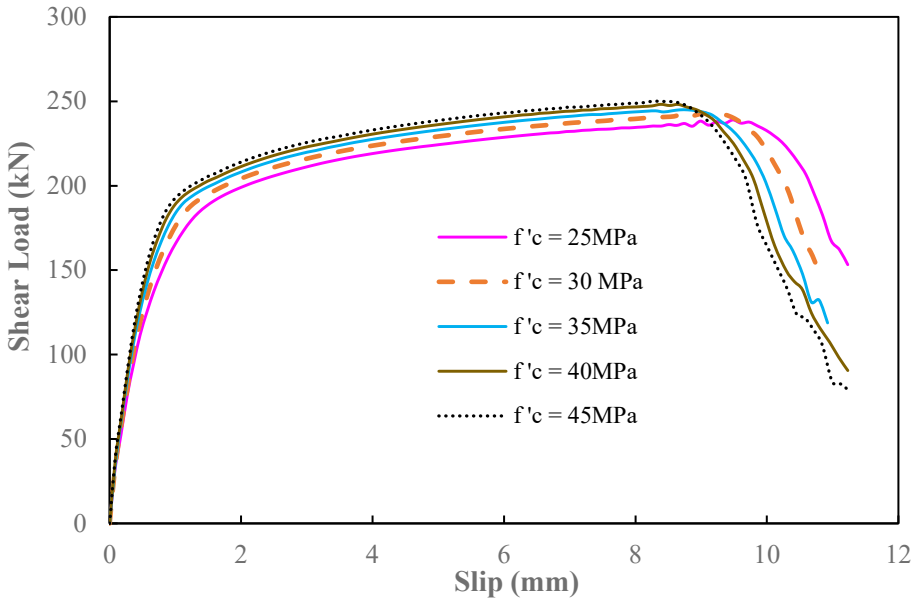

Figure 4.5. Effect of concrete strength on load-slip behavior for 30 mm shear stud

Concrete strength (MPa)	Ultimate slip (mm)	Maximum shear load (kN)	Shear load at ultimate slip (kN)
25	10.44	238.98	215.08
30	10.02	242.92	218.62
35	9.73	244.94	220.45
40	9.52	248.20	223.38
45	9.37	250.08	225.08

Table 4.5. Variation of ultimate slip and load with concrete strength for 30 mm shear stud

4.3. Comparison of FE Analysis Results with CSA S6-14 and EC4

As described in Section 2.3.1, The Canadian Standards Association, CSA S6-14 states that the factored shear resistance, q_r, of a headed stud shear connector shall be taken as lesser of the following equation (2-1),

$$q_r = 0.5\emptyset_{sc}A_{sc}\sqrt{(f'_cE_c)} \leq \emptyset_{sc}F_uA_{sc}$$

According to Eurocode-4, the static strength of shear stud in composite beam should be taken as the lesser of (Equation 2-2 and 2-3);

$$q_r = 0.8f_u(\pi d^2/4)/\gamma_v$$

$$q_r = 0.29\alpha d^2\sqrt{(f_{ck}E_{cm})}\ /\gamma_v$$

4.3.1. FE analysis results for 19 mm shear stud

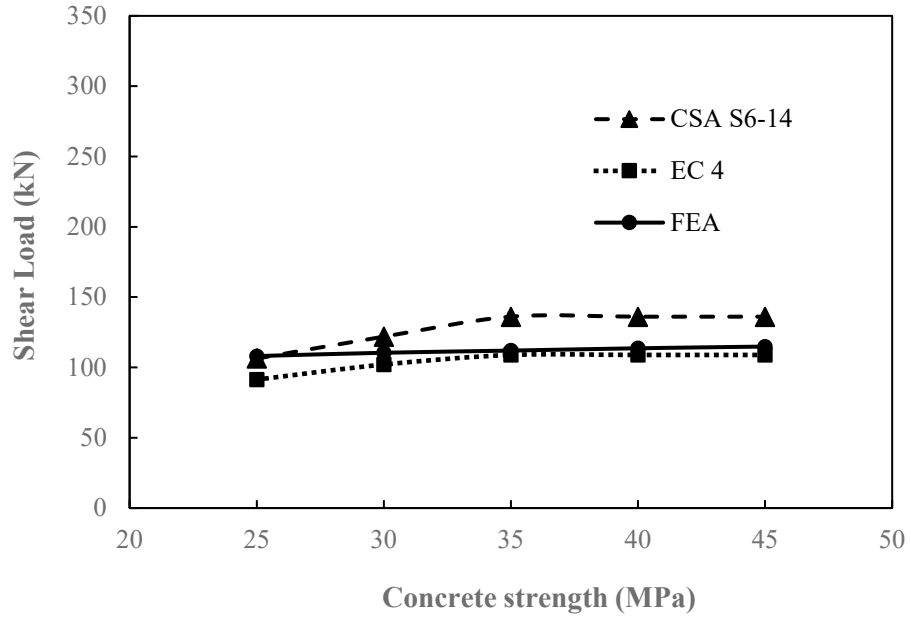

Figure 4.6. Comparison of shear capacity obtained from FE analysis with CSA S6-14 and EC4 for 19 mm headed shear stud

Concrete strength (MPa)	CSA S6-14 (kN)	EC4 (kN)	FEA (kN)	$P_{FEA}/P_{CSA\ S6-14}$	%	P_{FEA}/P_{EC4}	%
25	106.32	91.37	108.08	1.01	1.66	1.18	18.29
30	121.90	102.07	110.44	0.90	9.40	1.08	8.19
35	136.09	108.87	111.98	0.82	17.71	1.02	2.85
40	136.09	108.873	113.63	0.83	16.50	1.04	4.37
45	136.09	108.87	114.84	0.84	15.61	1.05	5.48

Table 4.6. Comparison of shear capacity obtained from FE analysis with CSA S6-14 and EC4 for 19 mm shear stud

4.3.2. FE analysis results for 22 mm shear stud

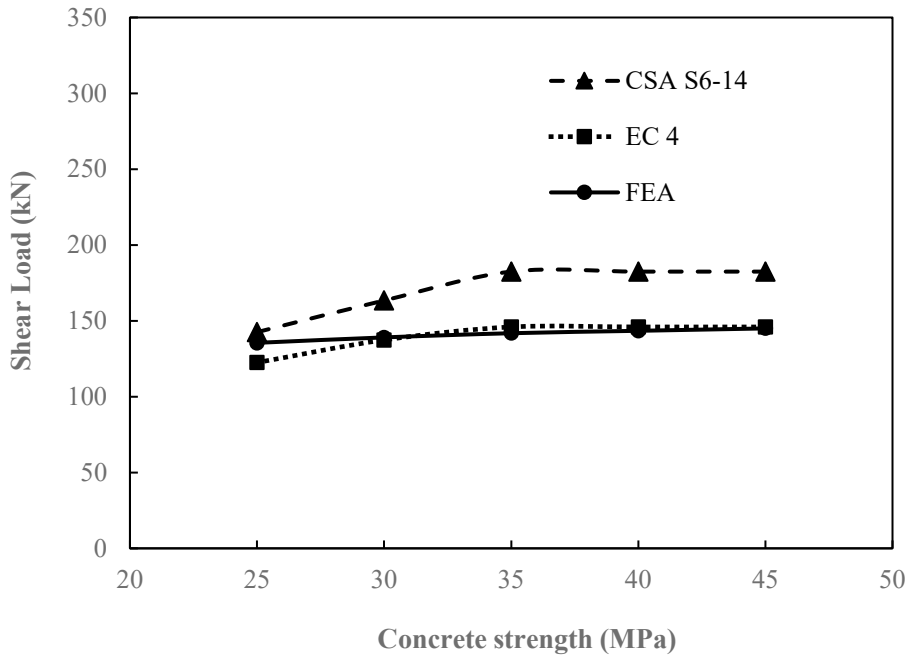

Figure 4.7. Comparison of shear capacity obtained from FE analysis with CSA S6-14 and EC4 for 22 mm headed shear stud

Concrete strength (MPa)	CSA S6-14 (kN)	EC4 (kN)	FEA (kN)	$P_{FEA}/P_{CSA\ S6-14}$	%	P_{FEA}/P_{EC4}	%
25	142.55	122.50	135.49	0.95	4.94	1.10	10.60
30	163.43	137.39	139.08	0.85	14.90	1.01	1.23
35	182.46	145.97	141.84	0.77	22.26	0.97	2.82
40	182.46	145.97	143.43	0.78	21.39	0.98	1.74
45	182.46	145.97	145.00	0.79	20.52	0.99	0.65

Table 4.7. Comparison of shear capacity obtained from FE analysis with CSA S6-14 and EC4 for 22 mm shear stud

4.3.3. FE analysis results for 25 mm shear stud

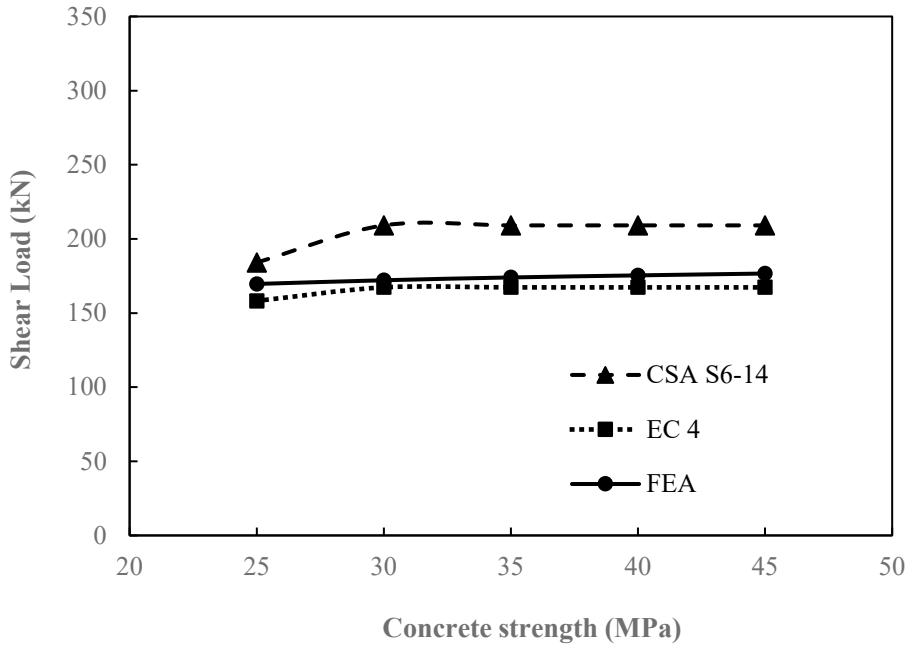

Figure 4.8. Comparison of shear capacity obtained from FE analysis with CSA S6-14 and EC4 for 25 mm headed shear stud

Concrete strength (MPa)	CSA S6-14 (kN)	EC4 (kN)	FEA (kN)	$P_{FEA}/P_{CSA\ S6-14}$	%	P_{FEA}/P_{EC4}	%
25	184.07	158.19	169.60	0.92	7.86	1.07	7.21
30	209.11	167.292	172.09	0.82	17.70	1.02	2.87
35	209.11	167.29	173.99	0.83	16.79	1.04	4.00
40	209.11	167.29	175.39	0.83	16.12	1.04	4.84
45	209.11	167.29	176.63	0.84	15.53	1.05	5.58

Table 4.8. Comparison of shear capacity obtained from FE analysis with CSA S6-14 and EC4 for 25 mm shear stud

4.3.4. FE analysis results for 27 mm shear stud

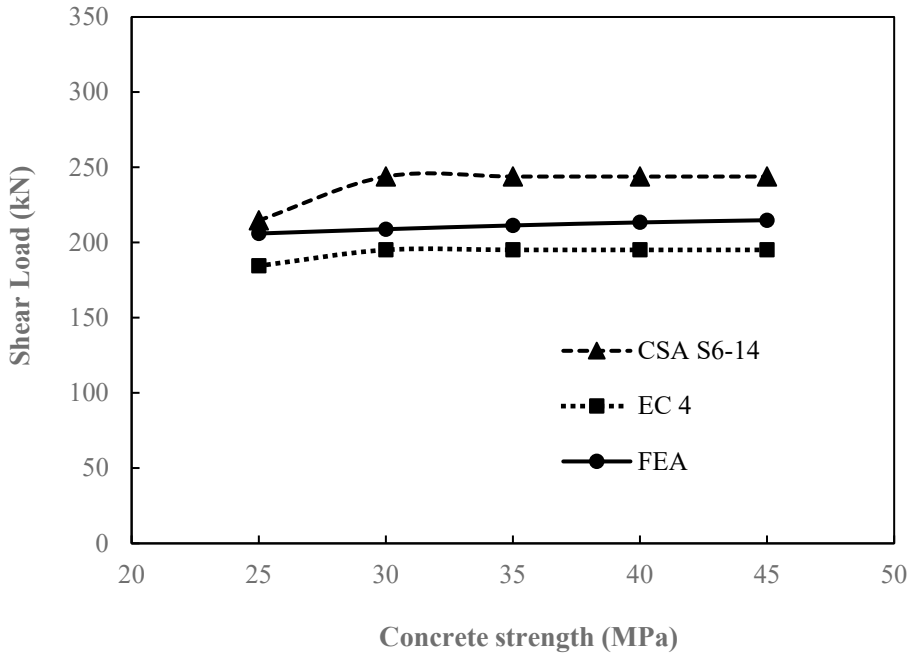

Figure 4.9. Comparison of shear capacity obtained from FE analysis with CSA S6-14 and EC4 for 27 mm headed shear stud

Concrete strength (MPa)	CSA S6-14 (kN)	EC4 (kN)	FEA (kN)	$P_{FEA}/P_{CSA\ S6-14}$	%	P_{FEA}/P_{EC4}	%
25	214.70	184.51	205.97	0.95	4.06	1.11	11.62
30	243.90	195.12	208.89	0.85	14.35	1.07	7.05
35	243.90	195.12	211.40	0.86	13.32	1.08	8.33
40	243.90	195.12	213.40	0.87	12.50	1.09	9.36
45	243.90	195.12	214.88	0.88	11.90	1.10	10.12

Table 4.9. Comparison of shear capacity obtained from FE analysis with CSA S6-14 and EC4 for 27 mm shear stud

4.3.5. FE analysis results for 30 mm shear stud

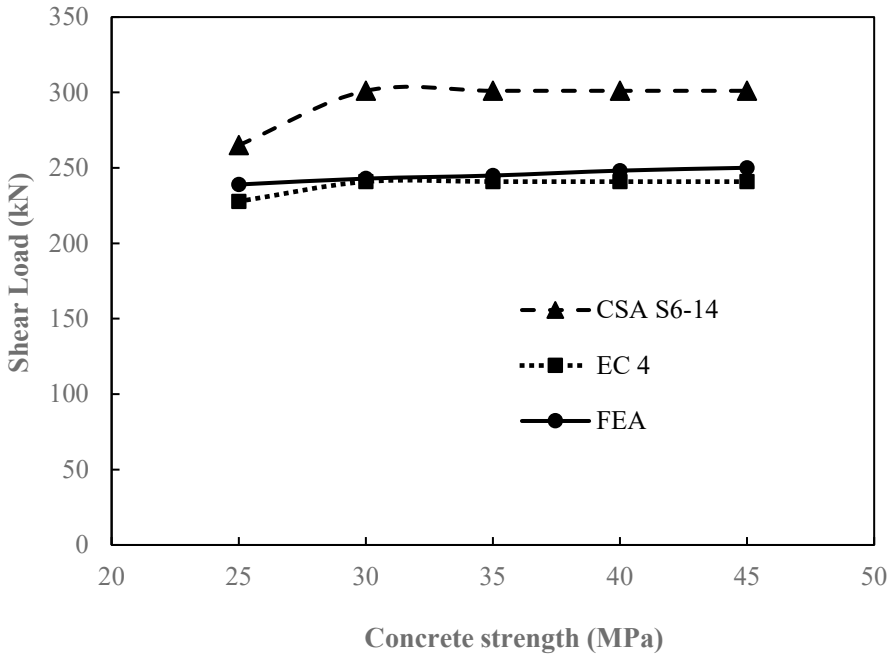

Figure 4.10. Comparison of shear capacity obtained from FE analysis with CSA S6-14 and EC4 for 30 mm headed shear stud

Concrete strength (MPa)	CSA S6-14 (kN)	EC4 (kN)	FEA (kN)	$P_{FEA}/P_{CSA\ S6-14}$	%	P_{FEA}/P_{EC4}	%
25	265.07	227.80	238.98	0.90	9.84	1.04	4.90
30	301.12	240.89	242.92	0.80	19.32	1.00	0.83
35	301.12	240.89	244.94	0.81	18.65	1.01	1.68
40	301.12	240.89	248.20	0.82	17.57	1.03	3.03
45	301.12	240.89	250.08	0.83	16.94	1.03	3.81

Table 4.10. Comparison of shear capacity obtained from FE analysis with CSA S6-14 and EC4 for 30 mm shear stud

4.4. Failure Modes

In the test of Lee *et al*. (2005), shank failure mode was reported for all stud diameters, such as 25, 27 and 30 mm which is also found from the FE analysis as shown in Figure 4.11. It can be noted here that for smaller shear studs, such as 19 mm, same type of failure mode was observed in the test of Gattesco and Giuriani (1996).

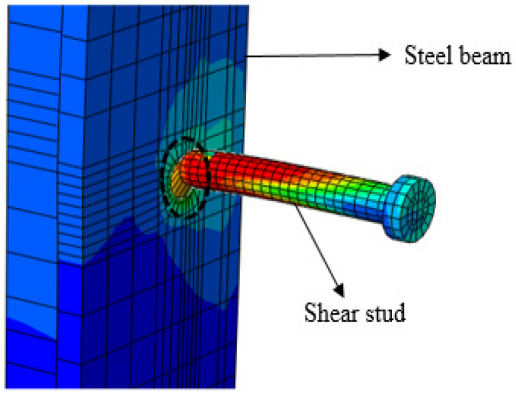

Figure 4.11: Shank failure mode

4.5. Headless Shear Stud

To investigate the shear capacity of headless shear stud, two smaller studs 19 and 22 mm and one large shear stud 25 mm are taken. The yield and ultimate strength of both headed and headless shear studs were 353 MPa and 426 MPa respectively. The headless shear stud and headed shear stud used in FEA are shown in Figure 4.12.

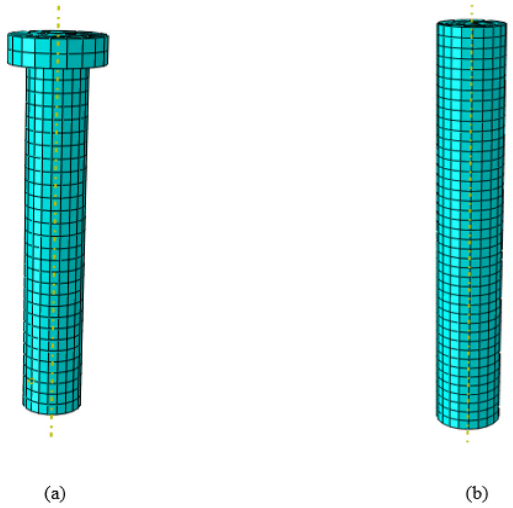

Figure 4.12: (a) Headed shear stud, (b) Headless shear stud

The comparison of shear capacity between headless and headed shear studs are presented in the following Figures and Tables.

Shear Stud Types	Ultimate slip (mm)	Maximum shear load (kN)
Headless	5.24	74.46
Headed	9.60	108.45

Table 4.11. Comparison of shear capacity with headless and headed shear stud (19 mm diameter)

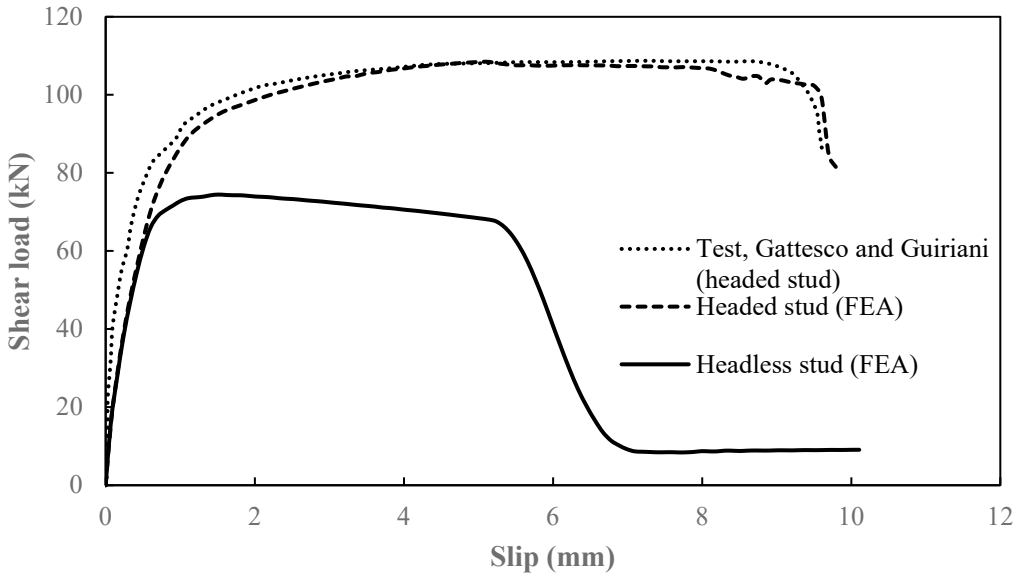

Figure 4.13. Comparison of shear capacity of headless shear stud with headed shear stud obtained from FE analysis (19 mm diameter)

From the Figure 4.13 and Table 4.11, it can be seen that the ultimate capacity of headless shear stud is very low compared to headed stud, by almost 1.46 times. Badie *et al.* (2002) attained a 17% higher load in a specimen having fully headed shear studs compared to the specimen containing alternate headed and headless shear studs. The ultimate slip for headed stud is 9.60 mm while for headless stud is only 5.24 mm. The similar trend is found for 22 and 25 shear stud also which are shown in Figure 4.14 and Figure 4.15.

Shear Stud Types	Ultimate slip (mm)	Maximum shear load (kN)
Headless	4.85	96.62
Headed	9.24	136.88

Table 4.12. Comparison of shear capacity with headless and headed shear stud (22 mm diameter)

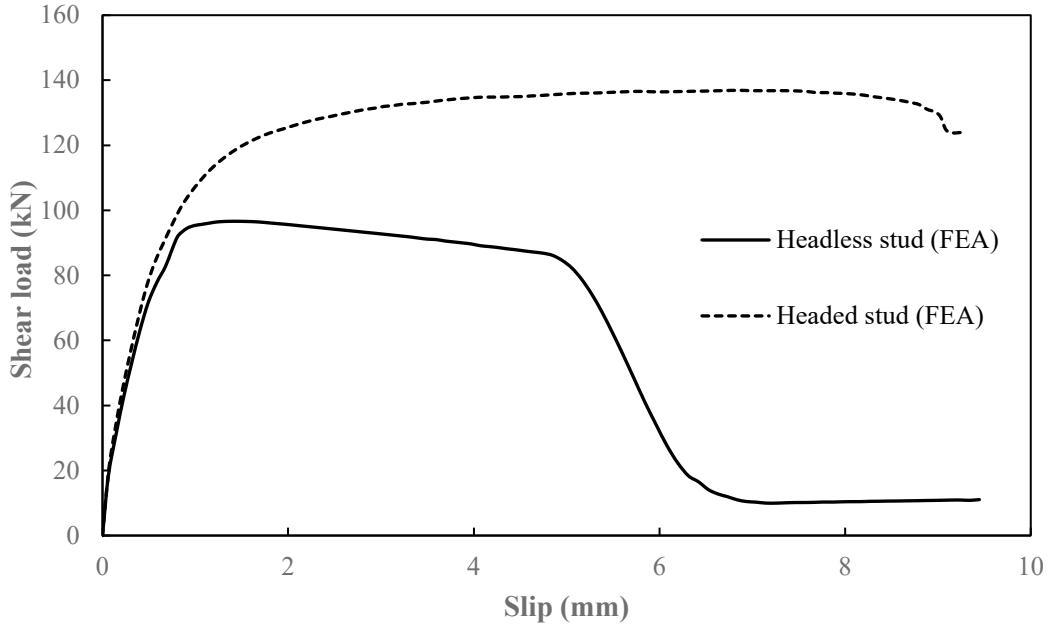

Figure 4.14. Comparison of shear capacity of headless shear stud with headed shear stud obtained from FE analysis (22 mm diameter)

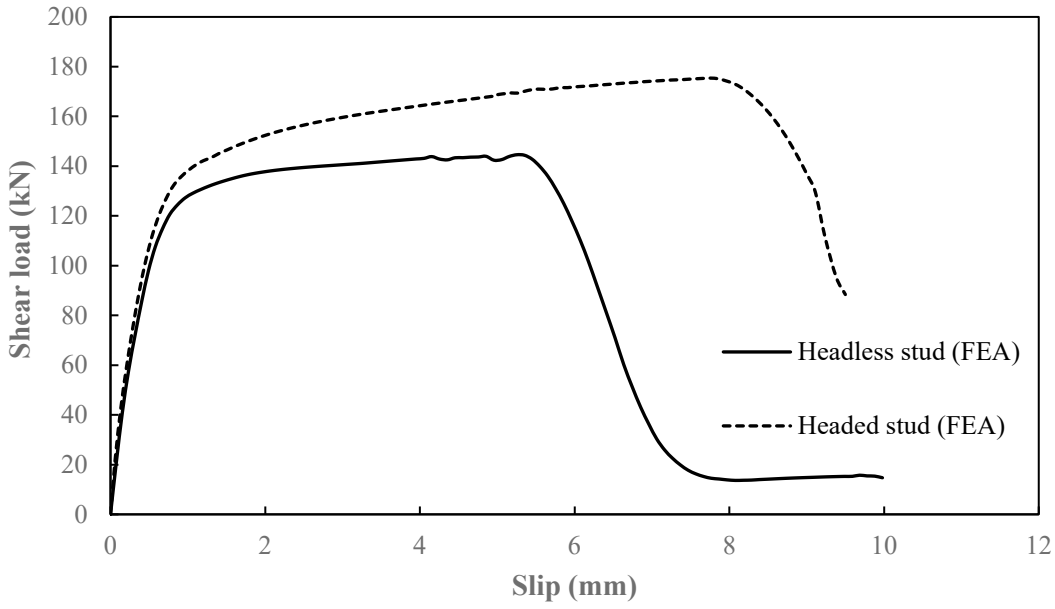

Figure 4.15. Comparison of shear capacity of headless shear stud with headed shear stud obtained from FE analysis (25 mm diameter)

Shear Stud Types	Ultimate slip (mm)	Maximum shear load (kN)
Headless	5.76	144.53
Headed	8.59	175.39

Table 4.13. Comparison of shear capacity with headless and headed shear stud (25 mm diameter)

4.6. Comparison of Previous Test Results with CSA S6-14 and EC4

From tables 4.6 - 4.10, it is observed that Canadian standard, CSA S6-14 generally overestimates the shear capacity of headed shear studs. The overestimation increases with the increase of concrete strength. Thus, for 19 mm shear stud diameter, as observed in Table 4.6, Canadian standard, S6-14 overestimates the shear strength as much as 17.7% when 35 MPa concrete is used. In addition, EC 4 ususally underestimates the shear capacities of the shear studs. For 19 mm dia shear stud, the underestimation is up to 18.3%, but for larger shear studs Equations 2-2 and 2-3 proposed in EC 4 are found to provide very close estimations when compared to the strengths obtained from FE analysis. To verify this issue, a comparison with previous test works on headed shear studs to investigate static strength using push-out specimen with CSA S6-14 and EC4 is shown in the following Table 4.14 and Figure 4.16.

Test Details	Dia of stud (mm)	Concrete Strength (MPa)	Height of Stud (mm)	Static Strength		
				CSA S6-14 (kN)	EC4 (kN)	Test (kN)
Hallam (1976)	19	48.2	76	119.36	95.49	151.20
Hallam (1976)	19	46.5	76	119.36	95.49	149

Hallam (1976)	19	28.1	76	116.06	95.49	116
Hallam (1976)	19	18.2	76	83.79	75.02	96
Hallam (1976)	19	24.2	76	103.76	89.53	107
Oehlers (1987)	22.2	45	155	185.21	148.17	146.75
Jayas (1987)	16	29.8	76	86.01	72.36	90.1
Oehlers (1990)	12.7	48.37	75	58.01	46.41	54.7
An and Cederwall (1994)	19	30.77	75	124.24	103.03	115
An and Cederwall (1994)	19	31.79	75	127.31	105.18	119.1
An and Cederwall (1994)	19	86.11	75	147.15	117.72	156.8
An and Cederwall (1994)	19	81.26	75	147.15	117.72	158.6
An and Cederwall (1994)	19	91.24	75	147.15	117.72	161
Gattesco and Giuriani (1996)	19	26	125	109.49	93.64	108.8
Badie et al. (2002)	22	32	155	129.24	103.39	127.2
Badie et al. (2002)	31.8	32	139.7	349.45	279.56	349
Loh et al. (2003)	19	26.2	125	110.12	94.09	101
Shim et al. (2004)	25	33.2	155	209.11	167.28	156.03
Shim et al. (2004)	25	45.3	155	209.11	167.28	180.1
Shim et al. (2004)	27	33.2	155	243.90	195.12	186.27
Shim et al. (2004)	27	53	155	243.90	195.12	211.2
Shim et al. (2004)	30	33.2	155	301.12	240.89	175.37
Shim et al. (2004)	30	53	156	301.12	240.89	232.27
Topkaya et al. (2004)	19	30.46	127	123.30	101.61	93.4
Hanswille et al. (2006)	22	43	125	200.71	160.56	181
Hanswille et al. (2006)	22	46	125	200.71	160.56	196
Xue et al. (2008)	13	50	65	58.98	47.18	73.87
Xue et al. (2008)	16	50	85	89.35	71.48	82.45
Xue et al. (2008)	16	30	85	86.44	71.48	77.15
Xue et al. (2008)	19	50	103	126.00	100.80	110.98
Xue et al. (2008)	19	30	103	121.90	100.80	100.49
Alkhatib (2012)	22.2	45	155	185.21	148.17	192.25

Table 4.14: Comparison of static strength from previous test works with CSA S6-14 and EC4

Figure 4.16 shows that CSA S6-14 usually overestimates static strength while EC4 gives a good prediction except some cases. For larger shear studs, the difference is much higher when compared with the test results with CSA S6-14. However, more experimental studies are required.

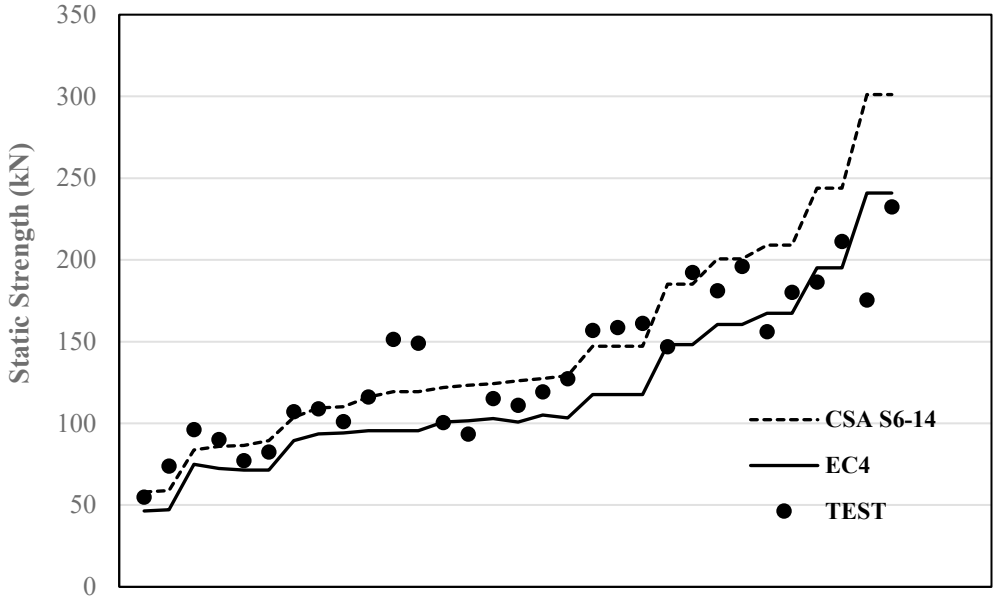

Figure 4.16: Comparison of static strength from previous test works with CSA S6-14 and EC4

4.7. Summary of Chapter

This chapter has presented the finite element analysis results of load-slip behavior for both standard and larger headed shear stud connector. To investigate the effect of concrete strength on load-slip behavior, five different concrete strengths have been taken. The results show that shear capacity increases with the increase in concrete strength but ultimate slip decreases. Concrete damage plasticity is defined in the FE model. So, with the increase in concrete strength, relative displacement between concrete slab and steel beam nodes around the stud decreases. Five different shear studs such as 19, 22, 25, 27 and 30 mm have been used to investigate the effect of stud

diameter on shear capacity of shear studs. It was found that with the increase of stud diameter, shear capacity and ultimate slip increases for a specified concrete strength. In the test of Lee *et al*. (2005) and Gattesco and Giuriani (1996), shank failure mode was reported. Similar failure mode has been observed for both standard and larger headed shear studs from finite element analysis. When FE analysis results were compared with current code of practices, Canadian Standard, CSA S6-14 is found to overestimate shear capacity of shear studs up to 22.3% while the European code, EC-4 usually gives conservative estimation. The overestimation by CSA S6-14 increases with the increase of stud diameter while EC-4 gives close estimation for larger shear studs. Thus, before more experimental and numerical study on larger shear studs are done, it might be safe to use European code EC-4 for predicting static shear capacity of larger headed shear stud connector.

Chapter 5 Fatigue Life Prediction Using Finite Element Analysis

5.1. Introduction

One of the major drawbacks of headed shear stud connectors is that they are very sensitive to fatigue and thus, care must be taken if used in fatigue prone sites. Repeated or fluctuating stress can initiate micro-cracks in materials which may propagate with the continued application of cyclic stress. This process is known as fatigue and the fatigue problem of shear studs has been paid a great attention in recent years. Fatigue failure can be dangerous since it occurs suddenly without significant prior deformations. The fatigue resistance of headed shear stud is best determined through testing which is very expensive and time consuming. It is often impractical, or sometimes impossible, to test full size structural components. As a result, analytical prediction models are often required as an alternative means. This chapter presents an approach for predicting fatigue life of shear stud using the developed FE push-out model discussed in Chapter 3 with slight modifications. Section 5.2 discusses the modifications in FE push-out model and material properties of headed shear studs. The approach for calculating fatigue crack initiation and crack propagation life will be discussed in Section 5.3. Validation of the developed FE approach is presented in Section 5.4. Section 5.5 will present comparison of test and FEA results with current code of practices, such as CSA S6-14, AASHTO LRFD, EC4, BS 5400. A parametric study to investigate effects of different parameters, such as concrete strength, stud spacing, slab thickness on fatigue life of headed shear studs are discussed in Section 5.6. Currently, there are no guidelines in CSA S6-14 about shear stud subjected to tensile loading. Shear stud is subjected to tension, especially in finger plate expansion joints, when vehicles are passed. The developed finite element based approach is used for fatigue life estimation of shear studs in tensile loading in Section 5.7.

5.2. Modifications in FE Model

Figure 5.1 shows two common fatigue failure modes, Mode A, in which crack initiates at the top of the weld collar and then propagates along the stud-weld interface; in Mode B, the crack initiates at the base of the weld collar and propagtes untill it reaches to the base of the weld collar again through the joist material. In the test of Lee et al. (2005), Mode B was reported which has been used in this thesis work.

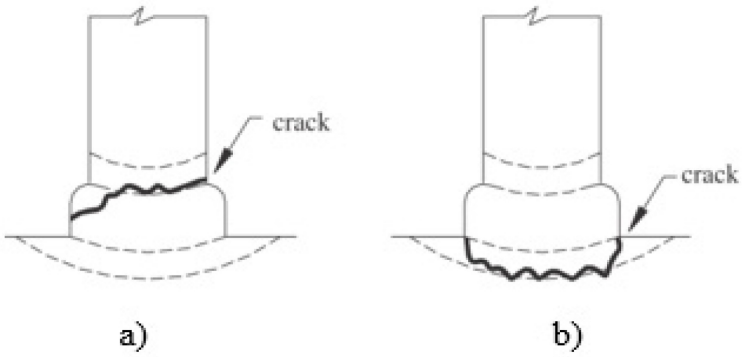

Figure 5.1. Fatigue failure mode; a) Mode A, b) Mode B (Lee *et al*. 2005)

Since fatigue failure mode B, most common in practical, is considered in this paper, welding of the shear stud is modeled with weld having weld collar height of 7 mm and weld base diameter of 31 mm. Figure 5.2 shows the dimensions of shear stud used in FE analysis. Arc stud welding which joins a base metal, such as steel, to a connector is followed generally for stud welding. It is done by a controlled electric arc process which melts the end of the stud connector to the base metal. The yield and ultimate strength of headed shear stud were 353 MPa and 426 MPa respectively as used in the test of Lee *et al*. (2005). The nonlinear plastic behavior of shear stud is introduced in FE model using a multi-linear isotropic hardening model and Ramberg-Osgood parameters, k' and n' as shown in Equation 5-1. The value of k' and n' has been collected from the structural engineering report of Josi and Grondin (2010).

$$\varepsilon = \frac{\sigma}{E} + \left(\frac{\sigma}{k'}\right)^{n'} \quad (5\text{-}1)$$

where k' and n' are 727 MPa and 0.15 respectively.

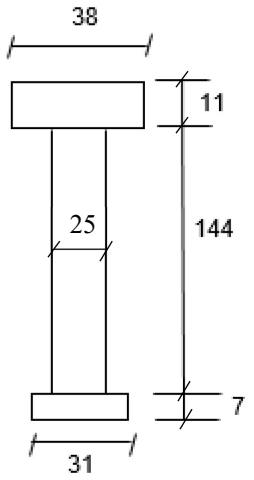

Figure 5.2. Dimensions of shear stud used in FE analysis

For both structural and reinforcement steel, bi-linear stress-strain relationships have been assumed representing a simple elastic-plastic model. Poisson's ratio is taken as 0.3 for both structural and reinforcement steel material. The yield strength of reinforcement steel and structural steel was 400 and 320 MPa respectively. The uniaxial stress-strain behavior of concrete described in Chapter 3 is also used here and concrete damage plasticity is defined in the FE model.

5.3. Prediction of Fatigue Life

The number of cycles a material can sustain before failure is known as fatigue life. The total fatigue life is the sum of crack initiation life and crack propagation life. The approach for the prediction of total fatigue life is described below.

5.3.1. Crack Initiation Life

Lee *et al.* (2005) tested 12 specimens for fatigue life investigation on three different stud diameters: 25, 27 and 30 mm. In this research work, five specimens of 25 mm diameter and two specimens of 27 mm shear stud have been investigated and an approach for fatigue life prediction of shear stud using push-out specimen has been proposed. The maximum and minimum load and stress ranges from the experimental program are shown in the following Table 5.1.

Specimen	Concrete Strength (MPa)	Maximum Load (kN)	Minimum Load (kN)	Stress Range (MPa)
FT25A2	30	73.6	0	150
FT25A3	30	83.4	0	170
FT25B1	40	63.8	0	130
FT25B2	40	73.6	0	150
FT25B3	40	87	0	177.3
FT27A1	30	73.5	0	128.4
FT27A2	30	85.9	0	150

Table 5.1. Load and stress ranges used in FE analysis (Lee *et al.* 2005)

ABAQUS dynamic explicit formulation is adopted for the analysis in this study. ABAQUS explicit formulaiton is popularly used for problems of impact, progressive damage and failure of material (Nguyen and Kim 2009). It has been applied in many problems such as crack and failure of concrete material. Dynamic explicit is a time control method since the stiffness matrices need not be inverted resulting relatively inexpensive increment compared to implicit analysis. It is important to note here that crack is not explicitely modeled in the FE model. Rather, the key factor assumed is that crack will generate in highly stressed area. The location of highly stressed area can be

identified from FE analysis. In the first time step, the model is fully loaded to maximum load. The load is then reduced to minimum load in the second time step, and finally it is reloaded to maximum load again in time step 3. After time step 2 and 3, the nominal strains in the X direction are recorded from the output file and the maximum nominal stress in X direction in time step 3 is also recorded. The critical location of push-out specimen was reported at the base of the weld collar (Lee *et al*. 2005) which can also be seen from Figure 5.3. Once strain and maximum stress at critical location are obtained, crack initiation life is calculated using Equation 5-2. The crack initiation properties are collected from the report of Josi and Grondin (2010).

$$\frac{\Delta\varepsilon}{2} = \frac{(\sigma'_f)^2}{\sigma_{max}E}(N_{init})^{2b} + \frac{\sigma'_f\,\varepsilon'_f}{\sigma_{max}}(N_{init})^{b+c} \tag{5-2}$$

where $\frac{\Delta\varepsilon}{2}$ is the strain range, σ_{max} is the maximum local stress accounting for plasticity, E is the modulus of elasticity, σ'_f is fatigue strength coefficient, ε'_f is fatigue ductility coefficient, b and c are fatigue strength exponent and fatigue ductility exponent respectively and N_{init} is the crack initiation life.

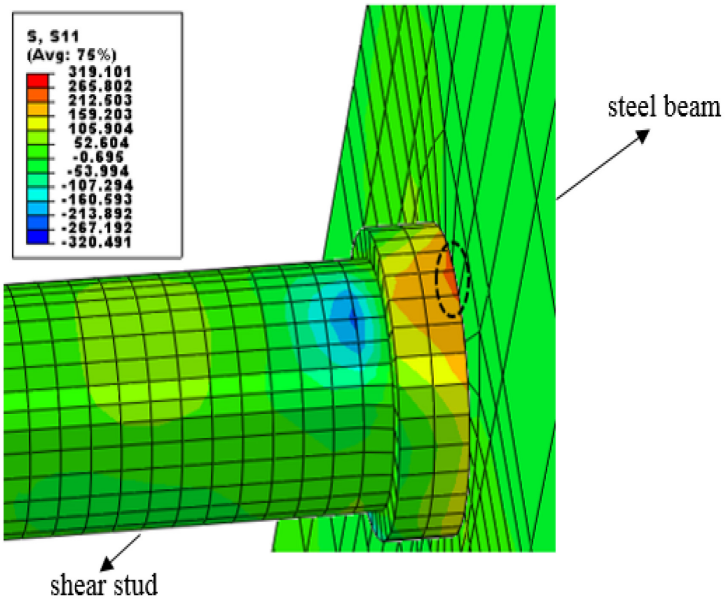

Figure 5.3. Critical location of shear stud at the base of weld collar

5.3.2. Crack Propagation Life

As soon as the crack is initiated, the crack front grows more and more until failure occurs. As described in Section 2.4.2.2, if the stress intensity factor is less than a certain value, then crack is not propagated known as threshold stress intensity factor range, ΔK_{th} (Dowling 2007). The following Equation 5-3 has been used to determine crack propagation life,

$$N_{prop} = \int_{a_o}^{a_f} \frac{da}{C\,(\Delta K^{\,m} - \Delta K_{th}{}^{m})} \tag{5-3}$$

where a_o and a_f are the initial and final crack size respectively. It is very important to note that as per guidelines of ASTM standard E647 (ASTM 2000), ΔK can be taken as $\Delta K = K_{max}$ if only tension portion of stress cycles are considered.

5.3.2.1. Initial and Final Crack Size

The distinction between crack initiation and crack propagation life is not easy to define. The approximate initial crack size is normally taken as engineering crack size which is visible to naked eye and normally 1 to 5 mm (Chen et al. 2005). If the crack size is too small, then small crack effects may need to be considered and linear elastic fracture mechanics (LEFM) method may not apply (Ellyin 1997). The initial crack size was assumed from 0.1 to 1 mm in the finite element analysis works on a steel plate (Josi and Grondin 2010). In this research work, different initial crack sizes were tried varying from 0.1 to 1 mm and found that initial crack size has a significant effect on fatigue life. Initial crack size of 1 mm was found to give a good correlation with test results.

As stated earlier, in fatigue failure mode B, the crack initiates at the base of the weld collar and propagates until it reaches to the base of the weld collar again through the joist material. As a

result, final crack size 31 mm, diameter of base of the weld collar, is taken which gives excellent correlation with the test results. It is important to note here that varying the final crack size doesn't change the total fatigue life too much and it is found that the effects of final crack size in total fatigue life prediction is insignificant.

5.3.2.2 Stress Intensity Factor

In fracture mechanics, stress intensity factor is used to predict the stress state near the crack tip caused by a load. There are three cracking modes used in fracture mechanics, such as Mode I, Mode II and Mode II as shown in Figure 5.4. Mode I is an opening (tensile) mode where the crack surfaces move apart and is the most common types. In Mode II, the crack surfaces slide apart in the direction perpendicular to the crack. In Mode III, the crack surfaces slide apart in a tearing manner known as out-of-plane shear mode.

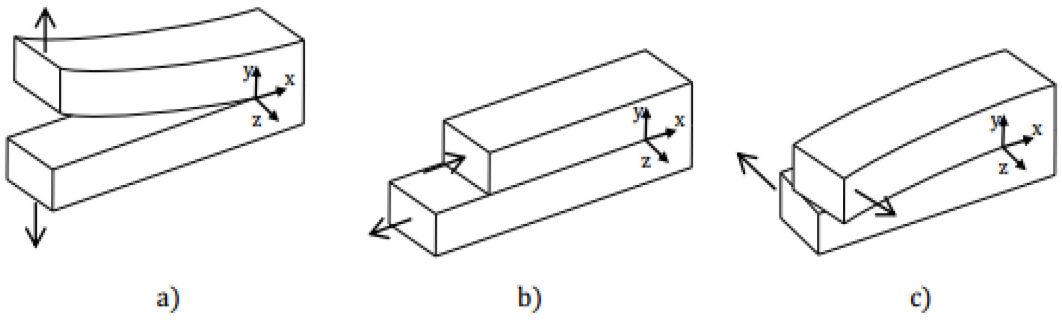

Figure 5.4. Cracking modes; a) Mode I, b) Mode II, c) Mode III

The stress intensity factor, k used in Equation 5-3 is determined by the following Equation 5-4 (Dowling 2007).

$$K = 1.12\, S\, \sqrt{(\pi a)} \tag{5-4}$$

where S is the nominal stress and a is the crack size.

5.4. Fatigue Life Calculation

The strain ranges and crack initiation and crack propagation life are listed in the following Table 5.2. In Section 5.4.2, the validation of the developed approach with test results will be presented.

5.4.1. Strain Range and Crack Initiation and Propagation Life

The difference between maximum and minimum strain obtained from the output files after step 3 and step 2 respectively is called strain range which are listed in the following Table 5.2.

Specimen	Strain range, $\frac{\Delta\varepsilon}{2}$	Crack Initiation life (cycles)	Crack Propagation life (cycles)
FT25A2	0.002613	33659	16927
FT25A3	0.003295	20253	18393
FT25B1	0.001369	342257	13182
FT25B2	0.002364	44327	17024
FT25B3	0.002839	19189	14618
FT27A1	0.00218	109397	26116
FT27A2	0.00367	17143	9654

Table 5.2. Strain range and crack initiation and crack propagation life obtained from FEA

5.4.2. Validation of developed FE analysis approach

The total fatigue life obtained from FE analysis for all fatigue specimens are listed below with test results in Table 5.3. An excellent correlation with the test results is observed.

Specimen	Total Fatigue Life (cycles)	
	Test (Lee *et al*. 2005)	FEA
FT25A2	44827	50586
FT25A3	60000	38646
FT25B1	387209	355439
FT25B2	61063	61351
FT25B3	5320	33807
FT27A1	142641	135513
FT27A2	22488	26797

Table 5.3. Comparison of FE analysis results with test results of Lee *et al*. (2005)

5.5. Comparison of FEA results with current code of Practices

The fatigue life equation proposed in AASHTO LRFD, CSA S6-14, EC4 and BS 5400 are used to calculate fatigue life and compared with test and FEA results which are shown in Table 5.4 and Figure 5.5.

Specimen	Stress range (MPa)	Total Fatigue Life (cycles)					
		Test	FEA	CSA S6-14	AASHTO LRFD	EC4	BS 5400
FT25A2	150	44800	50586	213630	11726	51772	81159
FT25A3	170	60000	38646	146754	3460	19021	29818
FT25B1	130	387200	355439	328175	40086	162657	254987
FT25B2	150	61063	61351	213630	11726	51772	81159
FT25B3	177.3	5420	33807	129363	2213	13588	21300

FT27A1	128.4	142641	135513	340597	44017	179597	281542
FT27A2	150	22488	26797	213630	11726	51772	81159

Table 5.4. Comparison of FEA results with current code of practices

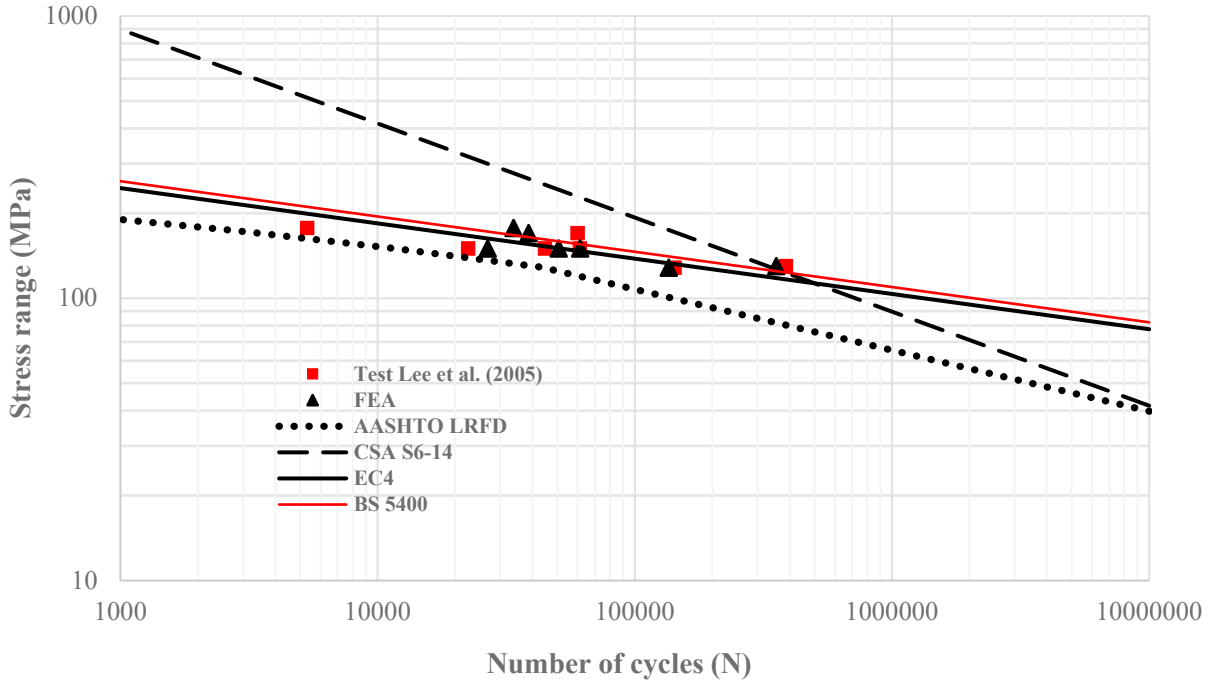

Figure 5.5. S-N curves

From the above Figure, it can be seen that when FE analysis results are compared with design code of practises, such as EC 4, CSA S6-14 and AASHTO LRFD, a significant underestimation is found in case of AASHTO LRFD while notable amount of overestimation is seen in case of CSA S6-14.

5.6. Parametric Study

In order to understand the influence of several parameters such as stud spacing, concrete slab thickness, concrete strength on fatigue life of shear stud, a parametric study is performed.

5.6.1. Effect of Slab Thickness

To investigate the slab thickness effects on fatigue life, parametric study is conducted with three different slab thicknesses (200, 250 and 300 mm). The results are shown in the following Table 5.5. It is observed that fatigue life decreases with the increase of slab thickness. This is due to the increase of shear forces which leads to the reduction of fatigue life.

Slab thickness (mm)	Fatigue Life (cycles)		
	FT25A2	FT25A3	FT25B1
200	50586	38646	355439
250	44593	21550	198937
300	32434	18214	101339

Table 5.5. Fatigue life variation with slab thickness

The following Figure 5.6 shows the variation of fatigue life with slab thickness for all specimens.

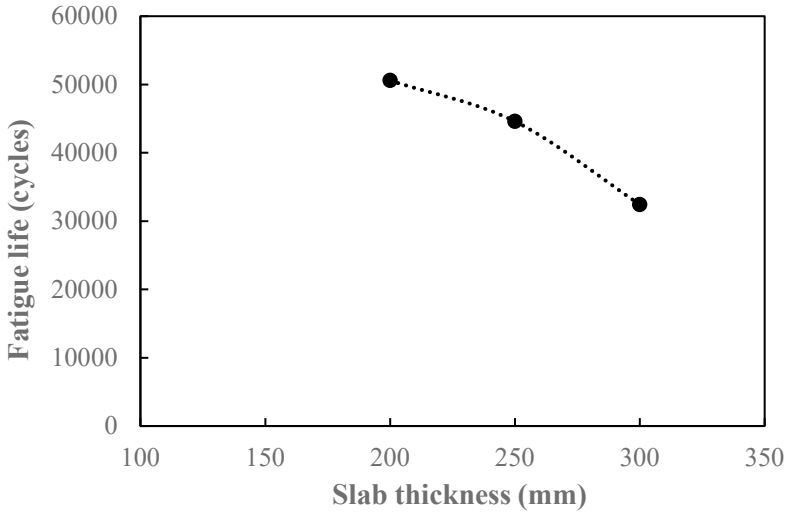

a)

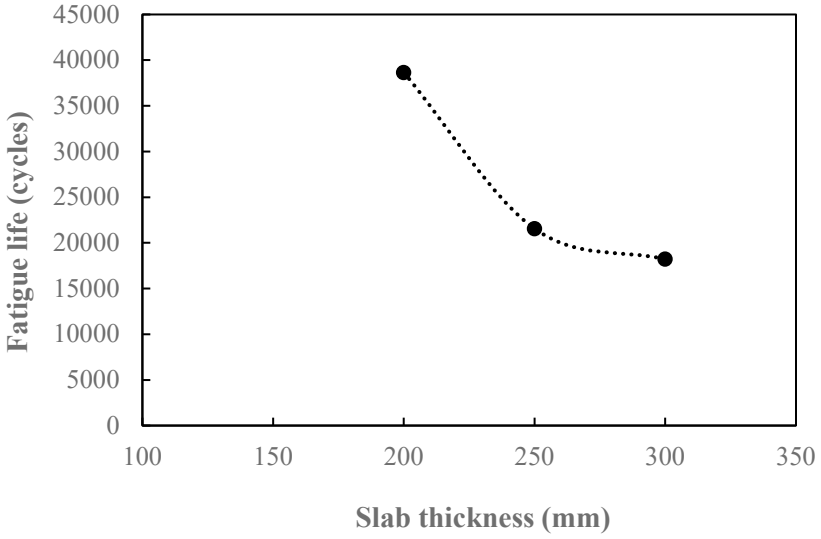

b)

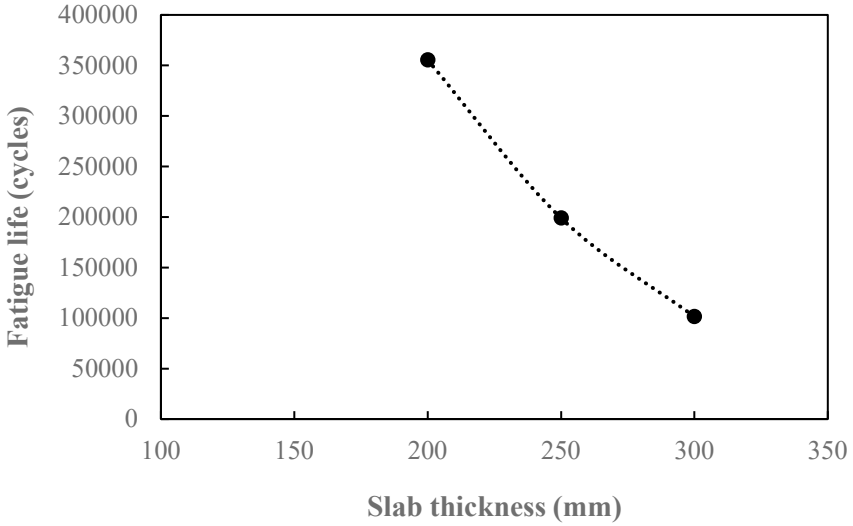

c)

Figure 5.6. Effect of slab thickness on fatigue life, a) FT25A2, b) FT25A3, c) FT25B1

5.6.2. Effect of Stud Spacing

To investigate the effects of stud spacing on fatigue life, three different stud spacings (200, 250 and 300 mm) are considered. Figure 5.7 shows the variation of fatigue life with the change of stud spacing for specimens FT25A2, FT25A3 and FT25B1. As can be seen from Table 5.6, a decrease in the fatigue life is observed with the increase of stud spacing for all fatigue specimen.

Stud Spacing (mm)	Fatigue Life (cycles)		
	FT25A2	FT25A3	FT25B1
200	134360	89275	376015
250	50586	38646	355439
300	22545	17143	231393

Table 5.6. Fatigue life variation with stud spacing

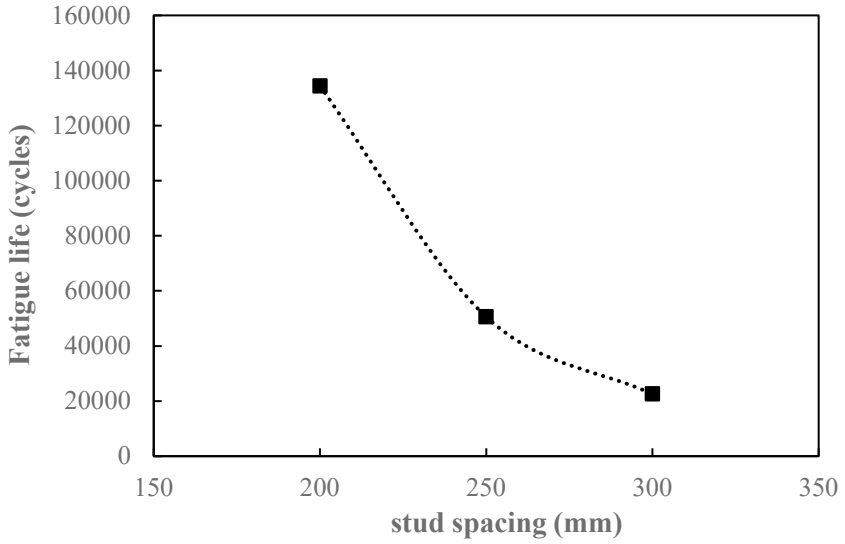

a)

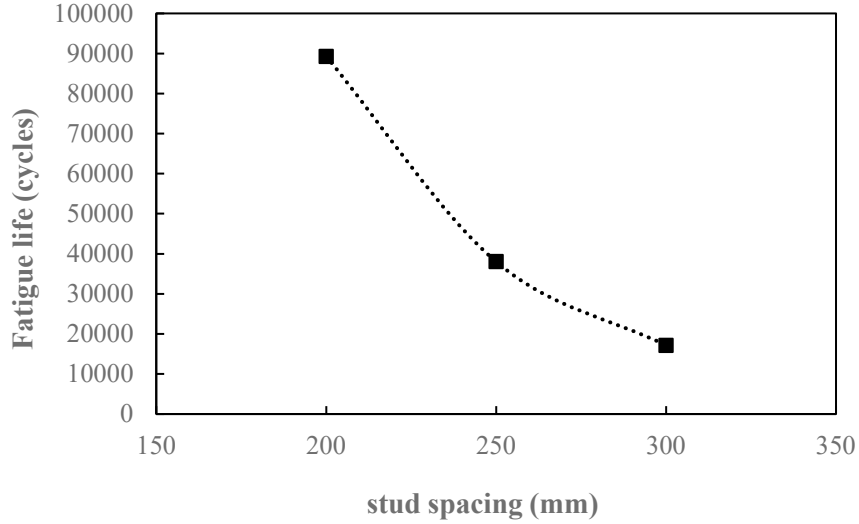

b)

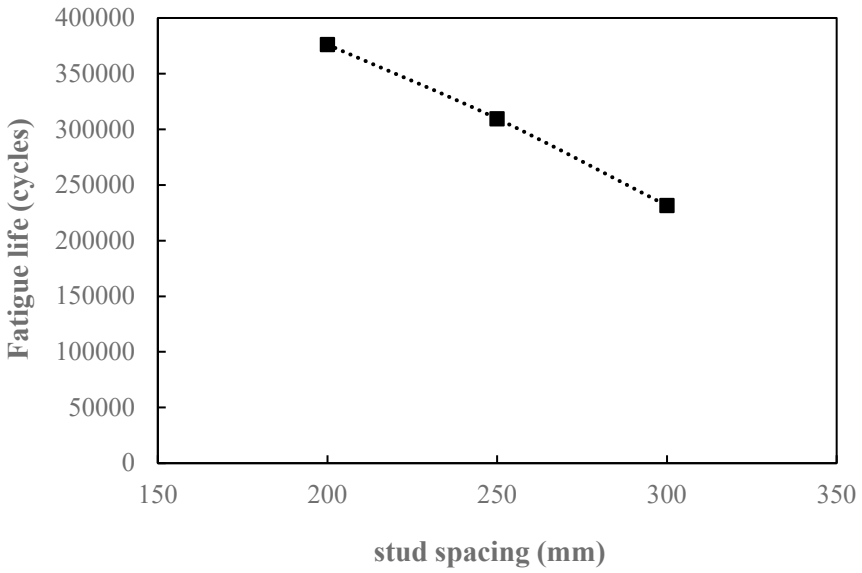

c)

Figure 5.7. Effect of stud spacing on fatigue life, a) FT25A2, b) FT25A3, c) FT25B1

5.6.3. Effect of Concrete Strength

From the tests, the strength of concrete was found to have minor effects on fatigue life of shear stud (Slutter and Fisher 1966). The mean compressive strength of all cylinders was around 30 MPa in their test. Now-a-days, higher concrete strenth is used in steel-concrete composite bridges. Thus, another parameter, concrete strength is taken to investigate it's effects on fatigue life. Five different concrete cylindrical compressive strengths (25, 30, 35, 40 and 45 MPa) are chosen. To account the effects of concrete strength, concrete damage plasticity is defined in the developed FE model. Results from analysis are shown in Table 5.7 and Figure 5.8. It can be observed that an increase in concrete strength leads to an increase in fatigue life but the increase is not significant.

Concrete Strength (MPa)	Fatigue Life (cycles)		
	FT25A2	FT25A3	FT25B1
25	41478	32919	296636

30	50586	38646	309500
35	55608	47197	318768
40	61351	66031	355439
45	62184	69791	450018

Table 5.7. Fatigue life variation with concrete strength

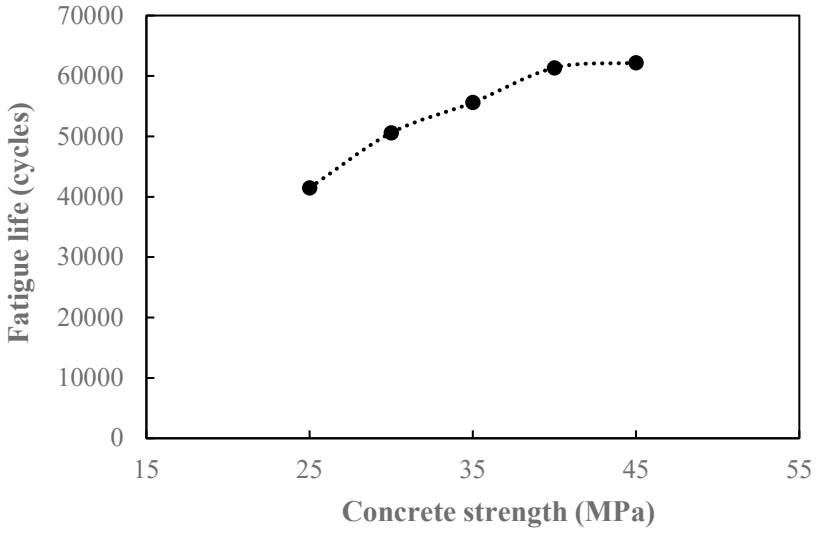

a)

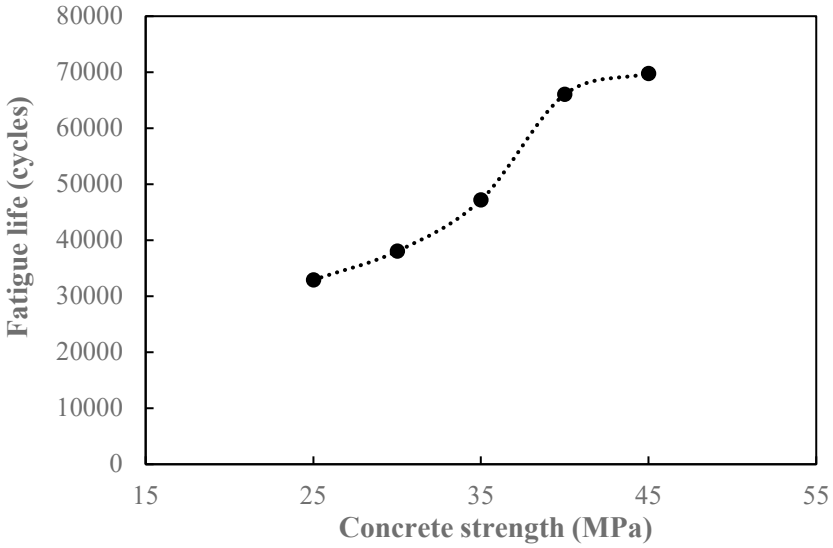

b)

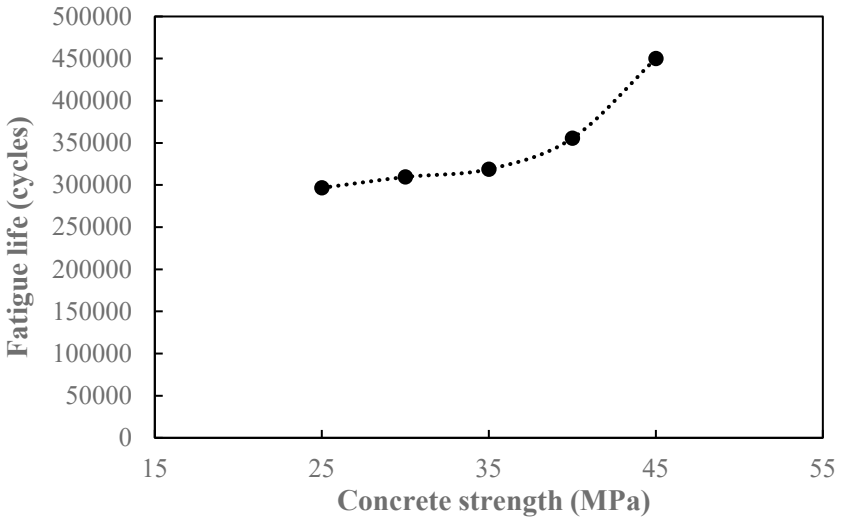

c)

Figure 5.8. Effect of concrete strength on fatigue life, a) FT25A2, b) FT25A3, c) FT25B1

5.7. Shear Stud Subjected to Tensile Loading

The shear studs are used in steel-concrete composite bridges primarily to transfer shear loads between steel beam and concrete slab. With the increase of using composite constructiion, conditions that lead to tension and combined shear and tension in headed shear studs are becoming more prevalent, especially in case of infill walls, connections to composite columns, or composite column bases (Pallares and Hajjar 2010). Few research works have been done recently on these type of conditions; shear stud in combined shear and tension (Shen and Chung 2017, Lin *et al.* 2014, Mirza and Uy 2010) and shear stud in tensile loading (Sutton *et al.* 2014, Pallares and Hajjar 2010). The previous works were limited to investigate the reduction in ultimate strength in case of axial and shear loading, and tensile strength in case of tensile loading. Currently, there are no guidelines in CSA S6-14 about fatigue life of shear stud subjected to tensile loading. In this thesis work, the effects of tensile loading on fatigue life of headed shear stud are investigated and the

developed finite element based approach for fatigue life estimation as discussed in Section 5.3 is used here to predict the total fatigue life when the shear studs are in tension.

FE model geometry, mesh, material properties, boundary conditions, contatct and interactions are same as previous except application of loading. The load is applied in such a way ensuring tension in shear studs. To do so, MPC constraint is used between the concrete slab surfaces and reference point (center of stud vertical line) as shown in Figure 5.9. The load is applied at the reference point ensuring uniform distribution of load.

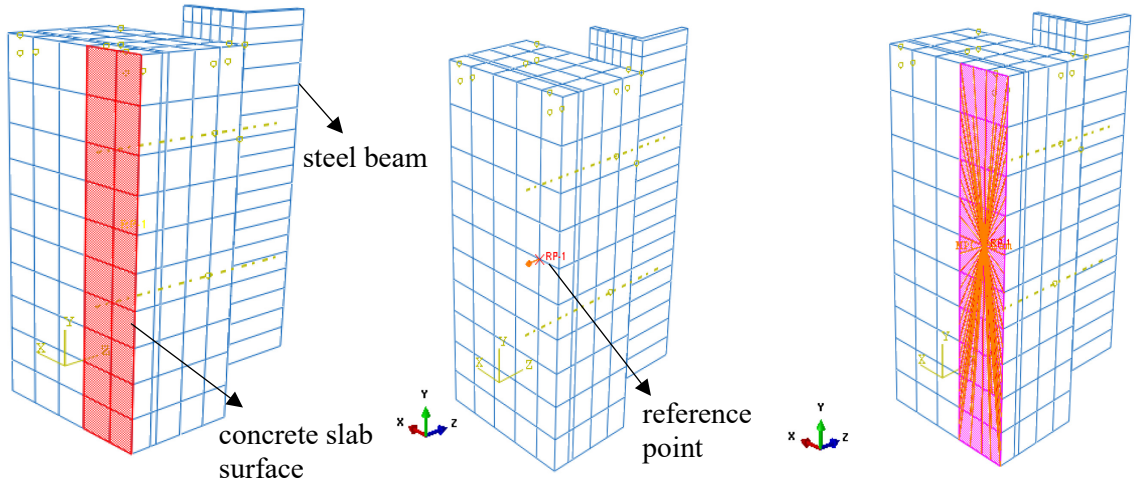

Figure 5.9. MPC constraint between concrete slab surfaces and reference point

Seven fatigue specimens have been used in the FE analysis to investigate the fatigue life. The stress ranges, concrete strength and ultimate strength of stud steel were collected from test of Lee *et al.* (2005) . In addition to 25 mm, shear stud of 27 mm is also taken. The maximum and minimum load and stress ranges are shown in Table 5.8.

Diameter of stud (mm)	Specimen	Concrete Strength (MPa)	Maximum Load (kN)	Minimum Load (kN)	Stress range (MPa)
25	FT25A2	30	73.6	0	150
	FT25A3	30	83.4	0	170
	FT25B2	40	73.6	0	150
	FT25B3	40	87	0	150
27	FT27A1	30	73.5	0	128.4
	FT27A2	30	85.9	0	150
	FT27A3	30	97.3	0	170

Table 5.8. Load and stress ranges used in FE analysis (Lee *et al*. 2005)

In the first time step, the model is fully loaded to maximum load. The load is then reduced to minimum load in the second time step, and finally it is reloaded to maximum load again in time step 3. After time step 2 and 3, the nominal strains in the X direction are recorded from the output file and the maximum nominal stress in X direction in time step 3 is also recorded. In case of shear loading, crack was reported to originate at weld collar base (Lee *et al*. 2005). As mentioned earlier, in Section 5.3, it is assumed that crack will form at most critical area (an area where stress is amximum) and the location of most critical area is identified by FE analysis. Figure 5.3 shows that the base of weld collar is most critical in case of shear loading indicating crack will form first at that position as test findings of Lee *et al*. (2005). In case of tensile loading, the most critical location is identified at base of weld from FE analysis as shown in Figure 5.10.

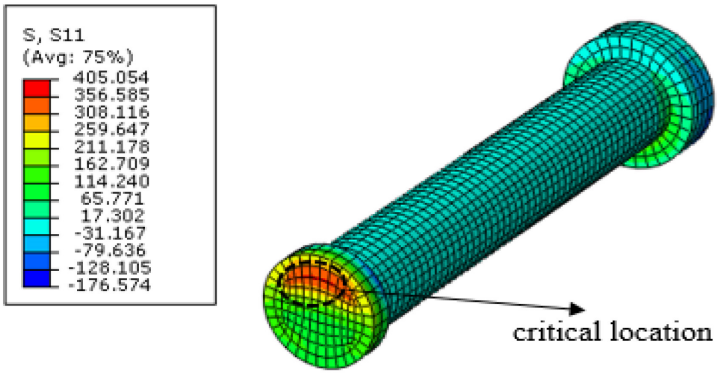

Figure 5.10. Critical loacation of shear stud in tensile loading (FT25A2 specimen)

5.7.1. Prediction of Fatigue Life

Equation 5-2 is used for crack initiation life and Equation 5-3 for crack propagation life. For crack propagation life, initial crack size is assumed as 1 mm and final crack size as 31 mm (weld base diameter) for 25 mm and 33 mm for 27 mm dia shear studs. It may be noted here that final crack size has very negligible effect on fatigue life (Blair and Stevens 1995). The crack initiation life, crack propagation life are listed below in the following Table 5.9.

Diameter of stud (mm)	Specimen	Strain range $\frac{\Delta\varepsilon}{2}$	Crack Initiation life (cycles)	Total fatigue life (cycles)
25	FT25A2	0.00200	20898	30197
	FT25A3	0.00212	16550	22591
	FT25B2	0.00193	22652	31584
	FT25B3	0.00229	14730	24071
27	FT27A1	0.00160	76902	90015

	FT27A2	0.00249	11510	22116
	FT27A3	0.00343	4113	14307

Table 5.9. Estimated fatigue life obtained from FE analysis

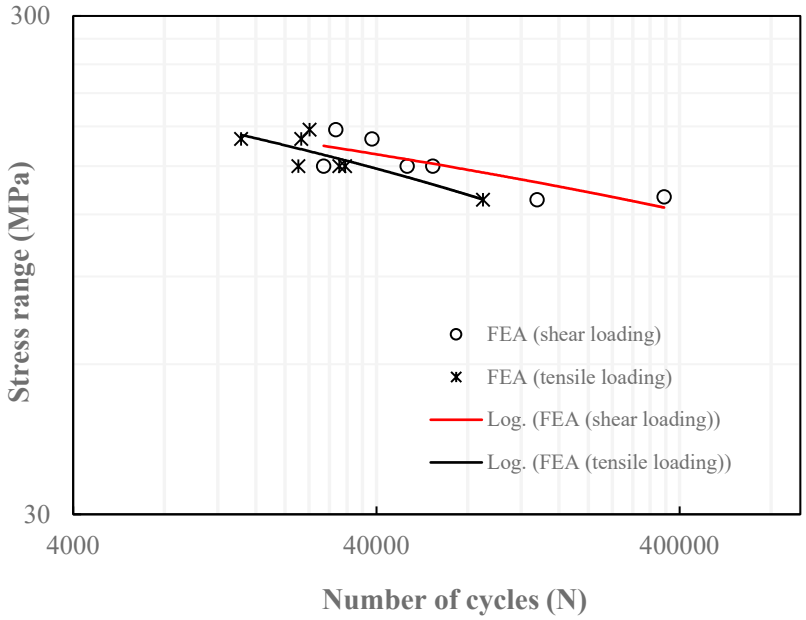

Figure 5.11. S-N curves

From Figure 5.11, a significant reduction in fatigue life is observed for all fatigue specimens when studs are in tension. It is important to note that current CSA S6-14 fatigue curve is developed based on push-out test where shear studs are in shear and slightly bending. So, this curve might not be safe to use for shear stud in tension. Now-a-days, engineers use their own judgement for design of shear stud in tension. Fatigue life of shear stud obtained from tensile loading is found less when compared with shear loading condition. Currently, there are no specific guidelines in CSA S6-14 about fatigue life of shear stud subjected to tensile loading. More experimental study is required in this area to develop a fatigue curve when shear stud connectors are in tension.

5.8. Summary of Chapter

This chapter presented the proposed finite element (FE) based approach for fatigue life estimation of headed shear stud connector. The proposed approach is well capable of predicting both crack initiation and crack propagation life. An excellent correlation is observed when FE analysis results were compared with the test results. It has been found that American code (AASHTO LRFD) significantly underestimates fatigue life while Canadian code (CSA S6-14) seriously overestimates fatigue life of headed shear stud. A parametric study has been performed with different concrete strength, stud spacing and concrete slab thickness. The parametric study reveals that the fatigue life increases with the increase of concrete strength but the effect is insignificant. Mode B fatigue failure mode is observed for shear loading condition where the crack is assumed to initiate at the base of stud weld collar which is similar to the finding of test results of Lee *et al.* (2005).

In case of tensile loading condition, the finite element analysis reveals a significant decrease in fatigue life when compared with shear loading. Thus, use of current fatigue curve in the Canadian code for fatigue life estimation of shear studs under tension might be unsafe. However, more experimental and numerical studies are required to form a fatigue curve when shear studs are in tension.

Chapter 6 Summary and Conclusions

6.1 Summary

The primary objective of this thesis was to investigate the load-slip behavior and fatigue life of headed stud shear connectors using finite element (FE) analysis. The basis of this study was in the form of parametric study conducted by finite element analysis representing the realistic push-out test behavior. A three-dimensional finite element (FE) model has been developed which was able to simulate exact load-slip behavior of shear studs. Two types of shear studs were studied i.e. large diameter (25, 27 and 30 mm) and standard diameter shear studs (19, 22 mm). Two experimental investigations were taken for comparison of the finite element analysis results. They include Gattesco and Giuriani (1996) for standard diameter and Lee et al. (2005) for large diameter shear studs and excellent correlation was found. Summary of the all studies conducted in this research are given below.

i) A detailed finite element model was developed considering both geometric and material non-linearites and validated against two tests.

ii) The developed FE model was used to investigate load-slip behavior of both standard and large diameter shear studs. The results obtained from FE analysis were compared with current code of practices such as Canadian code (CSA S6-14) and European Code (EC4). Two parameters i.e. strength of concrete and diameter of shear stud were considered to study their effect on shear capacity of headed shear studs.

iii) A finite element based approach for fatigue life estimation of shear studs using push-out specimen is proposed in Chapter 5. The FE model is validated against test results of Lee *et al*. (2005) to ensure its accuracy and reliability.

iv) The fatigue life obtained from finite element analysis were compared with American code (AASHTO LRFD), Canadian Code (CSA S6-14), European code (EC4) and British code (BS 5400).

v) The effects of concrete strength, stud spacing and slab thickness on fatigue life of shear studs were studied using the proposed FE based approach.

vi) Finally, shear studs subjected to tensile loading were analysed and fatigue life of studs were estimated using the same FE based approach used for shear loading.

6.2. Conclusions

An extensive parametric study with different stud diameters and concrete strength was performed using the develoed FE model to investigate the shear capacity and load-slip behavior of both small and larger shear studs. From this parametric study, following findings can be drawn:

i) Shear capacity increases with the increase of concrete strength but the slip decreases. Concrete damage plasticity is defiend in the developed FE model. So, with the increase of concrete stregth, relative displacement between concrete slab and steel beam nodes around the stud decreases.

ii) It has been found that with the increase of stud diameter, the ultimate slip increases for a certain concrete strength.

iii) Shank failure mode is observed for both standard (19 and 22 mm) and large diameter shear studs (25, 27 and 30 mm).

iv) The effect of shear stud head on shear capacity is found significant when capacity of headed shear stud is compared with headless shear stud.

v) It is observed that Canadian standard, CSA S6-14 generally overestimates the shear capacity of headed shear studs. The overestimation increases with the increase of concrete strength. Thus, for 19 mm shear stud diameter Canadian standard, S6-14 overestimates the shear strength as much as 17.7% when 35 MPa concrete is used. In addition, EC 4 ususally underestimates the shear capacities of the shear studs. For 19 mm dia shear stud, the underestimation is up to 18.3%.

vi) For 22 mm shear stud, CSA S6-14 is found to overestimate the shear capacity up to 22.3% when 35 MPa concrete strength is considered, while EC4 underestimates the shear capacity up to 10.6%.

vii) EC 4 underestimates the shear capacity as much as 7.2% and this underestimation decreases with the increase of concrete strength for 25 mm shear stud, whereas in case of CSA S6-14, about 17.7% overestimation is found.

viii) CSA S6-14 is found to overestimate shear capacity for both 27 and 30 mm shear studs. In case of EC4, the underestimation is found less compared to other diameters. Thus, only 4.9% undersetimation is noticed when 25 MPa concrete strength is considered for 30 mm shear stud.

In a nutsheel, Canadian Standard, CSA S6-14 is found to overestimate the static strength of headed shear stud up to 22.3% while the European code, EC4 ususally gives conservative estimation of shear capacity of headed shear stud.

A finite element based approach using the push-out test is proposed for fatigue life estimation of shear studs. Both crack initiation life and crack propagation life are estimated and a good correlation is found with test results. The following conclusions can be drawn from fatigue study.

i) The proposed approach is well capacble of predicting both crack initiation and crack propagation life.

ii) When FE analysis results are compared with design code of practises, such as EC4, CSA S6-14 and AASHTO LRFD, a significant underestimation is found in case of AASHTO LRFD, while notable amount of overestimation is seen in case of CSA S6-14.

iii) The parametric study revealed that the effect of concrete strength on fatigue life is insignificant.

iv) It is observed that fatigue life decreases with the increase of concrete slab thickness. This is due to the increase of shear forces which leads to the reduction of fatigue life. A decrease in the fatigue life is observed with the increase of shear stud spacing for all fatigue specimens.

v) In case of shear loading, Mode B fatigue failure mode is observed from FE analysis in which crack is assumed to initiate at base of the stud weld collar as observed in the test of Lee *et al*. (2005).

vi) In case of tensile loading, crack is found to initiate at base of the stud weld assuming crack will initiate at most stressed area. Fatigue life in this loading condition is found less for all fatigue specimens when compared to shear loading.

6.3. Recommendations for Future Work

Based on the findings and results obtained during this investigation the following recommendations can be made:

i) Current Canadian Standards Association, CSA S6-14 is found to overestimate shear capacity for both standard and large diameter shear studs. More experimental testing should be carried out for further investigation specially for large diameter shear studs.

ii) A notable amount of overerestimation in fatigue life is noticed in case of CSA S6-14 when compared with the results of FE analysis and test results of Lee *et al*. (2005) demanding more study to evaluate the current fatigue requirements of Canadian code.

iii) The FE analysis reveals a significant decrease in fatigue life of shear studs when they are in tension. Now-a-days, the design engineers use their own engineering judgements and no guidelines are available in the current Canadian code about shear studs subjected to tension. More experimental studies are required to form a fatigue curve when shear studs are in tension.

REFERENCES

Abaqus (2013). "Abaqus standard user's manual, 6.13." Dassault Systèmes.

Alkhatib, A. (2012). "Experimental Study of Behavior and Strength of Shear Studs in Composite Bridge Deck Construction." M.A.Sc dissertation, Department of Civil and Resource Engineering, Dalhousie University, Halifax, Nova Scotia, Canada.

American Association of State Highway and Transportation Officials, (AASHTO). (2012). "AASHTO LRFD Bridge Design Specifications." 6th Edition, Washington, D.C.

An, L. and Cederwall, K. (1994). "Push-out Tests on Studs in High Strength and Normal Strength Concrete." Journal of Constructional Steel Research, 36(1): 15-29.

ASTM Designation E 647-00: Standard Test Method for Measurement of Fatigue Crack Growth Rates. American Society for Testing and Materials, Philadelphia, USA.

Badie, S.S., Tadros, M.K., Kakish, F.H., Splittgerber, D.L. and Baishya, C.M. (2002). "Large Shear Studs for Composite Action in Steel Bridge Girders." Journal of Bridge Engineering, 7(3): 195-203.

Basquin, O.H. (1910). "The Exponential Law of Endurance Tests." Proceedings of the American Society for Testing and Materials, Vol. 10, pp. 625-630.

Blair, M. and Stevens, T.L. (1995). "Steel Castings Handbook." 6th Edition, ASM International, Materials Park, USA.

Bro, M. and Westberg, M. (2004). "Influence of Fatigue on Headed Stud Connectors in Composite Bridges." Master of Science Programme, Department of Civil and Environmental Engineering, Lulea University of Technology, Sweden.

BSI (1980). BS5400. "Steel, concrete and composite bridges - Part 10: Code of practice for fatigue." London, England.

BSI (2005). BS5400. "Steel, concrete and composite bridges - Part 5: Code of practice for the design of composite bridges." London, England.

Canadian Standards Association, (CSA). 2014. "Limit States Design of Steel Structures." CAN/CSA-S6-14: Toronto, Ontario, Canada.

Canadian Standards Association, (CSA). 2014. "Design of Concrete Structures." CAN/CSA-A23.3-14: Toronto, Ontario, Canada.

Chen, H., Grondin, G.Y. and Driver, R.G. (2005). "Fatigue Resistance of High Performance Steel." Structural Engineering Report NO. 258. Department of Civil Engineering, University of Alberta, Edmonton, Alberta, Canada.

Dowling, N.E. (2007). "Mechanical Behavior of Materials: Engineering Methods for Deformation, Fracture, and Fatigue." 3rd Edition, Pearson Prentice Hall, Upper Saddle River, USA.

Ellobody, E., Young, B. and Lam, D. (2006). "Behavior of normal and high strength concrete-filled compact steel tube circular stub columns." Journal of Constructional Steel Research, 62(7): 706-715.

Ellyin, F. (1997). "Fatigue Damage, Crack Growth and Life Prediction." Chapman & Hall, London, UK.

Eurocode 4. (1997). ENV 1994-2 Eurocode-4: "Design of composite steel and concrete structures, Part 2: Composite bridges." European Committee for Standardization (CEN), Brussels, Belgium.

Everett, R.A. (1992). "Comparison of Fatigue Life Prediction Methodologies for Rotorcraft." Journal of the American Helicopter Society, Vol. 37, No. 2, pp. 54-60.

Fisher, J.W., Kulak, G.L. and Smith, I.F.C. (1997). "A Fatigue Primer for Structural Engineers." ATLSS Report No. 97-11, Leigh University, Bethlehem, USA.

Fisher, J.W., Frank, K.H., Hirt, M.A. and McNamee, B.M. (1970). "Effect of Weldments on the Fatigue Strength of Steel Beams." NCHRP Report 102. Highway Research Board, National Research Council, Washington, D.C.

Gattesco, N. and Giuriani, E. (1996). "Experimental study on stud shear connectors subjected to cyclic loading." Journal of Constructional Steel Research, 38(1): 1-21.

Gattesco, N., Giuriani, E. and Gubana, A. (1997). "Low-Cycle Fatigue Test on Stud Shear Connectors." Journal of Structural Engineering, 123(2): 145-150.

Hallam, M.W. (1976). "The Behavior of Stud Shear Connectors Under Repeated Loading." Research Rep. R281, School of Civil Engineering, University of Sydney.

Hanswille, G., Porsch, M. and Ustundag, C. (2007). "Resistance of headed studs subjected to fatigue loading Part I: Experimental study." Journal of Constructional Steel Research, 63(4): 475-484.

Jayas, B.S. and Hussain, M.U. (1988). "Behavior of Headed Studs in Composite Beams: Push-out Tests." Canadian Journal of Civil Engineering, 15(2): 240-253.

Josi, G. and Grondin, G.Y. (2010). "Reliability-Based Management of Fatigue Failures." Structural Engineering Report No. 285. Department of Civil Engineering, University of Alberta, Edmonton, Alberta, Canada.

Klippstein, K.H. (1987)."Variable Amplitude Load Fatigue, Task A - Literature Review, Volume III - Supplementary Information on Constant Amplitude Fatigue Behavior." Report No. DTFH61-86-00036-III, U.S. Department of Transportation, Federal Highway Administration, Washington, D.C.

King, D.C., Slutter, R.G. and Driscoll, G.C. (1965). "Fatigue strength of 1/2-inch diameter stud shear connectors." NCHRP Report 103, Highway Research Record, Washington, D.C.

Lee, P.G., Shim, C.S. and Chang, S.P. (2005). "Static and fatigue behavior of large stud shear connectors for steel-concrete composite bridges." Journal of Constructional Steel Research, 61(9): 1270-1285.

Lee, K.C., Hassan, H.A. and George, E.R. (2010). "Review of Current AASHTO Fatigue Design Specifications for Stud Shear Connectors." url: http://dx.doi.org/10.1061/41130(369)29.

Lin, Z., Liu, Y. and He, J. (2014). "Behavior of stud connectors under combined shear and tension loads." Engineering Structures, Vol. 81, pp. 362-376.

Loh, H.Y., Uy, B. and Bradford, M.A. (2003). "The effects of partial shear connection in the hogging moment regions of composite beams Part I - Experimental study." Journal of Constructional Steel Research, 60(6): 897-919.

Maleki, S. and Bagheri, S. (2008). "Behavior of channel shear connectors, Part I: Experimental study." Journal of Constructional Steel Research, 64(12): 1333-1340.

Mainstone, R.J. and Menzies, J.B. (1967). "Shear connectors in steel-concrete composite beams for bridges, Part I." Concrete, 1(9): 291-302.

Miner, M.A. (1945). "Cumulative damage in fatigue." Journal of Applied Mechanics, Vol. 12, pp. 159-164.

Mirza, O. and Uy, B. (2008). "Behavior and Design of Headed Shear Connectors in Composite Steel-Concrete Beams." Doctoral dissertation, School of Engineering, University of Western Sydney, Australia.

Mirza, O. and Uy, B. (2010). "Effects of the combination of axial and shear loading on the behavior of headed stud steel anchors." Engineering Structures, 32(1): 93-105.

Mundie, D.L. (2011). "Fatigue Testing and Design of Large Diameter Shear Studs Used in Highway Bridges." M.A.Sc dissertation, Department of Civil Engineering, Auburn University, USA.

Naithani, K.C., Gupta, V.K. and Gada, A.D. (1988). "Behavior of shear connectors under dynamic loads." Materials and Structures/Materiaux et Constructions, 21, pp. 359-363.

Nguyen, H.T. and Kim, S.E. (2009). "Finite element modeling of push-out tests for large stud shear connectors." Journal of Constructional Steel Research, 65(10-11): 1909-1920.

Oehlers, D.J. and Foley, L. (1985). "The fatigue-strength of stud connections in composite beams." Proceedings of the Institution of Civil Engineers, 79(2): 349-364.

Oehlers, D.J. (1990). "Deterioration in strength of stud connectors in composite bridge beams." Journal of Structural Engineering, 116(2): 3417-3431.

Ollgaard, J.G., Slutter, R.G. and Fisher, J.W. (1971). "Shear strength of stud connectors in lightweight and normal weight concrete." AISC Engineering Journal, 8:55-64. url: htp://preserve.lehigh.edu/engr-civil-environmental-fritz-lab-reports/2010.

Ovuoba, B. and Prinz, G.S. (2016). "Fatigue Capacity of Headed Shear Studs in Composite Bridge Girders." Journal of Bridge Engineering, 04016094:1-9. url: http://dx.doi.org/10.1061/(ASCE)BE.1943-5592.0000915.

Pallares, L. and Hajjar, J.F. (2010). "Headed steel stud anchors in composite structures, Part II: Tension and interaction." Journal of Constructional Steel Research, 66(2): 213-228.

Paris, P. and Erdogan, F. (1963). "A Critical Analysis of Crack Propagation Laws." Transactions of the ASME, Vol. 85, pp. 528-534.

Seracino, R., Oehlers, D.J. and Yeo, M.F. (2003). "Behavior of stud shear connectors subjected to bi-directional cyclic loading." Advances in Structural Engineering, 6(1): 65-75.

Shariati, A., Ramlisulong, N.H., Suhatril, M. and Shariati, M. (2012). "Various Types of Shear Connectors in Composite Structures: A Review." International Journal of Physical Sciences, 7(22): 2876-2890.

Shen, M.H. and Chung, K.F. (2017). "Experimental investigation into stud shear connections under combined shear and tension forces." Journal of Constructional Steel Research, Vol. 133, pp. 434-447.

Shim, C.S., Lee, P.G. and Chang, S.P. (2001). "Design of shear connection in composite steel and concrete bridge with precast decks." Journal of Constructional Steel Research, 57(3): 203-219.

Shim, C.S., Lee, P.G. and Yoon, T.Y. (2004). "Static behavior of large stud shear connectors." Engineering Structures, 26(12): 1853-1860.

Slutter, R.G. and Fisher, J.W. (1966). "Fatigue strength of shear connections." Leigh University Institute of Research, Bethlehem, PA, USA.

Smith, K.N., Watson, P. and Topper, T.H. (1970). "A stress-strain function for the fatigue of metals." Journal of Materials, 5(4): 767-778.

Stephens, R.I., Fatemi, A., Stephens, R.R. and Fuchs, H.O. (2001). "Metal Fatigue in Engineering." 2nd Edition, John Willey and Sons, New York, USA.

Sutton, J.P., Mouras, J.M., Samaras, V.A., Williamson, E.B. and Frank, K.H. (2014). "Strength and Ductility of Shear Studs under Tensile Loading." Journal of Bridge Engineering, 19(2): 245-253.

Tavernelli, J.F. and Coffin, L.F. Jr. (1962). "Experimental Support for Generalized Equation Predicting Low Cycle Fatigue (incl. Discussion by S.S. Manson)." Transactions ASME, Journal of Basic Engineering, Vol. 84, pp. 533-541.

Topkaya, C., Yura, J.A. and Williamson, E.B. (2004). "Composite Shear Stud Strength at Early Concrete Stages." Journal of Structural Engineering, 130(6): 952-960.

Vianna, J. da. C., Costa-Neves, L.F., Vellasco, P.C.G. da S. and De Andrade, S. A. L. (2009). "Experimental assessment of Perfobond and T-Perfobond shear connectors' structural response." Journal of Constructional Steel Research, 65(2): 408-421.

Viest, I.M. (1956). "Investigation of Stud Shear Connections for Composite Concrete and Steel T-Beams." Journal of the American Concrete Institution, 27(8): 875-891.

Wang, Y. (2010). "Fatigue Repair Technique Investigation - Hole Drilling and Expansion Method." Doctoral dissertation, Department of Civil Engineering, University of Alberta, Edmonton, Alberta, Canada.

Xie, E. and Valente, M.I.B. (2011). "Fatigue Strength of Shear Connectors." Research Report. University of Minho, Guimaraes, Portugal.

Xue, W., Ding, M., Wang, H. and Luo, Z. (2008). "Static Behavior and Theocratical Model of Stud Shear Connectors." Journal of Bridge Engineering, 13(6): 623-634.

APPENDIX

A sample of FE analysis output file for fatigue specimen FT25B1 (Shear loading):

Time (sec)	Nominal strain (NE11)	Nominal stress (S11)
0	4.79E-07	0
0	2.52E-07	1.93469
0.60016	1.77E-06	1.84951
0.60016	2.14E-06	19.8372
1.20009	2.57E-05	18.7514
1.20009	2.26E-05	65.085
1.80001	9.33E-05	60.8759
1.80001	7.90E-05	140.586
2.40022	2.12E-04	130.688
2.40022	1.77E-04	225.556
3.00008	3.44E-04	222.06
3.00008	3.08E-04	275.823
3.60019	4.67E-04	276.478
3.60019	4.63E-04	288.706
4.20006	5.70E-04	295.879
4.20006	6.35E-04	297.008
4.80016	6.82E-04	305.851
4.80016	8.24E-04	298.3
5.40003	7.66E-04	306.47
5.40003	9.95E-04	294.583
6.00011	8.61E-04	302.569
6.00011	1.12E-03	290.903
6.60006	1.00E-03	298.848
6.60006	1.26E-03	283.808
7.20006	1.09E-03	291.855
7.20006	1.36E-03	276.269
7.80018	1.11E-03	283.455
7.80018	1.41E-03	270.489
8.4002	1.09E-03	275.377
8.4002	0.001411	263.515
9.00006	1.06E-03	266.871
9.00006	1.37E-03	256.985
9.60016	1.03E-03	260.588
9.60016	1.30E-03	253.802
10.2	1.02E-03	256.309
10.2	1.26E-03	253.323
10.8001	1.07E-03	255.954
10.8001	0.001278	257.189

11.4002	1.29E-03	260.956
11.4002	0.001467	256.673
12.0001	1.63E-03	262.741
12.0001	0.00182	255.73
12.6001	2.02E-03	261.143
12.6001	0.002227	250.785
13.2001	2.46E-03	255.361
13.2001	0.002632	242.381
13.8001	2.80E-03	244.471
13.8001	0.002892	241.842
14.4	3.12E-03	243.466
14.4	0.003051	236.434
15.0001	3.37E-03	235.711
15.0001	0.003149	232.614
15.6001	3.62E-03	225.948
15.6001	0.003237	231.181
16.2	3.82E-03	224.086
16.2	0.003316	230.676
16.8	3.98E-03	224.23
16.8	0.003389	232.079
17.4001	4.10E-03	226.235
17.4001	0.003474	235.792
18	4.22E-03	229.096
18	0.003571	239.134
18.6001	4.30E-03	232.548
18.6001	0.003635	144.653
19.2002	0.00411	147.241
19.2002	0.00349	-69.5253
19.8	0.003587	-41.0492
19.8	0.003114	-173.973
20.4001 (2nd time step)	0.003199	-141.691
20.4001	0.002875	-100.979
21.0002	0.003312	-73.0776
21.0002	2.98E-03	68.6866
21.6002	0.003721	76.3989
21.6002	0.003269	156.034
22.2	0.003966	147.234
22.2	3.42E-03	77.7832
22.8001	3.81E-03	72.5366
22.8001	3.29E-03	-74.3294
23.4001	0.003441	-60.2213
23.4001	3.03E-03	-147.13
24.0002	0.003231	-118.269

24.0002	2.90E-03	-88.2248
24.6	0.003341	-62.3237
24.6	2.99E-03	15.5859
25.2001	0.003592	27.2271
25.2001	0.003168	39.1582
25.8001	0.003676	42.9338
25.8001	0.003214	-47.4006
26.4002	0.003486	-35.729
26.4002	0.003067	-152.754
27	0.003219	-126.032
27	2.88E-03	-182.044
27.6001	0.003071	-154.272
27.6001	2.80E-03	-144.871
28.2001	0.003141	-119.618
28.2001	2.86E-03	-98.8769
28.8002	0.003255	-80.5839
28.8002	2.94E-03	-117.551
29.4	0.003225	-99.7143
29.4	2.90E-03	-188.795
30.0001	0.003024	-166.58
30.0001	2.76E-03	-232.549
30.6001	0.002658	-218.24
30.6001	2.50E-03	-247.685
31.2002	0.002407	-236.117
31.2002	2.32E-03	-245.149
31.8	0.002357	-235.176
31.8	0.002287	-243.648
32.4001	0.002356	-235.267
32.4001	0.002284	-254.853
33.0001	0.002218	-246.801
33.0001	0.002172	-275.013
33.6002	0.001892	-264.933
33.6002	0.00192	-292.748
34.2	1.49E-03	-280.232
34.2	0.001629	-303.826
34.8001	1.16E-03	-290.779
34.8001	0.001399	-309.759
35.4001	9.48E-04	-296.985
35.4001	0.001251	-315.137
36.0002	7.85E-04	-302.76
36.0002	1.14E-03	-319.838
36.6	0.000559	-309.463
36.6	0.000973	-321.071

37.2001	2.15E-04	-313.102
37.2001	7.33E-04	-321.422
37.8001	-0.00021	-314.581
37.8001	4.48E-04	-321.562
38.4002	-6.54E-04	-315.772
38.4002	0.000149	-318.714
39	-0.00104	-315.491
39	-0.00011	-317.488
39.6001	**-0.00143**	-317.034
39.6001	-0.0004	-316.169
40.2001 (3rd time step)	-0.00182	-318.022
40.2001	-0.00069	-316.032
40.8002	-2.18E-03	-318.692
40.8002	-0.00097	-312.167
41.4	-2.28E-03	-314.219
41.4	-0.00104	-238.863
42.0001	-2.13E-03	-251.186
42.0001	-0.00093	-127.802
42.6001	-1.86E-03	-156.824
42.6001	-0.00074	-42.5539
43.2002	-0.00165	-84.6127
43.2002	-0.0006	-32.4444
43.8	-0.00159	-78.1465
43.8	-0.00058	-73.829
44.4001	-0.00167	-113.585
44.4001	-0.00064	-89.5815
45.0001	-0.00171	-124.121
45.0001	-0.00066	-34.5613
45.6002	-0.0016	-74.0407
45.6002	-0.00057	56.5273
46.2	-0.00138	5.77901
46.2	-0.00042	118.809
46.8001	-0.0012	66.1215
46.8001	-0.00028	132.356
47.4001	-0.00113	81.1916
47.4001	-0.00024	115.537
48.0002	-0.00116	66.0683
48.0002	-0.00026	116.463
48.6	-0.00116	68.0372
48.6	-0.00025	154.843
49.2001	-1.05E-03	110.571
49.2001	-0.00017	201.423
49.8001	-7.95E-04	167.847

49.8001	-1.30E-05	233.653
50.4002	-5.19E-04	208.676
50.4002	0.000182	244.467
51	-3.59E-04	223.531
51	0.0003	244.723
51.6001	-3.20E-04	226.081
51.6001	0.00033	246.331
52.2001	-2.87E-04	229.016
52.2001	0.000358	255.271
52.8002	-1.60E-04	238.451
52.8002	0.000463	268.355
53.4	5.68E-05	251.533
53.4	6.42E-04	278.636
54.0001	2.70E-04	262.197
54.0001	8.12E-04	283.355
54.6001	4.11E-04	268.056
54.6001	9.20E-04	283.694
55.2002	4.63E-04	269.895
55.2002	0.000961	283.72
55.8	4.87E-04	270.841
55.8	0.00098	287.437
56.4001	5.49E-04	274.101
56.4001	0.00103	293.861
57.0001	6.60E-04	279.541
57.0001	0.001116	300.2
57.6002	7.91E-04	285.795
57.6002	0.001218	**303.873**
58.2	8.83E-04	289.613
58.2	1.29E-03	303.818
58.8001	9.08E-04	290.006
58.8001	**0.001309**	299.966
59.4001	9.01E-04	286.959
59.4001	0.001303	300.253
60	9.01E-04	287.615
60	0.001305	275.890

PUBLICATIONS:

1. Mia, Md Manik and Bhowmick, Anjan (Presented), “Static Strength of Headed Shear Stud Connectors Using Finite Element Analysis”, 6th International Conference on Engineering Mechanics and Materials, CSCE, May 31-June 3, 2017, Vancouver, Canada.

2. Mia, Md Manik and Bhowmick, Anjan (Presented), “Fatigue-Life Prediction of Shear Stud using Finite Element Analysis”, 6th International Conference on Engineering Mechanics and Materials, CSCE, May 31-June 3, 2017, Vancouver, Canada.